Wheat Straw-Clay-Polypropylene Hybrid Composites

by

Amirpouyan Sardashti

A thesis
presented to the University of Waterloo
in fulfillment of the
thesis requirement for the degree of
Master of Applied Science
in
Chemical Engineering

Waterloo, Ontario, Canada, 2009

AUTHOR'S DECLARATION

I hereby declare that I am the sole author of this thesis. This is a true copy of the thesis, including any required final revisions, as accepted by my examiners.

I understand that my thesis may be made electronically available to the public.

Amirpouyan Sardashti

ABSTRACT

The preparation of polymeric hybrid composite consisting of organic and inorganic fillers is of interest for industries like automotive, construction and packaging. In order to understand and predict the physical and chemical properties of these hybrid composites, it is necessary to fully understand the nature and properties of the employed fillers. In this study, the preparation of polypropylene hybrid composite consisting of wheat straw and clay was investigated. A detailed study was performed on wheat straw from South Western Ontario region. The effect of grinding the straw and compounding it with polypropylene was investigated. Experiments were carried out to identify the thermal stability of the ground wheat straw with respect to their size and composition. It was important to identify a correlation between these properties in order to minimize the straw degradation by processing and also to improve the final properties of the hybrid composite. The composite samples were prepared through melt blending method using a co-rotating twin-screw extruder. Sample test bars were prepared by injection moulding. The composition of the constituents of the hybrid composite; percentages of wheat straw, clay and coupling agent, were varied in order to investigate their influence on thermal stability, water resistance and mechanical properties.

The results of the study indicated that grinding the wheat straw with a hammer mill produced particles with different sizes and shapes. It was found that through the grinding system all particles, regardless of their size, had a multi-layered structure similar to the plant structure. Further hammer milling did not produce plant particles with long aspect ratios that would be expected in a defibrillation process. Analysis of the chemical composition of wheat straw particles of different sizes and shapes was used to measure the ratio of hemicelluloses: lignin and the ash content. It was found that the large particles contained more amount of lignin whereas smaller particles had larger amount of ash content. The thermal stability of the particles was found to be a function of particle size rather than the lignin content. Particle size analysis on the wheat straw particles after the extrusion process indicated a reduction in the particle length and aspect ratio.

The thermal stability of the composites was found to be enhanced by the addition of clay particles at higher temperature and the addition of coupling agent at lower temperatures. Increasing the amount of wheat straw and clay content increased the flexural modulus and reduced the resistance for water absorption. Increasing the amount of coupling agent also increased the flexural modulus and resistance for water absorption. The morphological study by scanning electron microscopy revealed that coupling agent increased the interfacial interaction between the particles and the polymer matrix.

ACKNOWLEDGEMENTS

I would like to express my sincerest gratitude to Dr. Leonardo C. Simon, my supervisor, for all his assistance, guidance and supervision through my graduate research.

I also would like to thank Dr. Ali Elkamel and Dr. Christine Moresoli, my thesis committee members, for accepting to be readers of my thesis, and for all their help and guidance.

I would also like to thank all my friends and colleagues especially Barbara Guetller, Zena Ng, Dr. Ravindra Reddy, Dr. Sang-Young Anthony Shin, and Mahsa Golbabaie for all their valuables assistance.

Further, I would like to acknowledge the financial support and assistance provided by the Ontario BioCar Initiative (ORF-MRI) grant, NSERC-Discovery grant and to the industrial partners A. Schulman Inc. and Omtec Inc.

DEDICATION

I would like to dedicate this thesis to my parents, Mohammad Reza and Soudabeh Sardashti for all their love and support throughout my life.

TABLE OF CONTENTS

LIST OF FIGURES

LIST OF TABLES

LIST OF ABBREVIATIONS

"

$

µ

3

A

C

D

E

F

G

H

K

L

M

N

O

P

R

S

T

U

W

X

Δ

Λ

1 INTRODUCTION

1.1 MOTIVATION AND OBJECTIVES

Environmentally friendly polymer composites obtained from natural bio-derived reinforcements have received considerable attention during the recent past due to cost effectiveness and increased environmental awareness (Bledzki, Faruk et al. 2006, Panthapulakkal, Sain 2007). Several bio-based fibers such as wood, sisal, jute, flax, abaca, banana, oil palm, pineapple leaf, and bamboo have been studied as reinforcements for polymers (Saheb, Jog 1999). Among natural fibers (NF), wood was the most extensively and more frequently used reinforcement for polymers. However, due to expensive manufacturing process of wood fibers, inexpensive and sustainable alternatives such as agricultural waste have attracted considerable interest. Wheat straw is one of such agro-derived materials with applications in polymer composites (Hornsby, Hinrichsen et al. 1997b, Panthapulakkal, Sain 2006). In general the term natural fiber is used to designate materials (used as fiber or filler in composites) that are derived from plant tissue containing cellulose fibers on the cell wall.

Natural fiber polymer composites have found applications in construction, transportation and packaging sectors. Despite their relative low cost, improved mechanical properties, light weight, recyclability and environmentally friendliness of composites with natural fibers, poor resistance to water absorption restricts their use in many structural and out-doors applications. The poor resistance of those composites to water absorption is due to hydrophillic nature of natural fibers (Marcovich, Reboredo et al. 1998). The hydrophilicity of natural fiber also leads to incompatibility with hydrophobic polymer matrix and hence reduces the interfacial interaction between natural fiber and polymer. Several research attempts have been made in order to improve interfacial interaction between natural fibers and polymer matrices. Most of the studies in this area have focused on reducing the

hydrophilic nature of the natural fibers through various physical or chemical modifications (Arbelaiz, Fernández et al. 2005).

Incorporation of coupling agents enhanced the interfacial interaction between natural fiber and polymer matrix and also resistance for water absorption (Panthapulakkal, Sain et al. 2005). Surface modification of natural fibers with organo-silane compounds are used to improve the interfacial interaction between the fiber and polymer matrix and hence improved mechanical properties. Hybridization of the compsites formulation by using a natural fiber and another fiber with good resistance to water absorption seemed to be an interesting alternative. Glass fiber is one of the most studied materials along with natural fibers such as hemp, sisal, bamboo and oil palm fruit bunch fiber to enhance the resistance for water absorption and mechanical properties of composites (Thwe, Liao 2002)

Wheat straw is a relatively inexpensive agricultural by-product since wheat is planted primarily for food. In Ontario, wheat straw can be used for animal bedding or mushroom composting. Many farmers believe that the straw should be left in the field to improve the soil quality and reduce the use of fertilizers. Although this hypothesis could have economic impact on the supply of wheat grain or straw, there is no conclusive study at the present moment available in the literature.

Organo-clays have been known as good reinforcements or functional fillers in polymers (Ray, Okamoto 2003). When organo-clays are used as reinforcements for polymers, the composite resulted may be either a conventional microcomposite or a nanocomposite. The type of composite formed depends on the type of polymer and the method used for preparation. Nanocomposites are obtained when the layered structures of clays are exfoliated and the conventional composites are obtained when clay particles are either clumped together or poorly intercalated by the polymer.

The present study reports the experimental investigation on the preparation and characterization of wheat straw-clay-polypropylene hybrid composites. This document starts with a literature review on bio-based composites and natural fibers in Chapter 2. The materials and methods are described in Chapter 3. The results of natural fiber and composite characterization are discussed in Chapter 4. Finally the conclusions and recommendations are presented in Chapter 5.

2 LITERATURE REVIEW

2.1 BIOCOMPOSITES: DEFINITION AND APPLICATION

Composite materials are attractive because they allow combining properties in ways that are not found in the nature. These materials often have high mechanical properties with light weight structure. A typical composite consists of a discontinuous reinforcement phase embedded in a continuous matrix phase. Biocomposites are composites materials comprising one or more phase(s) derived from a biological origin (Fowler, Hughes et al. 2006). According to the ASTM (American Society of Testing and Materials) standard, bio-based materials are materials that contain "carbon based compound(s) in which the carbon comes from contemporary (non-fossil) biological sources (ASTM International 2008c). Therefore, it can be concluded that the biocomposites are materials made from renewable and sustainable agricultural or forestry biomasses stocks, including agricultural wastes, wood or other plants. The main components in renewable plant biomass are starch, lignin, cellulose and hemicellulose.

Other definitions of biocomposites are also found in the literature. Biocomposites are composites materials made from natural fiber/particles and petroleum-derived non-biodegradable polymers like PP (Polypropylene), PE (Polyethylene), and epoxies or biopolymers such as PLA (Polylactic Acid) and PHA (Polyhydroxyalkanoates) which are biodegradable in nature, as shown in Figure 2-1. It should be noted that composite materials made from biopolymers of PLA and PHA along with synthetic fibers of carbon or glass fibers are also defined as biocomposites.

Reinforcement of plastics by natural fibers began with cellulose fiber in early 18^{th} century and was later developed. Glass fiber was started being used in the early 1940s and glass fiber reinforced plastics were extensively used during the past 80 years. Resurgence of

interest of using natural fibers are seen due to environmental and health concern (Fowler, Hughes et al. 2006).

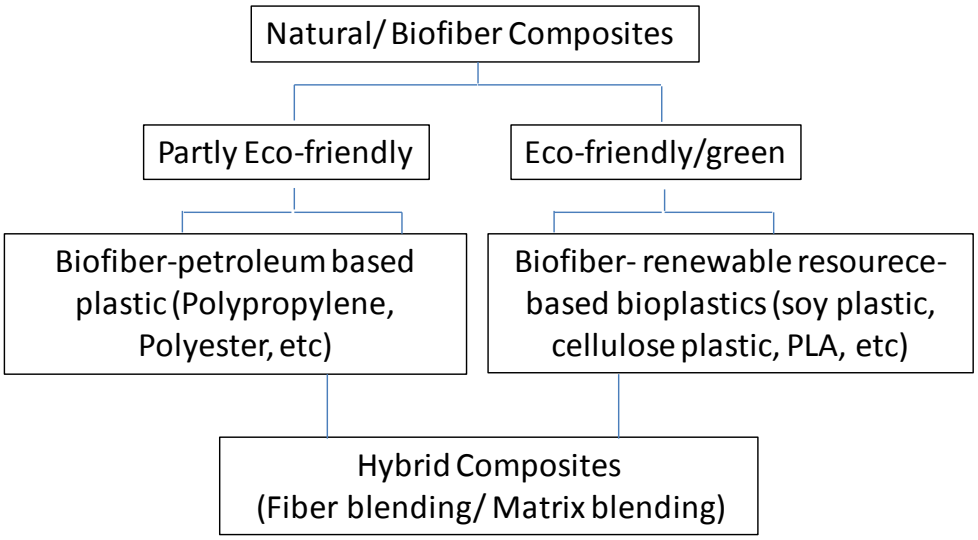

Figure 2-1 Classification of Biobased Composites (Mohanty, Misra et al. 2005)

Interest in natural fibers as fillers and reinforcement for polymeric matrices is growing fast particularly due to their comparable properties with glass fiber. It has been predicted that the demand in the North American market for natural fibers to be used in plastic industry will grow 15 % to 20 % per year in automotive application and to 50 % or more per year in building products. The European and North American markets for natural fiber reinforced plastic composites reached 685,000 tonne, valued at 775 million US$ (US Dollars) in 2002 (Mohanty, Misra et al. 2005). Further, total use of biofibres in the European automotive sector was found to be between 50,000 and 70,000 tonnes in 2005 and is predicted to rise to more than 100,000 tonnes by 2010 as shown in Figure 2-2 (Bledzki, Faruk et al. 2006). Furthermore, the number of research publications in the area of biocomposites has continuously increased as shown in Figure 2-3 (constructed based on information obtained from Scifinder research discovery tool and Scholars Portal Search research data base).

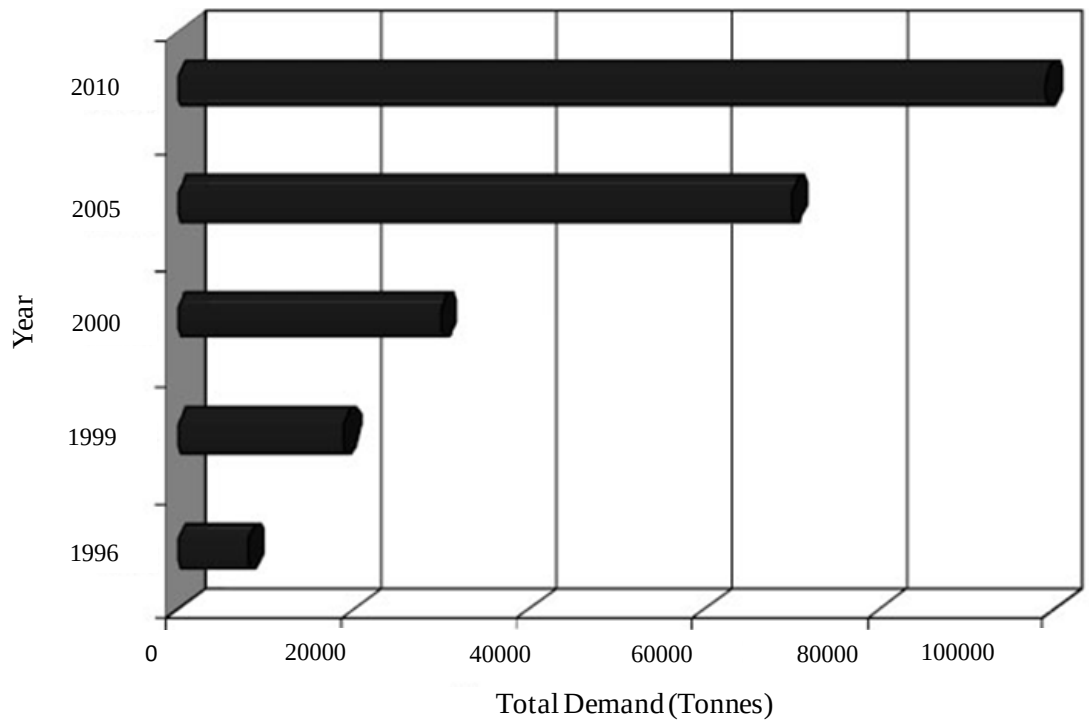

Figure 2-2 Application of Biofiber in West European Automotive Market (Bledzki, Faruk et al. 2006)

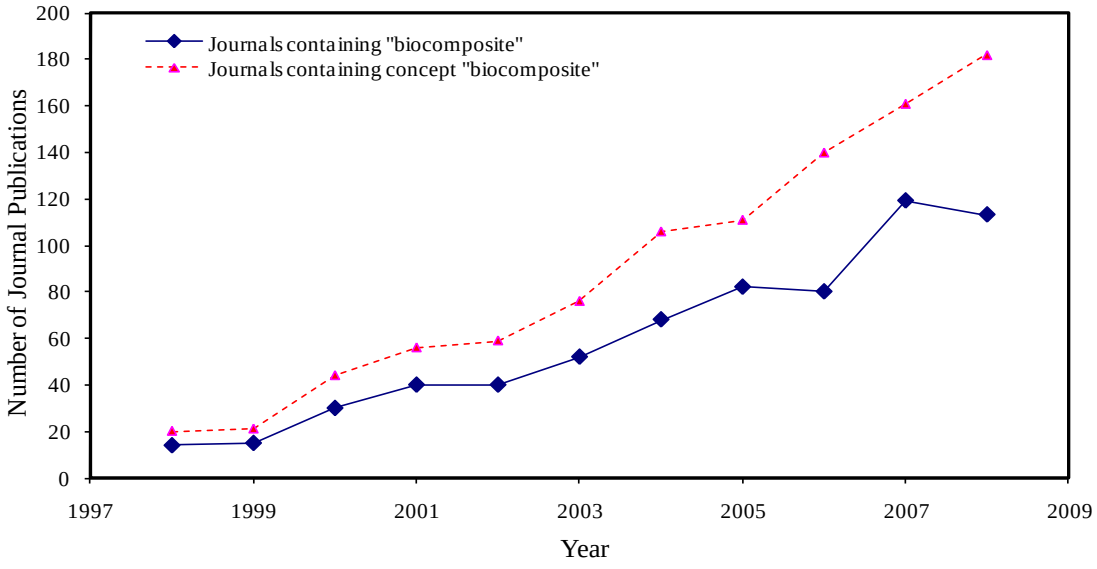

Figure 2-3 Increase in the Number of Publications in Regards to Biocomposites

In the last decade, biofiber reinforced polymer composites have been embraced by European car makers for door panels, seat backs, headliners, package trays, dashboards, and trunk liners (Bledzki, Faruk et al. 2006). Daimler is currently using abaca fiber in exterior application of floor protection for passenger cars. Mercedes S class nowadays (Figure 2-4) have 27 components made from natural fiber reinforced composites with total weight of 43 kg .Ford is using kenaf fibers in different models.

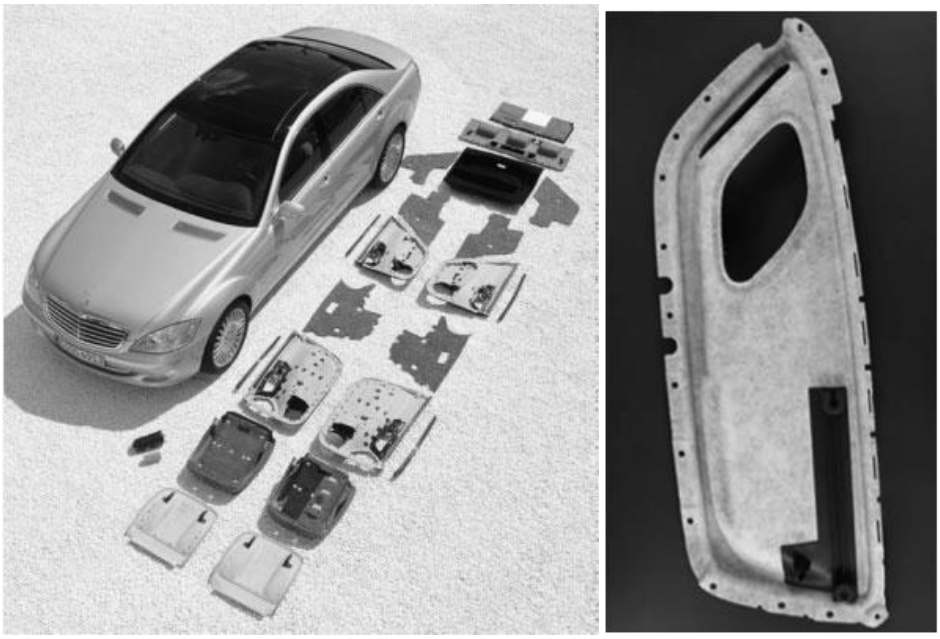

Figure 2-4 Mercedes S Class Automotive Componenst Made from Different Biofiber Reinforced Composites (left) (Bledzki, Faruk et al. 2006, Holbery, Houston 2006)

The techniques that are used to manufacture the biocomposites are based on existing plastic processing methods. They can be used with thermoplastics or thermosettings. For thermoplastic composite, the manufacturing methods include extrusion, injection moulding and compression moulding. One of the main limitations of compounding and injection moulding is that only relatively short natural fibers can be used (Fowler, Hughes et al. 2006). If longer fibers are to be used, alternative methods such as co-mingling in the form of a non-woven fleece should be implemented.

2.2 FIBERS AS REINFORCEMENT IN COMPOSITES

Most polymers especially thermoplastics do not possess high physical properties. In order to use these polymers in applications where superior properties are required, they are usually combined with various reinforcing fibers or fillers. The effect of a reinforcing material is dependent on the aspect ratio, size, size distribution, and the dispersion of the material in the polymer. High level of polymer reinforcement can be obtained from fibers made from electrical glass fibers due to their high aspect ratio (Maier, Calafut 1998). When natural fibers have high aspect ratios, they serve as reinforcement by enhancing the strength and stiffness of resulting composite (Mohanty, Misra et al. 2000). At the same time, plastic matrices cover the porous structures of the fibers and serve as adhesive to hold the fibers together. According to their origin, natural fibers can be classified into two main groups: nonwood natural fibers and wood fibers. Non wood natural fibers in turn can be classified into straw, leaf, bast, seed, and fruit origin. The best example of these natural fibers are sisal and pineapple for leaf family, flax, hemp and kenaf for bast family, cotton for seed, coconut husk for fruit family, and rice and wheat for straw family.

The major components of all these natural fibers are cellulose, hemicellulose and lignin along with minor amount of pectin, wax, and proteins. The composition of these components can vary based on factors such as age, type, and the origin of the plant. These natural fibers are hydrophilic in nature due to the existence of the surface hydroxyl groups with moisture content from 8 to 13 wt-%. Other properties of fibers such as density, strength and stiffness depend on the internal structure and the composition of the fiber components. Lignin content is believed to have influences on structure and morphology of the fibers whereas the waxy substances influence the fibers wettability and adhesion characteristics (Mohanty, Misra et al. 2000). High tensile and flexural properties of the fiber are believed to be due to cellulose content; however it should be mentioned that other parameters such as age and type of the plant can directly change these properties. Some of

the chemical composition and structural parameters of commonly used natural fibers are shown in Table 2-1 and Table 2-2.

Table 2-1 Chemical Composition and Structural Parameters of Some Natural Fibers (Mohanty, Misra et al. 2000)

Types of Fiber	Cellulose wt-%	Lignin wt-%	Hemicellulose wt-%	Pectin wt-%	Wax wt-%	Microfibrillar (deg)	Moisture Content wt-%
Bast							
Jute	61-71.5	12-13	13.6-20.4	0.2	0.5	8.0	12.6
Flax	71.0	2.2	18.6-20.6	2.3	1.7	10.0	10.0
Hemp	70.2-74.4	3.7-5.7	17.9-22.4	0.9	0.8	6.2	10.8
Ramie	68.6-76.2	0.6-0.7	13.1-16.7	1.9	0.3	7.5	8.0
Kenaf	31-39	15-19	21.5	--	--	--	--
Leaf							
Sisal	67-78	8-11	10-14.2	10.0	2.0	20.0	11.0
PALF	70-82	5-12	--	--	--	14.0	11.8
Henequen	77.6	13.1	4-8	--	--	--	--
Seed							
Cotton	82.7	--	5.7	--	0.6	--	--
Fruit							
Coir	36-43	41-45	0.15-0.25	3-4		41-45	8.0

Table 2-2 Comparative Properties of Some Natural Fibers with Manmade Fibers (Mohanty, Misra et al. 2000)

Fiber	Density (g/cm^3)	Diameter (μm)	Tensile Strength (MPa)	Young's Modulus (GPa)	Elongation at break (%)
Cotton	1.5-1.6	25-200	287-800	5.5-12.6	7-8
Jute	1.3-1.45	--	393-773	13-26.5	1.16-1.5
Flax	1.5	--	345-1100	27.6	2.7-3.2
Hemp	--	--	690.0	--	1.6
Ramie	1.5	--	400-938	61.4-128	1.2-3.8
Sisal	1.5	50-200	468-640	9.4-22	3-7
PALF	--	20-80	413-1627	34.5-82.51	1.6
Coir	1.2	100-450	131-175	4-6	15-40
E-glass	2.5	--	2000-3500	70.0	2.5
S-glass	2.5	--	4570.0	86.0	2.8
Aramid	1.4	--	3000-3150	63-67	3.3-3.7
Carbon	1.7	--	4000.0	230-240	1.4-1.8

A comparison of properties of natural fibers and synthetic fibers shows that in general, natural fibers have a lower density and lower absolute mechanical properties than synthetic fibers. However either no or small inferiority between the natural and synthetic fiber properties is observed if the comparison is made based on the values of the specific properties. Figure 2-5 illustrates a comparison made between composites from different natural fibers and composites constructed from synthetic fibers. It is clear that fibers like flax, hemp and ramie are well suited for polymer reinforcement and can compete with glass fiber.

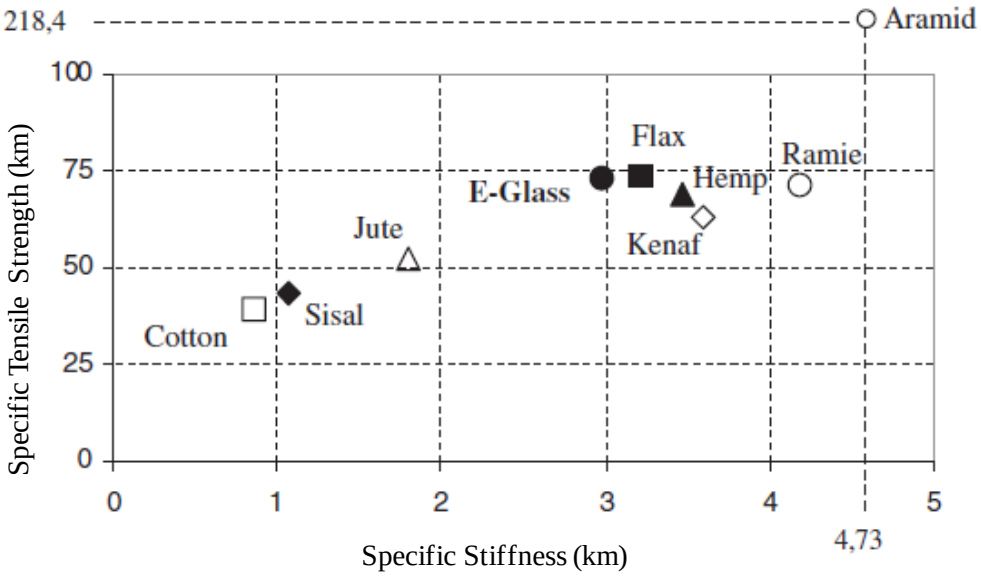

Figure 2-5 Specific Stiffness and Specific Tensile Strength for Different Natural Fibers Compared to E-Glass Fibers (Mueller, Krobjilowski 2003)

2.3 FILLERS AS REINFORCEMENT IN COMPOSITES

Fillers are defined as a variety of solid particulate materials (inorganic, organic) that may be irregular, circular, fibrous or plate-like in shape and are used in reasonably large volume loadings in plastic. Fillers have been extensively employed in plastic industries for two main reasons: (a) lowering the price and (b) modification of the properties of polymers such as hardness, viscosity or color. By selective use of fillers, certain properties are enhanced and thus reinforcement is possible. Therefore, selected fillers are currently employed to improve properties such as heat resistance, electrical characteristics, strength, and rheological properties. These fillers are called functional fillers since they facilitate the improvement of material properties. Hamerton has defined functional fillers as discontinuous additives; the form, shape, and/or surface chemistry of which have been suitably modified with the objective of improving the mechanical properties of the polymer, particularly strength (Hamerton 2006).

The most commonly used inorganic fillers are calcium carbonates, metal oxides like alumina (aluminum oxide) and titanium dioxide, clays and aluminum silicates such as China clay and mica, silica and silicates such as talc, and carbon black (organic). Calcium carbonates are the mineral fillers used in the largest amount in the plastics industry and are used to improve the processabilty and surface finish. Alumina is used where high electrical resistivity and thermal conductivities are required. Titanium dioxide and zinc oxide are both mainly used as ultra violet light absorbers. Carbon black is mainly used in tyres in large scale, but smaller quantities are also used as pigments in thermoplastics and in inks and paints. Table 2-3 is a representation of filler classification based on chemical family. It should be noted that fillers can also be classified based on their shape or aspect ratios.

Table 2-3 Various Fillers Based on Chemical Family Classification (Hamerton 2006)

Chemical Family	Examples
Inorganic	
Oxides	Glass (spheres, hollow spheres, flakes), MgO, SiO_2,Sb_2O_3, Al_2O_3
Hydroxides	$Al(OH)_3$, $Mg(OH)_2$
Salts	CaCO3, BaSO4, Phosphates
Silicates	Talc, Mica, Kalin, Wollastonite, Montmorillonite, Nanoclays, Feldspar, Asbestos
Metals	Boron, Steel
Organic	
Carbon, graphite	Carbon black, Carbon nanotubes, Graphite

Research has been directed at producing composites with the objective of substituting inorganic fillers with organic fillers obtained from sustainable sources. Wake has argued that there are two main sources of organic fillers: (a) wood waste in the form of sawdust and offcuts obtained in the fabrication of timber or (b) agricultural by-products like stems and husks (Wake 1971). Agricultural wastes such as cobs, husks, hulls are good candidates to be used as fillers in plastic industries. Further, waste products remained after processing the plants such as soy flakes, have potentials to be used as fillers in the plastic industries. Other cellulosic fillers such as nutshell flour, cellulose pulp fillers, cotton fillers and cloth yarn have also been used as fillers in plastics industry.

2.4 BIOCOMPOSITE COMPOSITION

2.4.1 THE MATRIX: POLYPROPYLENE

In the development of the biocomposites there are certain challenges related to materials and processing. The processing temperature of the materials should be high enough to allow flow of the material but low enough to avoid thermal degradation of natural fibers. Therefore, the choice of matrix to create bio-composites is limited.

A study conducted by Nova Institute in 2000 reported that both thermosets and thermoplastics were being used in automotive industry in equal measure; however, there has been a shift in using more thermoplastics attributed to the fact that thermoplastics exhibit a reduced environmental impact over thermosets at the end of the life of the products. Typical examples of thermoplastics used in composite industries are polypropylene, polyethylene, polyvinylchloride, polycarbonate and polyamide.

Polypropylene (PP) is the most commonly used one. Polypropylene is prepared by polymerization of propylene, a gaseous by-product of petroleum refining, in the presence of a catalyst under carefully controlled heat and pressure (Maier, Calafut 1998). Figure 2-6 shows molecules of polypropylene which are made by subsequent addition of many propylene monomers. A long and linear chain of carbon atom is formed with methyl groups attached to every other carbon atom.

Propylene Monomers

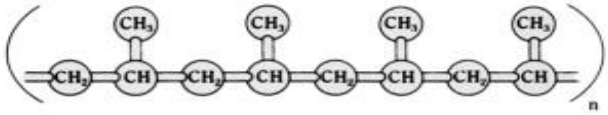

Polypropylene Chain

Figure 2-6 Molecules of Propylene and Polypropylene (Maier, Calafut 1998)

Polypropylenes which possess structural regularity are isotactic, in which the methyl groups are stationed all on one side of the main chain or syndyotactic, in which methyl groups alternate regularly on both sides of the chain (Galanti, Mantell 1965). Polypropylene can also be amorphous (atactic) at which no structural regularity is observed (random orientation of molecule). Figure 2-7 represents polypropylene molecules with different structural configuration.

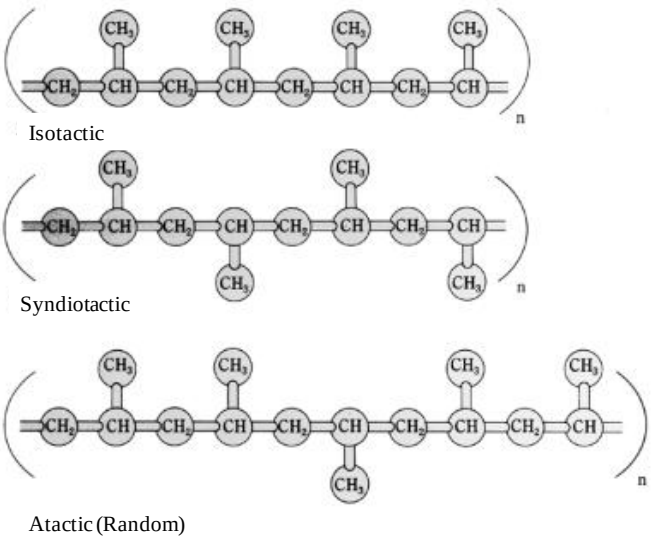

Figure 2-7 Steriochemical Configuration of Polypropylene (Maier, Calafut 1998)

The moderate cost and good properties of polypropylene contribute to a high demand for polypropylene. The density of the polypropylene (around 0.9 g/cm^3) is low compared to other polymers, for example polyethylene terephthalate (around 1.4 g/cm3), polyamiade (around 1.15 g/cm^3), and polycarbonate (around 1.2 g/cm^3). Polypropylene also excels in physical properties such as toughness, resilience, permeability, chemical and abrasion resistance along with excellent melt processabilty over other polymers. However, PP in general needs some special consideration due to its low polarity and usually coupling agents are used to bond the polymer (matrix) to the dispersed phase (fiber or filler). Based on specific applications, anti-oxidants and ultraviolet (UV) stabilizers should be used with polypropylene.

Polypropylene is used in different applications such as transportation, packaging, textiles, and appliances. In automotive polypropylene is the most commonly used polymer. In Opel Astra for example, 68 % of the thermoplastic components are composed of polypropylene, compared to 10 % Nylon (polymamide), 6 % Acrylonitrile-butadiene-styrene polymer

(ABS), 4 % polyethylene and 12 % other thermoplastics (Maier, Calafut 1998). Figure 2-8 is a representation of few applications of polypropylene in transportation and appliances.

Figure 2-8 (a) Polypropylene Door Handle on the BMW 3 Series (b) Under the Hood Application of Polypropylene (c) and (d) Application of Polypropylene in Appliances (Maier, Calafut 1998)

2.4.2 WHEAT STRAW

Agricultural by-products can alleviate the shortage of wood resources as renewable fillers in countries where there are few forestry resources (Ashori, Nourbakhsh 2009a). Agricultural by-products have a lower cellulose content compared to wood (White, Ansell 1983). Factors such as availability and renewability of these agricultural by-products are important factors which contribute to their acceptance in different industries.

Wheat straw is one of such agro-derived materials (Hornsby, Hinrichsen et al. 1997a). The price of wheat straw in 2008, in Ontario, based on an annual average was around $0.10-0.15/lb (Ng 2008). Approximately 120 million tonnes of these residues are generated by

wheat crops of which only a small percentage is being used in application such as feed stock and energy production (Alemdar, Sain 2008). Half the straw in North America is simply burned on the fields just to get rid of it or else it is buried in greater quantities than what is needed to replenish organic matter in the soil; both of these practices contribute to important environmental problems (Mohanty, Misra et al. 2005)

WHEAT STRAW PHYSICAL AND CHEMICAL STRUCTURE

The cell wall in wheat straw is a natural composite composed of cellulose microfibrils in an amorphous matrix of hemicellulose and lignin. These cellulosic microfibrils are very tough in nature and impart high mechanical properties. The amorphous lignin and hemicellulose are believed to be responsible for the physical and chemical properties such as biodegradability and sensitivity to moisture. The composition of these constituent can vary according to different types of wheat straw and the place of cultivation. Further, composition may differ in the same species for different climates, geographic places, or ages (Golbabaie 2008). Table 2-4 compared the composition of wheat and rice straws. Note that the amount of silica in rice straw is about twice the amount found in wheat straw.

Table 2-4 Chemical Composition of Straw, Percent of Dry Matter (Mohanty, Misra et al. 2005)

Straw	Cellulose	Hemicellulose	Lignin	Silica	Protein
Wheat	39	36	10	6	3.6
Rice	33	26	7	13	4.2

An extensive study on the characterization of Ontario crop fibers of wheat and soybean for use in biocomposites was done by Golbabaie (Golbabaie 2008). The author investigated fiber properties with respect to particle size distribution, morphology, chemical composition on the surface, interaction with moisture and resistance to high temperature degradation. The study discussed the morphology of mature wheat straw pointing out the multilayer structure of epidermis (outer layer), vascular bundles, parenchyma bundles, and sclerenchyma bundles. Sclerenchyma bundles were found to be distributed either in

conjunction with the vascular bundles or in separate bundles consisting exclusively of this cell type. Figure 2-9 and Figure 2-10 indicate the morphology of the wheat straw.

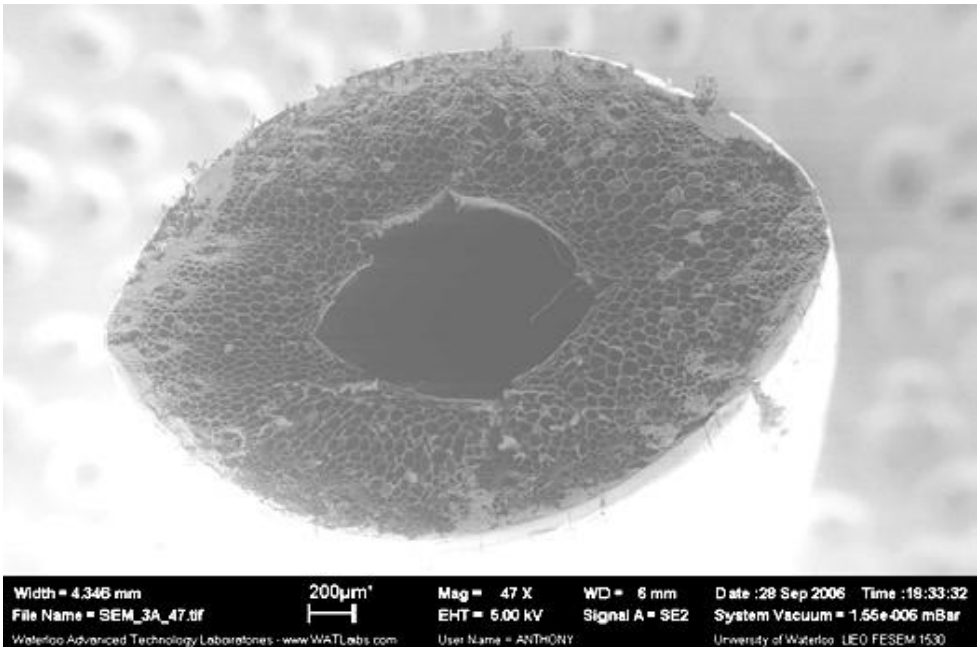

Figure 2-9 Scanning electron micrograph of Wheat Straw Cross Section (Golbabaie 2008)

The degree of lignifications appears to be highest in the hard red winter cultivar, lowest in the soft red winter cultivar, and intermediate in soft white winter cultivar. However, in all cultivars, lignification is greatest in the vascular bundles and sclerenchyma cells (Golbabaie 2008).

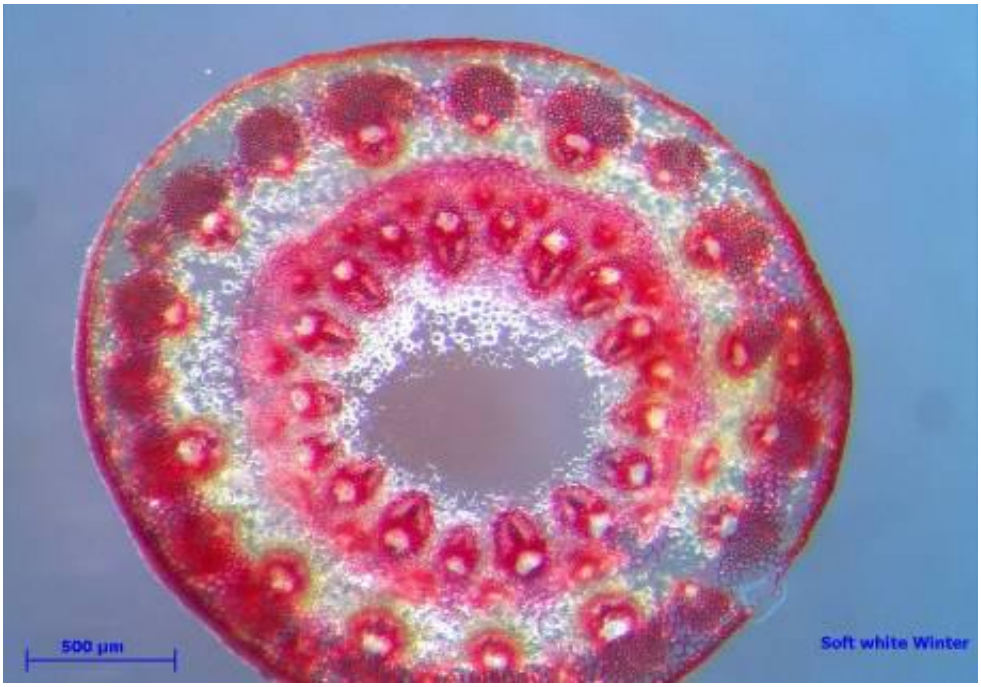

Figure 2-10 Optical Micrograph of Soft White Winter Wheat Straw Cross Section: Red Spots are Indication of Lignin Concentration in the Straw (Golbabaie 2008)

Further it was found that the properties of particles or components derived from crop plant stem material will depend on where in the stem they originate, as well as the method used to produce them. In terms of morphology after grinding, Golbabaie concluded that particles contain a layer of epidermis still attached to underlying stem tissue including sclerenchyma and parenchyma creating a multi layered structure.

The thermal stability of the particles was studied under two atmospheres; air and nitrogen. It was found that particles are more prone to thermal degradation under air atmosphere than nitrogen. It was also found that the rate of thermal degradation is very similar in both atmosphere but the onset temperature of degradation is lower in air atmosphere.

Another extensive study was done by Kruger on wheat straw polypropylene composites where mechanical and water absorption properties of composites were obtained based on

parameters such as filler content, processing at different conditions, and addition of additives (Kapustan Krüger 2007). The author observed that addition of coupling agent increased the compatibility between the hydrophilic wheat straw fillers and the hydrophobic polypropylene creating a better interfacial bonding and consequently resulting in better mechanical properties as well as better resistance to water absorption. The study further concluded that the processing conditions such as temperature and screw rotation speed can directly influence the final properties of the compression moulded biocomposite. Moreover, it was found that the particle size of the wheat straw used in the study also can dictate the physical properties.

WHEAT STRAW SURFACE MODIFICATION

The wheat straw outer surface is composed of a layer consisted of wax, silica and small amount of protein which serves to protect the outer layer of straw (epidermis) against moisture loss. This layer prevents strong bonding with polymeric matrices and makes straws not good candidates as reinforcement in resins. Recently, there have been attempts in which various pre-treatment of wheat straw using methods such as mechanical, chemical and enzyme treatments are applied to either remove these layers or completely separate the cellulose fibers from the wheat straw.

Mohanty et al. have reported on Han et al. study on the effect of ethanol-benzene (EB) extraction of straw on the properties of wheat particleboard and found that the EB treatment removes the wax from the straw surface facilitating the adherence of urea formaldehyde (UF) resins to the active hydroxyl site of cellulose (Mohanty, Misra et al. 2005). They further reported on Zhang et al. study on the effects of enzyme treatment (Mohanty, Misra et al. 2005). The strawboards in the study showed improved mechanical and dimensional stability. Alemdar et al. have obtained cellulose nanofibers from wheat straw by a chemical treatment followed by a mechanical treatment (Alemdar, Sain 2008).

2.4.3 CLAY MINERALS

The size reduction increases fillers interfacial area. Better interfacial adhesion between the filler and polymer has consequences in the final properties. Usuki et al. have reported that if the reinforcing material in the composite can be dispersed on nanometer level and can be bound to the matrix by chemical bonding, then significant improvements in the mechanical properties of the material can be achieved or unexpected new properties may be discovered (Usuki, Kojima et al. 1993)

Clays are known to be good reinforcing materials due to their platelet structure. According to International Association for the study of clays (AIPEA) clays are defined as naturally occurring materials composed of fine grained minerals, which become plastic at appropriate water content and gets harden when dried or fired (Maniar 2004). When well dispersed in the polymer matrix, a small amount of clay can dramatically change the thermal and flame properties, mechanical properties, and gas permeability of the polymer (Zhang, Jiang et al. 2006; Li, Ton-That et al. 2007; Xu, Tang et al. 2007).

CLAY PHYSICAL STRUCTURE

Clays are crystalline materials of very fine particle size with lateral dimensions ranging from 150 to less than one micron. The aspect ratio of clays is very high with values from 100 to 1500 and surface areas of 700- 800 m^2/g (Zeng 2005). The clay particles are layered materials with layer thickness of around 1 nm. The layers form stacks with a gap between them called the interlayer or gallery (Ray, Easteal 2007). Each platelet has very high strength and stiffness and can be regarded as a rigid inorganic polymer.

Clay platelets are mainly composed of two main building blocks called tetrahedral silicate layer (Figure 2-11) and octahedral gibbsite or brucite layer (Figure 2-12). The tetrahedral

layers consist of continuous sheets of silica tetrahedra which are linked together via three corners to form a hexagonal mesh and to adjacent layers via the fourth corner. The octahedral layers consist of flat layers of edge-sharing octahedra, each formally containing cations like Mg^{2+} or Al^{3+} at its center and OH^- or O^{2-} at corners.

Isomeric substitution within the layers generates negative charges that are counterbalanced by alkali and alkaline earth cations (typically Na^+, Mg^{2+}, Al^{3+}, Ca^{2+}) situated inside the galleries (Ray, Okamoto 2003). Isomorphic substitution of Al with Mg, Fe, Li in the octahedron sheets and/or Si with Al in tetrahedron sheets gives each three-sheet layer an overall negative charge, which is counterbalanced by exchangeable metal cations residing in the interlayer space, such as Na, Ca, Mg, Fe, and Li (Pavlidou, Papaspyrides 2008).

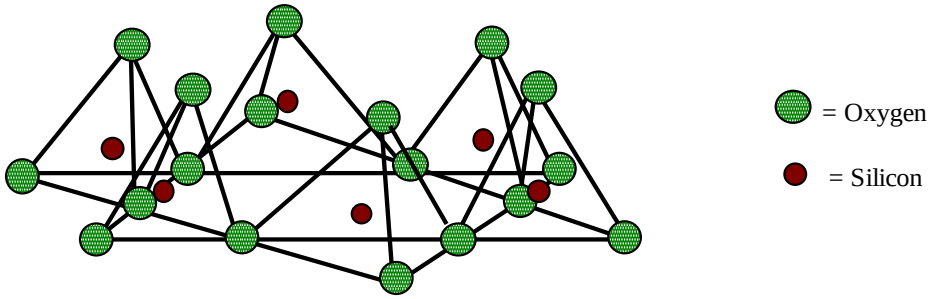

Figure 2-11 Tetrahedral Silicate Sheet Structure of Clays

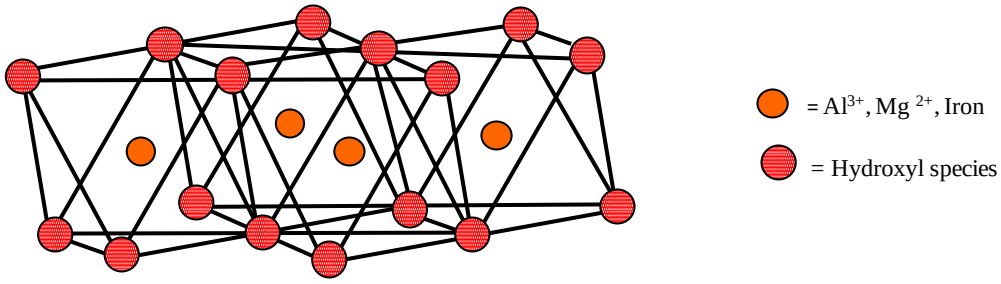

Figure 2-12 Octahedral Gibbsite or Brucite Sheet Structure of Clays

Smectite clays are one of the most commonly used clays in plastic industries. The clays which belong to the smectite family are consisted of 1 nm thick layers of aluminum octahedron sheet sandwiched in between two silicon tetrahedron sheets. These layers are held together by van der Waals and electrostatic forces.

Sodium montmorillonite (smectites) used in this study (shown in Figure 2-13) possesses high strength, high stiffness, high aspect ratio and high surface area. Moreover, it is naturally abundant and inexpensive.

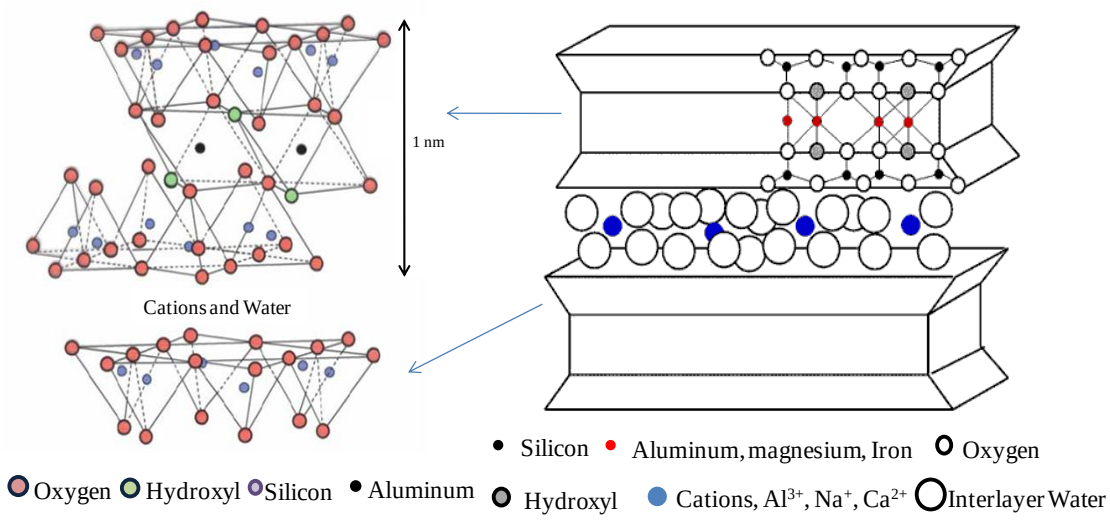

Figure 2-13 Molecular Structure of Montmorillonite Clay (Hussain 2006)

CLAY SURFACE MODIFICATION

Polymers with non-polar structure do not interact with polar fillers. Another way of looking at the surface interaction is by considering the surface of natural clays as hydrophilic, thus having a better interaction with hydrophilic polymers than with hydrophobic polymers. The incompatibility between the polymer and clay particles often causes agglomeration of clay

mineral in the polymer. Therefore, in order to create composites with good filler dispersion it is necessary that a chemical surface modification of clay be used.

Such modified clays are commonly referred to as organoclays (Zeng, Yu et al. 2005). Zhang et al. have reported that to obtain a nanocomposite the inorganic clay must be modified with some organic surfactants, usually an onium salt, which replaces the inorganic cations and makes the gallery space of the clay sufficiently organophilic to permit the entry of a monomer or polymer (Zhang, Jiang et al. 2005). These organic modifiers mostly exchange the positively charged inorganic gallery cations with bulky ions such as ammonium cations (polar head) connected to short hydrocarbons (non-polar tails) as shown in Figure 2-14.

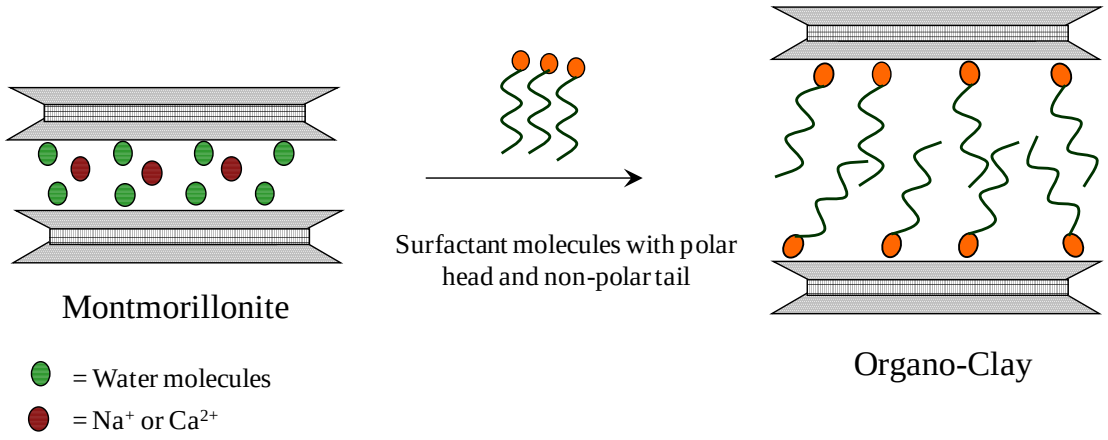

Figure 2-14 Surface Modification of Montmorillonite Clay with Organic Modifiers

2.4.4 ADDITIVES

Various additives are used in the formulation of thermoplastics and its composites. Lubricants, release agents, pigments, antioxidants, ultra violet (UV) stabilizers and dyes are added to polymeric materials to prevent undesired processing effects and to improve and modify the properties of the finished polymer (Bachert, Werner 2000).

COUPLING AGENT

The surface energy difference between the polymer and natural fibers or fillers is a constraint in creating such composites. Since the interfacial bonding between NF and the polymer dictates the composite final properties, it is necessary to use compatibilizers. Maier et al. have reported that coupling agents are bifunctional molecules in which one end reacts with polar, inorganic materials, while the other end reacts with organic, nonpolar substrates (Maier, Calafut 1998).

Generally, coupling agent such as silane, titanate, and maleic anhydride grafted to the polymers like polypropylene grafted maleic anhydride (PP-MA) and polyethylene grafted maleic anhydride (PE-MA), zirconate, and aluminates are used in polymer industries. PP-MA and PE-MA are effective coupling agents used with thermoplastics. These coupling agents are characterized by their molecular weights and the percentage of the maleic anhydride grafted to the polymer.

Panthapulakkal et al. have shown that incorporating coupling agents ethylene- (acrylic ester) -maleic anhydride and ethylene- (acrylic ester)-glycidylmethacrylate with high density polyethylene (HDPE) gave enough strength and rigidity to the composite to be used for structural materials (Panthapulakkal, Sain et al. 2005). The improved mechanical property of the composites is due to the esterification between the anhydride groups of the coupling agent and the hydroxyl groups of cellulose (Zhang 2005) as shown in Figure 2-15. Maier et al. also showed that composites made with fibers treated with maleated PP (PP-MA) had reduced water absorption compared to composites made without coupling agent (Maier, Calafut 1998).

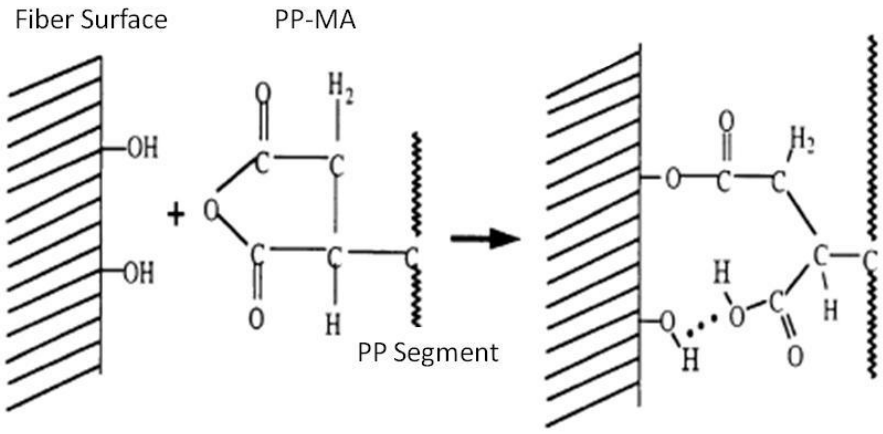

Figure 2-15 Mechanism of PP-MA Reacting with a Lignocellulosic Hydroxyl Group (Rowell 2007)

ANTI-OXIDANTS

Polymer degradation can be activated by heat, shearing forces, oxygen or chemical factors which in return result in a drastic change in mechanical, chemical, and appearance of the polymers (Feldman 2002). Figure 2-16 illustrates main causes of failure in more than 5,000 plastic articles done by Rapra Technology limited. It is apparent that close to 20 % of the failure is due to polymer degradation caused by heat, UV and chemical attack.

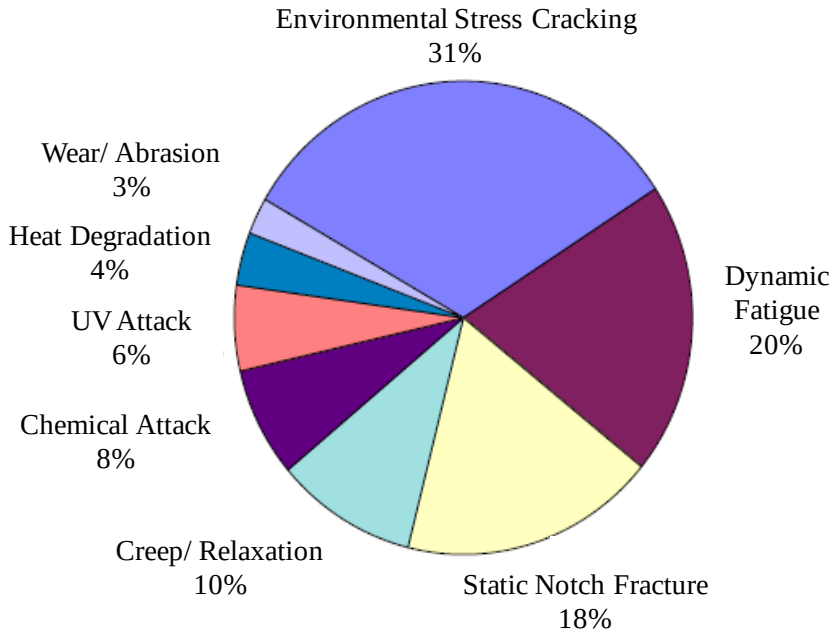

Figure 2-16 Causes of Failure in Plastic Articles (Maier, Calafut 1998)

Anti-oxidants are mainly added to polymers to prevent thermal oxidation of polymers. Anti-oxidants are classified into two main groups: (a) the chain breaking anti-oxidants (primary and secondary antioxidants) and (b) the preventive anti-oxidants.

The chain breaking anti-oxidants have two mechanisms: chain breaking donor (primary) and chain breaking absorbent (secondary). A chain breaking donor anti-oxidant is a radical scavenger and prevents the oxidation by reducing the alkylperoxide free radicals as shown in Figure 2-17. Examples of this type of anti-oxidant are phenols and arylamines which are capable of delocalization of the unpaired electron in their aromatic ring structure.

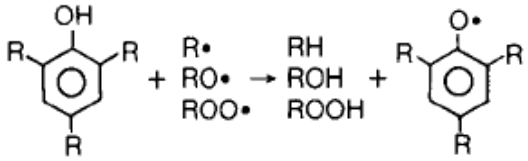

Figure 2-17 Stabilization Reaction of Primary Anti-Oxidants (Maier, Calafut 1998)

A chain breaking acceptor (secondary) on the other hand prevents the oxidation by decomposing hydroperoxides as shown in Figure 2-18. An example of these types of stabilizers is aminoxyl which has high tendency to attract hydrogen.

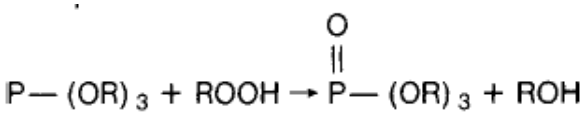

Figure 2-18 Stabilization Reaction of Secondary Anti-oxidants (Maier, Calafut 1998)

The preventive anti-oxidants are generally used to control the onset of pro-oxidant activities. Acid scavengers, metal deactivators, and light stabilizers are few examples of these anti-oxidants.

The two mostly used commercially available anti-oxidants for polyolefin are: (a) Irganox 1010, a phenolic chain breaking, H donor and (b) Irgafos 168, a phosphate chain breaking ROOH decomposer. The chemical structures of these two anti-oxidants are shown in Figure 2-19. Phosphates are secondary anti-oxidants (see Figure 2-19 (b)), that convert unstable hydroperoxides to alcohols.

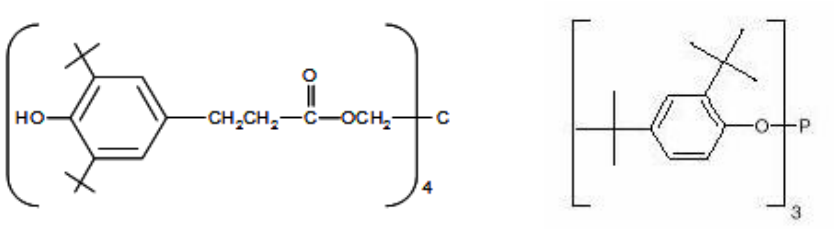

(a) (b)

Figure 2-19 Chemical Structure of the Anti-oxidants (a) Irganox 1010 and (b) Irgafos 168

2.5 COMPOSITE PROCESSING TECHNIQUES

The selection of processing techniques to manufacture a composite is critical. The final shape, cost, performance and ease of manufacturing are the essential concepts to be considered during selection. In the case of thermoplastic natural fiber composites, the distribution, dispersion, orientation and the interfacial bonding of the NF are the major drivers for the selection. Compounding is a process when the several components of the formulation are put together. Then injection moulding and compression molding are two processing techniques widely used in manufacturing thermoplastic natural fiber composites.

2.5.1 COMPOUNDING

The main purpose of compounding process is to create a pellet which is suitable for further processing and manufacturing operations. Compounding by extrusion has been used due to high levels of consistency in the pellets. Compounding process usually includes feeding the raw material followed by applied shear and heat within the extruder barrel. Due to high shear, agglomerations of raw materials are inhibited and melt mixing takes place which in return creates a homogenized molten mixture.

The extrusion process can be equipped with a de-volatilization unit to remove the moisture and other volatiles that may be present in natural fibers. At the end of the extruder there is a die followed by a pelletization step. The molten compound leaving the die can be immersed in a water bath to solidify the compounded extrudate that is then carried through the knives of the pelletizers. The final compounded material is a homogeneous mixture of all components in the formulation that can be used in manufacturing the final composite.

Rizvi et al. have reported that the inherent moisture and other volatiles, present in wood flour (WF) are released during the heating and are retained in the mix as a gaseous or liquid state until the extrudate comes out of die (Rizvi, Park et al. 2008). The entrapment of these fluids leads to deterioration of the surface quality of the extrudate.

In the compounding processes of NF, co-rotating twin screws are widely used since desired homogenous mixing is obtained. Other screw configuration like counter rotating twin screws, single screw and various types of batch mixers have also been used in NF composite production.

One drawback involved in using extruders is the loss of fiber properties due to high shear and temperatures. Rowell has concluded that regardless of the shape and size of the fiber before processing, the fiber loses length and width during extrusion (Rowell 2007). Rowell discussed that in order to use longer fibers, new technologies for mixing are needed to insure an even distribution of biomass in thermoplastic matrix. Likewise, Yam et al. reported that fiber length, and consequently the mechanical properties, are sensitive to extrusion parameters such as temperature and screw configuration (Yam, Gogoi et al. 1990).

2.5.2 INJECTION MOULDING

Injection moulding is a process for the mass production of products. It is very versatile in terms of the wall geometries and thickness. This technology is widely used in automotive and packaging applications where excellent dimensional tolerance, low cost, and short production cycles are required. The injection moulding of natural fiber composites is a new segment in industry and only 5 % of the worldwide market of plastics reinforced with natural polymers is dedicated to injection moulding process (Leao, Teixeira et al. 2008).

Reciprocating screws (shown in Figure 2-20) are currently standard for injection moulding and the shearing action of the screw accounts for 70-90 % of the heat required to melting the composite pellets that are fed to the hopper. The products made from injection moulding are believed to have some superior properties compared to those made from other processing methods such as extrusion or compression molding. Rowell has reported that injection molded composites have a surface rich in thermoplastic that surrounds and protect the biomass from coming into contact with moisture hence reducing the water absorption properties of the composites (Rowell 2007).

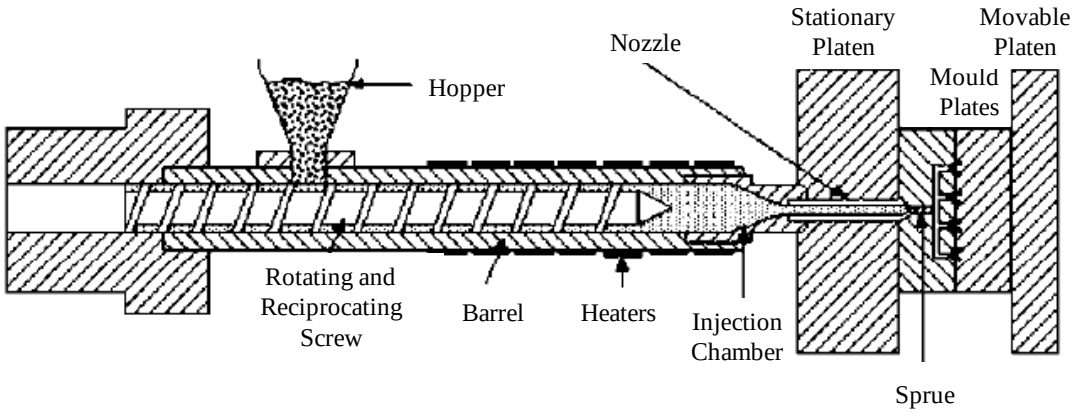

Figure 2-20 Typical Reciprocating Screw Injection Moulding Unit (Maier, Calafut 1998)

2.6 COMPOSITE PROPERTIES

2.6.1 MECHANICAL PROPERTIES

The effects of selection of processing techniques, processing conditions, and additives are reflected in the mechanical properties of composites. It is reported that mechanical performance of a fiber reinforced plastic composite primarily depends on three main factors: strength and modulus of the fiber, strength and chemical stability of the resin and effectiveness of the bond between resin and fiber (Joseph, Varghese et al. 1996). Joseph has further argued that fiber diameter, fiber length, volume fraction of fibers, alignment and packing arrangement of fibers are important factors governing properties of the composite. The aspect ratio of the fibers, the ratio of the fiber length to its width, is an indication of fiber's ability to transfer stress. Migneault et al. concluded that fibers with low aspect ratios cause stress concentration leading to lower strength (Migneault, Koubaa et al. 2008). In agreement with Migneault, Stark et al. have reported that the rigidity and strength of the composites is mainly governed by the aspect ratio of the fiber not the length of the fiber (Stark, Rowlands 2003).

On the other hand, Lee et al. concluded that increasing fiber length improved the mechanical properties of wood plastic composites (Lee, McDonald et al. 2001). Similarly, Joseph et al. have reported that the length of the fiber should be above a critical length for effective stress transfer from matrix to fiber (Joseph, Varghese et al. 1996). Further, Kruger has argued that fiber debonding from the matrix will occur when the fiber is shorter than its critical length while a high composite strength and breaking of the composites under stress are likely to be seen when the fibers length is greater than the critical length (Kapustan Krüger 2007). The fiber bonding is another point that governs the final mechanical properties of the composites. In order to have an effective stress transfer from the matrix to the fiber, a good interfacial bonding should be between the two phases. It is reported that the higher the bond strength, the lower the critical length and vice versa.

In order to obtain flexural properties of composites such as flexural strength, flexural modulus and flexural yield strength, a three point bending test based on ASTM D790-3 (ASTM International 2008d)is commonly used in which a typical stress-strain curve according to mechanical properties is obtained and used for calculation of the properties.

2.6.2 THERMAL PROPERTIES

Temperature can affect the behaviour of the natural fiber when the composite is manufactured and the physical properties of the composite containing natural fiber.

Low thermal stability of most natural fibers is an obstacle in production of biocomposites. In order to avoid degradation of the natural fibers, the processing temperature is kept below the degradation temperature of the NF (usually below 200 ^{o}C). The degradation of the natural fibers can lead to brittleness and poor mechanical integrity of thermoplastic composites. Ng has reported that the degradation of natural fibers is undesirable and the consequences include loss in mechanical strength, increased brittleness and darkening of the composite (Ng 2008).

The most common technique to investigate the thermal stability of the natural fiber is thermal gravimetric analysis (TGA). In this technique, a sample is heated up in a specified environment, usually air, nitrogen or helium, and is thermally decomposed or oxidized. The degree of decomposition is obtained from the material weight loss with comparison to a reference in accordance to the temperature. Temperature is increased from room temperature to 800 ^{o}C where all natural fiber components are decomposed. Information obtained from TGA can further be used to create a decomposition mechanism for the natural fibers.

The physical properties of the final composite are affect by temperature. These properties are associated with thermal degradation or changes in the morphology of the polymer matrix (amorphous and crystalline phase). As a consequence, temperature can affect the mechanical properties of the composites. It is usual to measure the melting and the crystallization/melting behaviour to obtain understanding on the crystallinity of the thermoplastic matrix. These properties are obtained by differential scanning calorimetry (DSC).

It is believed that the introducing natural fibers to polymer will increase the crystallinity of the composite since fibers act as nucleating agents (Ng 2008, Araujo, Waldman et al. 2008). The increase in crystallinity is explained by transcrystallinity effect provided by interaction between the fiber and the matrix. Without the presence of the fiber, the process of crystallization reaches its chain formation balance in forming perfectly aligned spherollites (Mohanty, Misra et al. 2005). Addition of fibers disturbs the balance among crystals by attracting them to the natural fibers surface and result in attractive forces between the polymer crystals and the fibers creating a transcrystalline interphase. This creates a transcrystalline interphase which in turn increases the mechanical properties of the composite.

2.6.3 PROCESSABILITY (MELT FLOW)

The melt flow property of the NF composites is an important parameter in manufacturing processes such as injection moulding and extrusion. The melt flow index (MFI) is commonly used to indicate the ease for processability. An appropriate selection of polymer with proper MFI will ensure wetting of the fiber which consequently can improve the physical properties of the final composite. The measurement of MFI is reported in standard units of g/10 min and is based on ASTM D1238 (ASTM International 2008a). MFI is inversely proportional to the viscosity of polymers and is an indication of the polymers

molecular weight. Therefore, a high MFI polymer has low viscosity and a low molecular weight. Ng has showed that that the addition of agricultural fillers results in an increase in viscosity of the composite material, indicated by MFI decrease or torque increase (Ng 2008). It should be noted that parameters such as fiber length, fiber proportion, and fiber type exert an important impact on the rheological properties of the composites as well.

2.6.4 WATER ABSORPTION PROPERTIES

It is known that the performance of natural fiber composites is dependent on factors such as property of the individual components and their interfacial compatibility. One of the main drawbacks in using natural fibers is the high affinity of the fibers towards water absorption. Arbelaiz et al. reported that amorphous cellulose and hemicellulose are mostly responsible for the high water uptake of natural fibers, since they contain numerous easy accessible hydroxyl groups which give strong hydrophilic character to natural fiber (Arbelaiz, Fernández et al. 2005). The moisture absorption by composites containing natural fibers has several adverse effects on their properties and thus affects their long-term performance (Arbelaiz, Fernández et al. 2005). Sain et al. concluded that increased moisture in NF composites not only deteriorate mechanical properties but also provides necessary conditions for biodegradation and also change in dimensions (Sain, Wang et al. 2006).

In order to use NF composites in different applications, physical and chemical treatments should be used to improve the water resistance properties. Methods such as alkalization, washing or boiling natural fibers in basic solutions of sodium or potassium hydroxide, can remove unwanted fiber components. Such treatments however should be accompanied with other chemical agents like compatibilizers in order to increase the compatibility between the polar natural fiber and the non-polar polymer.

The water absorption behaviour of composites is measured by the immersion test according to ASTM D570-98 (ASTM International 2008b). The increase in the weight of the composites according to their immersion time can identify the affinity of the composite towards moisture and further, it can be used to investigate the kinetics of water absorption.

3 MATERIALS AND METHODS

3.1 MATERIALS AND INSTRUMENTS

Table 3-1 and Table 3-2 illustrate materials and equipments involved in preparation of wheat straw-clay-polypropylene composites.

Table 3-1 List of Materials and Chemicals Used in the Study

	Type / Grade	Supplier / Manufacturer
Filler		
Clay	Cloisite® 15A, organically modified montmorillonite	Southern Clay Products Inc., USA
Wheat Straw	AC Mountain, soft white winter variety	Woodrill farms, Ontario, Canada
Materials/ Chemicals		
Antioxidants	Irganox 1010, phenolic	Ciba Inc., Canada
	Irgafos 168, phosphate	Ciba Inc., Canada
Coupling Agent	Fusabond MD-353D, maleic anhydride grafted polypropylene	DuPont, Canada
Polymer	Pro-fax 6301, homopolypropylene, MI 12	A. Schuman Inc., Ohio, USA
Solvent	Xylene $C_6H_4(CH_3)_2$, 98.5 %	VWR, Canada

Table 3-2 List of Equipments Used in the Study

Equipment	Manufacturer
Analytical balance AB304-S	Mettler Toledo
Band saw (for bars) Racer V50 V50929	Racer machinery Co.
DSC Q2000	TA Instruments
FESEM gold coating unit Desk II with Argon (inert gas)	Denton Vacuum, USA
Field Emission Scanning Electron Microscope (FESEM) Leo 1530 with EDX/OIM PV9715/69 ME	Leo Gemini AMETEK Inc., Germany
Flywheel by end cutter, 93ZP-0.6	Flying Horse, China
Grinder	IKA® Werke
Grinder KSM2 Aromatic Coffee Grinder	Braun GmbH, Germany
Injection Moulding Apparatus RR/TSMP	Ray-Ran, UK
MFI Dynisco Polymer Test D4001DE	Alpha Technologies
MiniLab Extruder Haake	Thermo Electron Corporation
MiniMat	Maple Instruments
Oven 5890A GC	Hewlett Packard
Rotary Hammer Mill Pulverizer, 5hp	Meadow Mills, USA
SDT 2960 Simultaneous DTA-TGA	TA Instruments, Canada
Stereo Microscope MZ6, equipped with transmitted-light base TL BFD and digital camera	Leica Microsystems GmbH, Germany
Testing Sieve Shaker RO-TAP, 1/4 H.P	W.S.Tyler Inc.
TGA Q500	TA Instruments, Canada
Tzero Hermetic low-mass pan and lid (DSC)	TA Instruments, Canada
U.S standard testing sieves	VWR, Canada
XRD Instrument, 30 kV, 30 mA, with Cu Kα radiation	Bruker Instrument Inc, Canada.

3.2 GRINDING

In order to prepare wheat straw for compounding process, bales of wheat straw were taken to Omtec Inc. located in Mississauga for grinding. Prior to grinding all bales were examined for any obvious contamination due to winter storage. Straws were first fed to a flywheel by end cutter to reduce their sizes approximately to 3-5 cm. The cut wheat straw was then fed to a directly coupled, rotary hammer mill for grinding. Grinding was performed at 60 min intervals followed by 15-20 min cooling cycles taking approximately a week to grind 16 bales of wheat straw each weighing close to 23 kg. The ground wheat straw was screened through 2 sieves with mesh sizes of 16 (0.5 mm opening) and 35 (1.19 mm opening) giving three ground wheat straw (gWS) batches named as Large: Size<Mesh16, Mid: Mesh16<Size<Mesh35, and Fine>Mesh35. The chopping and grinding units are two separate units provided by different manufacturers. OMtec Engineering has developed a system to connect the two systems.

3.3 PARTICLE SCREENING

Further screening was performed on the three batches of ground wheat straw obtained from grinding process. Each batch (Large, Mid, Fine) was screened through five 8 "diameter sieves with mesh sizes according to Table 3-3 . The sieving was performed by a Tyler RO-Tap Sieve Shaker (old style) driven by 1/4 H.P. motor operating at 1750 rpm.

Table 3-3 Mesh Number and Opening of Selected Sieves

Mesh Number	Opening (mm)	Opening (in)
18	1.00	0.0394
25	0.71	0.0278
35	0.50	0.0197
60	0.25	0.0098
100	0.15	0.0059

3.4 COMPOUNDING

Wheat straw-clay-polypropylene composites (WSCPPC) were prepared by melt blending method using a Haake Minilab Micro-compounder (Minilab) from Thermo Electron Corporation, a co-rotating conical twin-screw extruder (see Figure 3-1). The operating conditions of the extruder were set at 190 ^{o}C and 40 rpm. All the components of composite - wheat straw, polypropylene, clay, coupling agent and antioxidants - were hand blended to get a uniform mixture prior to feeding the extruder. As the mixture of components passed through the screws of twin-screw extruder, melting and mixing took place and a homogenized extrudate exited through the flush orifice. The extrudate was cut into smaller pieces proper for the next processing step by scissors (see Figure 3-2).

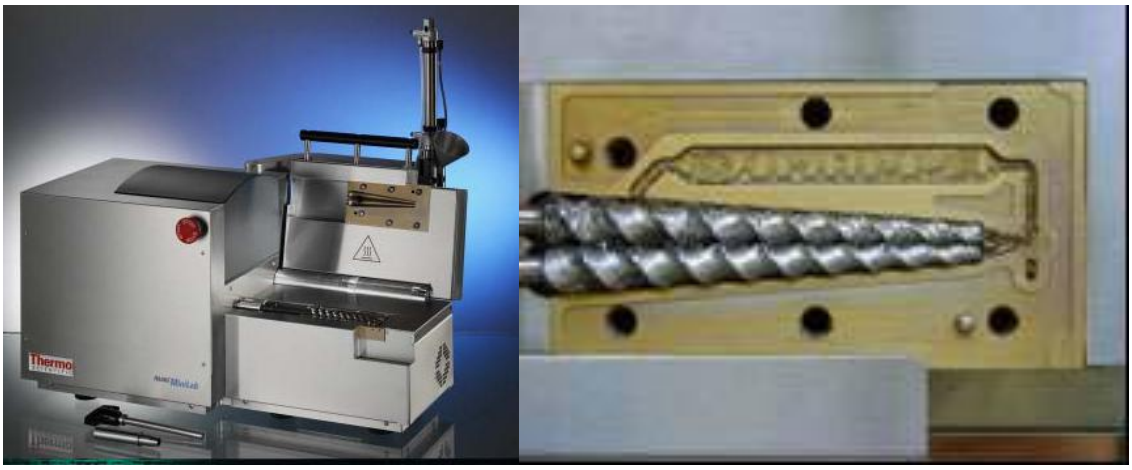

Figure 3-1 Haake Minilab Micro-Compounder Used for Compounding WSCPPCs ((left) and its Conical Screws (right)

Figure 3-2 WSCPP Pellets Obtained From Compounding Process by Minilab

Large Scale compounding was carried out with the assistance of our industrial partner A.Schulman Inc. in Akron, Ohio. Three sizes of wheat straw and a previously made polymer master batch provided by A.Schulman Inc. were fed into a twin screw 25 mm extruder. Wheat straw and the polymer batch were both fed separately by agitating feeders placed on top of the extruder inlet. The extruder was set at 190 ^{o}C and 200 rpm. The extrudate was sent through a water bath placed right after the flush orifice and then to a pelletizer to produce pellets with sizes around 0.5 to 1 cm.

3.5 INJECTION MOULDING

The resulting WSCPPCs pellets were then injection moulded using a Ray-Ran Laboratory injection molding machine (RR/TSMP) to get test bars according to ASTM standards (ASTM International 2008b) with dimensions according to Table 3-4. The injection molding was performed keeping the barrel temperature at 190 ^{o}C and mold tool temperature at 50 ^{o}C with injection periods of 15 sec at 100 psi. A measured amount of pellets were transferred to the barrel and were compressed few times by a pneumatic piston

connected to high pressure air to reduce the bulk. Once the composite was fully plasticized, indicated by a fall from the die orifice, a small amount of polymer was purged to the atmosphere, then such excess was cut and injection quickly took place. The barrel was recharged with WSCPPCs pellets after each injection. Once cooled to room temperature, the test sample bars were removed from the mold (Figure 3-3) and were inspected for voids and other possible defects. To erase the thermal history of the WSCPPC test bars, injection molded specimens were annealed in an Hewlett Packard 5890A GC air circulating oven at 150 ^{o}C for 10 min and then cooled down to room temperature at a rate of 10 ^{o}C/min.

Table 3-4 Dimension of Test Bars for Property Testing

	Water Absorption	Flexural Properties
Length (mm)	63.5 ± 0.2	31.8 ± 0.2
Width (mm)	12.7± 0.2	12.7± 0.2
Depth (mm)	3.3 ± 0.2	3.3 ± 0.2

Figure 3-3 WSCPP Test Sample Bars Obtained From Injection Molding Process

3.6 CHARACTERIZATION METHODS

3.6.1 MORPHOLOGY

The morphology of ground wheat straw and WSCPPCs was analyzed by using scanning electron microcosy (SEM) with the LEO 1530 microscope equipped with Gemini field emission column (FESEM) and EDX/OIM PV9715/69 ME. The composite samples for SEM analysis were prepared by freeze breaking after cooling the sample in liquid nitrogen. A small piece of freeze broken sample was fixed to an aluminum stub using double-sided conductive tape. Prior to loading the samples for SEM analysis, the freeze broken part of the samples were sputter coated with gold with approximate thickness of 10 nm.

3.6.2 CHEMICAL COMPOSITION ANALYSIS

Chemical composition analysis of Acid Detergent Fiber (ADF), Neutral Detergent Fiber (NDF), and lignin content were performed on ground wheat straws at AgriFood Laboratories located in Guelph, Ontario. Tests consisted of soaking the wheat straw in either neutral or acid detergents followed by proper washing, filtering, and drying (Garcia, Infante et al. 1997). These methods are based on single extraction of soluble components. The residue left from the filtration process is then analyzed and correlated to straw components.

3.6.3 PARTICLE SIZE ANALYSIS

The wheat straw particles were spread on a glass slide in a way that none would over lap or touch each other. The images were taken by stereomicroscope Leica MZ6 (63x magnification) equipped with transmitted-light base TL BFD and digital camera. The image analysis was initially performed by using the ImajeJ Java-based image processing

program. The software converts and stacks 16-bit and 32-bit images to 8-bits by linearly scaling them from minimum-maximum to 0-255 (0 being white and 255 black). The dimension of the fibers/ particles was obtained by drawing the best fitting ellipse around the particle (done by ImageJ). The length of the major and minor axis of the drawn ellipse corresponds to the length and the width of the items of interest as shown in Figure 3-4. This methodology does not account for the 3 dimensional nature of the particle, thus assuming that 2 dimensions are sufficient to describe each particle in the population. The image processing program also counts the number of objects by scanning each image. For each ground WS size, approximately 200 to 300 particles were analyzed.

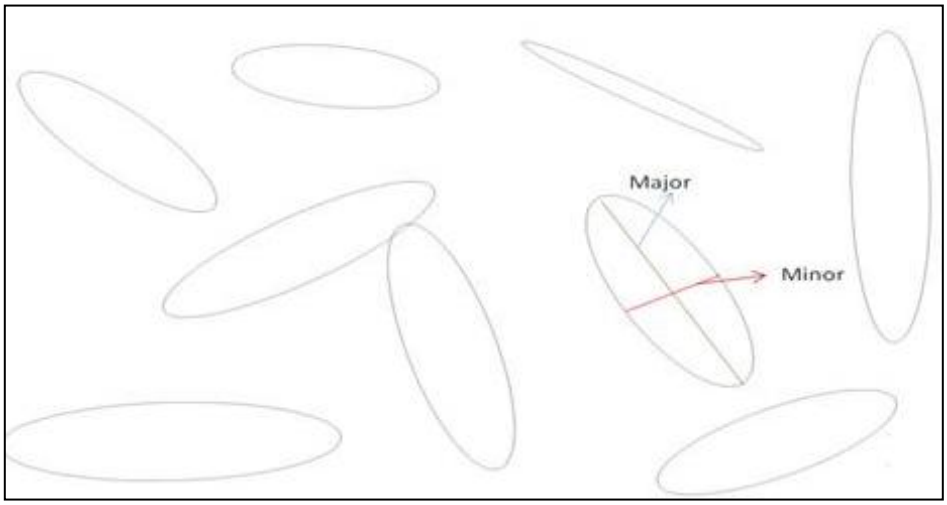

Figure 3-4 Best Fitting Ellipses Drawn by ImageJ Data Analyzer

3.6.4 PARTICLE DENSITY

The density of three batches of ground wheat straw was measure by a gas pycnometer at Porous Material Inc. located in Ithaca, New York. The measurements were obtained by using Boyle's law which is used in order to measure the changes in the volume and pressure of the initial state of a fixed quantity of gas by introducing a minor change at the same temperature (Richards, Bouazza 2007). A premeasured amount of the ground wheat straw was introduced to a gas pycnometer and the change of the pressure was measured.

The measured pressure then is used to obtain the volume of the particles. The density of the particles was simply found by dividing the volume of the particles by their weight. For each measurement, 10 gas pycnometry analysis were performed and the results were averaged.

3.6.5 PARTICLE EXTRACTION

The extruded samples of WSCPPCs were subjected to solvent extraction in boiling xylene to separate particles from the matrix and other components in the formulation. Solvent extraction process was carried out based on ASTM D2765 with a minor difference of using a Whatman 41 ashless filter paper. A known amount of composites was placed in the filter paper formed into a packet and was exposed to reflux xylene in a round-bottomed flask fitted with condenser. The extraction process was run for 24 hours, during which solvent was replaced by new xylene. At the end of 24 hours, the filter paper envelope was placed in a fume hood for another 24 hours to dry. The extracted samples of particles were analyzed for particle size.

3.6.6 THERMAL PROPERTIES

THERMAL GRAVIMETRIC ANALYSIS (TGA)

TGA was determined in a Q500 TGA controlled by a TA processor connected to a computer for data analysis. The experimental conditions were as follows: Initial temperature 40 ^{o}C; Final temperature 800 ^{o}C; heating rate of 10 ^{o}C min^{-1}; sample size close to 5 mg; under nitrogen at a flow rate of 15 ml/min. Calibration for the temperature was done based on the Curie point of Nickel (temperature at which Nickel losses its magnetic properties) and the room temperature, recorded by a very accurate thermometer. At Curie point, a reduction in weight is measured by the instrument and the temperature is corrected for the deviation between the true Curie temperature and the recorded temperature. No base

line correction was necessary since the instrument measures the tare weight of the samples. The degree of material weight loss in accordance to the temperature was measured by Universal Analysis 2000 (TA Instruments, 4.5A Build 4.5.0.5).

DIFFERENTIAL SCANNING CALORIMETRY (DSC)

DSC was determined in a Q2000 DSC controlled by a TA processor connected to a computer for data analysis. The experimental conditions were as follows: Cycle 1: Initial temperature 40 ^{o}C; Final temperature 200 ^{o}C; heating rate of 10 ^{o}C min^{-1}; sample size close to 5 mg; under nitrogen at a flow rate of 15 ml/min, Cycle 2: Initial temperature 200 ^{o}C; Final temperature 40 ^{o}C; cooling rate of 10 ^{o}C min^{-1}; under nitrogen, Cycle 3: Initial temperature 40 ^{o}C; Final temperature 200 ^{o}C; heating rate of 10 ^{o}C min^{-1}. Cycle 1 was used to remove the thermal history of the WSCPPCs. Cycle 2 and 3 were used to evaluate the thermal properties of the material. DSC calibration was done with the TzeroTM method. The calibration experiment was run firstly without any samples or pans in order to obtain a baseline followed by a calibration experiment involving a 96.21 mg sapphire disk (without pans) on the sample and reference positions; the temperature range was 0 °C to 400 °C under nitrogen. TzeroTM Technology provides an additional thermocouple sensor and an automated calibration routine that allows all the thermal characteristics of the cell (those affecting the ordinate baseline, and those affecting the temperature scale) to be addressed. The DSC graphs were analyzed by Universal Analysis 2000 (TA Instruments, 4.5A Build 4.5.0.5).

3.6.7 WATER ABSORPTION

Water absorption test was conducted based on ASTM D570-2001. In order to obtain the conditioned weight of the composite, three injected molded specimens were placed in an air circulating oven at 105 ^{o}C-108 ^{o}C for approximately one hour. Then the specimens were

placed in a desiccator (8-10 wt-% RH) and weighed to 4 decimal places by a Mettler Toledo analytical balance (AB304-S). The recorded weight is called the conditioned weight of the test sample bars.. Water absorption values (wet weight) were recorded at first 4, 12, and 24 hrs of immersion, then every 24 hours for a week, and then every week thereafter for a total of 22 weeks. The amount of water absorbed by each composite was calculated by the following equation taken from ASTM D-570-98:

$$Increase\ In\ Weight\ (Wt-\%) = \frac{Wet\ Weight - Conditioned\ Weight}{Conditioned\ Weight} \times 100 \qquad \text{Equation 3-1}$$

Knowledge of diffusivity coefficient and transport properties is critical for predicting the water absorption behavior of the composite and their physical and mechanical properties. Equation 3-2 was used to model the diffusion behaviour of the composite specimens.

$$\frac{M_t}{M_m} = kt^n \qquad \text{Equation 3-2}$$

Where M_t (wt-%) is the amount of moisture in the sample at time t, M_m is the equilibrium moisture (wt-%); k and n are both kinetic parameters. Constant n is a representation of the behavior of the diffusion process (Case I or Fickian, Case II, and Non Fickian) and k represents the interaction between the composite and water (Espert, Vilaplana et al. 2004). Natural logarithm of Equation 3-2 was taken in order to calculate the values of n and k and Equation 3-3 was obtained:

$$log\left(\frac{M_t}{M_m}\right) = log(k) + n\ log(t) \qquad \text{Equation 3-3}$$

Moreover, D, diffusivity parameter of the composites which is a representation of how fast the water molecules enter the composite material was calculated by Equation 3-4. Slope taken from the linear part of the water absorption graphs were used to calculate diffusivity.

$$\frac{M_t}{M_m} = \frac{4}{h}\left(\frac{D}{\pi}\right)^{\frac{1}{2}} t^{\frac{1}{2}} \qquad \text{Equation 3-4}$$

3.6.8 MELT FLOW INDEX (MFI)

Flow properties of the WSCPPs were measured by a Dynisco D4001DE MFI tester at 230 ^{o}C and 2.16 kg load through an 8 mm die based on ASTM 1238 (method A). Approximately 5 g of the composite pellets obtained from extrusion process were placed inside the heated barrel for 360 seconds to melt after which 4 to 5 samples were cut and collected for the MFI measurement.

3.6.9 X-RAY DIFFRACTION (XRD)

The XRD analysis of samples was recorded on Bruker D8 FOCUS instrument operating at 30 kV and 30 mA with a Cu Kα radiation source (λ= 1.5404Å). The XRD patterns were recorded between the 2θ values 2.0-30 with step size of 0.05. The test samples were prepared by hot pressing the composite pellets obtained from compounding process at 180 ^{o}C for 2 minutes at 3000 psi followed by cooling at room temperature. In terms of the clay, the powder was place inside the XRD sample holders for the measurement. The XRD patterns were used to measure the variation of basal spacing of clay from the Braggs`s equation according to Equation 3-5.

$$d = \frac{\lambda}{2\sin\theta} \qquad \text{Equation 3-5}$$

3.6.10 FLEXURAL PROPERTIES

Flexural properties of the samples were investigated on sample specimens prepared by injection molding by a MiniMat2000 miniature material tester from Maple Instrument equipped with a load cell of 1000 N. Conditioning the sample and analysis procedure were as per ASTM D790-03 with a minor change in the dimensions of the test specimens due to equipment constraints. The injection moulded samples were cut in halves using a band saw

(Racer V50 V50929aw, from Racer Machinery Co). The analysis was done based on a fixture span to material thickness ratio of 6:1 (span: 18 mm, sample thickness: 3mm).

3.6.11 MIXTURE DESIGN AND OPTIMIZATION

Design-Expert (v.7) software was used to generate the design points of the experimental mixture design of wheat straw-polypropylene composite. The generated design points was further simplified based on considerations such as running minimum design points and linear blending properties of wheat straw and polypropylene. The software was also used to run statistical analysis to get the fittest model. The software provides complete analysis tool for mixture design including analysis of variance, model diagnostics, generating graphs of 3D response surface, contour plot and multi-objective optimization tools.

4 RESULTS AND DISCUSSION

4.1 CHARACTERIZATION OF GROUND WHEAT STRAW

4.1.1 YIELD OF WHEAT STRAW BATCHES AND FRACTIONS

The output of the grinding process was evaluated by measuring the yield of wheat straw particles for a given range of particle size. The yield was measured at the weight percentage (wt-%) based on the amount of wheat straw before grinding (bale) and after grinding for a given batch. In order to identify the weight percentages of the three ground wheat straw (gWS) batches and gWS fractions, sieves were weighed before and after the screening process. The weight percentages of each fraction per gWS batches and per WS bales are summarized in Table 4-1. Averages were calculated based on three measurements.

Table 4-1 Mass Distribution Recovery of Ground Wheat Straw Fractions

Large							**Total wt -%**
	<18	18-25	25-35	35-60	60-100	>100	
Wt-% / Batch	45.3	40.2	12.	1.53	0.18	0.42	
Wt-% / WS Bale	13.13	11.66	3.59	0.44	0.05	0.12	28.99
Mid							
	<18	18-25	25-35	35-60	60-100	>100	
Wt-% / Batch	1.02	18.86	39.41	35.29	4.82	0.59	
Wt-% / WS Bale	0.45	8.3	17.34	15.53	2.12	0.26	44.00
Fine							
	<18	18-25	25-35	35-60	60-100	>100	
Wt-% / Batch	0.1	0.89	4.4	43.09	33.43	18.07	
Wt-% / WS Bale	0.03	0.24	1.19	11.64	9.03	4.88	27.01

It was found that 44 wt-% of the gWS obtained was in the Mid size range and the rest was evenly distributed between the Fine and Large batches. It was found that close to 98 wt-% of the wheat straw particles in the Large batch were mainly from fractions separated by

mesh sizes of 35 and below. Similarly, approximately 94 wt-% of gWS from Mid and Fine batches were screened by mesh sizes of 18 to 60 and 35 to above100 respectively. This implied that 95 wt-% of the ground wheat straw obtained from the grinding system were from fractions of (a) Large<35, (b) 18<Mid<60, and (c) 35<Fine<100.

4.1.2 PARTICLE DENSITY

Particle density of the Large, Mid, and Fine batches of gWS were measured by a gas pycnometer and results obtained showed good reproducibility. The density values were found to be between 1.3 g /cm^3 and 1.6 g /cm^3 as indicated in Table. These values were found to be in the density range reported in the literature (Hornsby, Hinrichsen et al. 1997b, Thermo Haake 2002).

Table 4-2 Measured Particle Density of gWS Batches by Gas Pycnometry Performed at Porous Material Inc.

	gWS Batch ID		
	Large	Mid	Fine
Average Density (g/cm3) (Based on 10 Measurements)	1.653±0.015	1.431±0.028	1.425±0.061

4.1.3 PARTICLE SIZE ANALYSIS

PARTICLE SIZE ANALYSIS ON A BLEND BATCH

Particle size analysis was performed on a blended batch of gWS (combination of all three sizes) to obtain total gWS particle length, width, and aspect ratio distributions. It should be noted that the mixing was based on a random selection of 44 wt-% gWS from Mid size batch and equal portions of Large and Fine batches (28 wt-%) to simulate the product of the

actual grinding process. Results for particle's length, width, and aspect ratio distributions are shown in Figure 4-1 (a), (b), and (c) respectively.

It was found that particle's length data ranges between 50 and 7,000 µm with close to 70 % of the particles having a length value between 1,000 to 4,000 µm. Average length value was found to be 2,000 µm. The width distribution was found to be limited to 50 and 2,000 µm with almost 85 % of the particles with width values between 100 and 1,000 µm. This resulted in an average width value of 506 µm. Similarly, Hornsby et al. found that ground wheat straw obtained by hammer milling had particle's mean length values of 2,300 µm (Hornsby, Hinrichsen et al. 1997b)

On the other hand, Mohanty found mean length values of 1,400 µm and 2,000 µm and mean width values of 15 µm and 22 µm for wheat straw and hemp after grinding by a Wiley mill (Mohanty, Misra et al. 2005). This indicated that average length of wheat straw particles will be lower if a hammer mill is used.

The aspect ratio (AR) of the gWS, the ratio of the length of the particles to its width, was found to be limited between 1 and 40. About 65 % of the particles have aspect ratios below 5 indicating that most of the ground wheat straws obtained by hammer milling were in the form of particles rather than fibers. Fowler et al. have reported that in certain processes, such as chemical or thermo-mechanical pulping, much of the aspect ratio can be maintained; however, grinding by hammer milling reduces the fibers to a particulate form, with low aspect ratio (Fowler, Hughes et al. 2006).

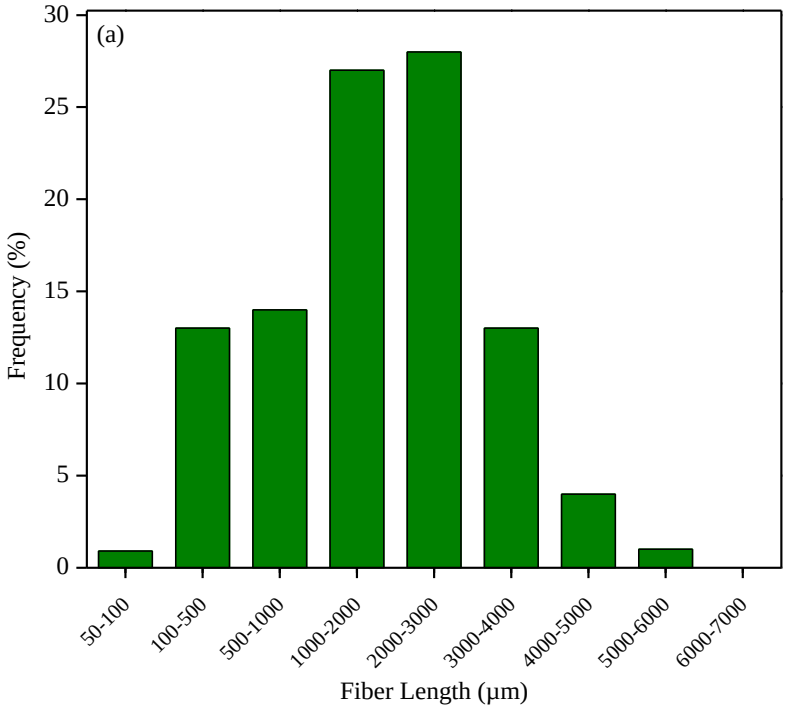
(a)
Frequency (%)
0
5
10
15
20
25
30
50-100
100-500
500-1000
1000-2000
2000-3000
3000-4000
4000-5000
5000-6000
6000-7000
Fiber Length (µm)

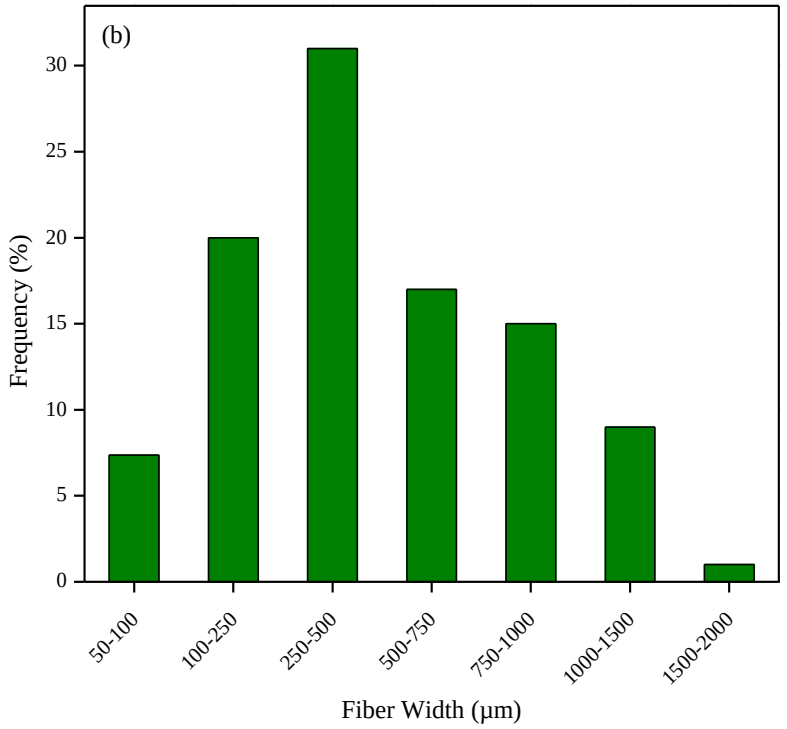
(b)
Frequency (%)
0
5
10
15
20
25
30
50-100
100-250
250-500
500-750
750-1000
1000-1500
1500-2000
Fiber Width (µm)

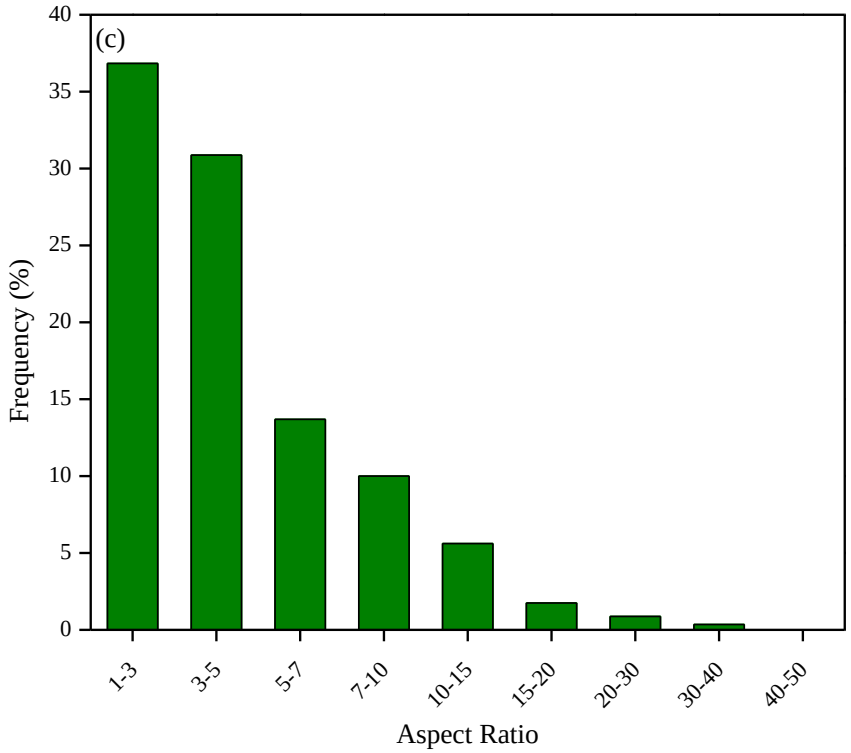

Figure 4-1 Blended Batch of Ground Wheat Straw (a) Particle Length Distribution (b) Particle Width Distribution (c) Particle Aspect Ratio Distribution

In order to have a better visual presentation of the length and aspect ratio distributions, a three dimensional diagram was constructed using Statistica software and is shown in Figure 4-2. Based on information from Figure 4-2 it is observed that majority of the particles are between 1,000 and 4,000 µm with aspect ratio between 1 and 10.

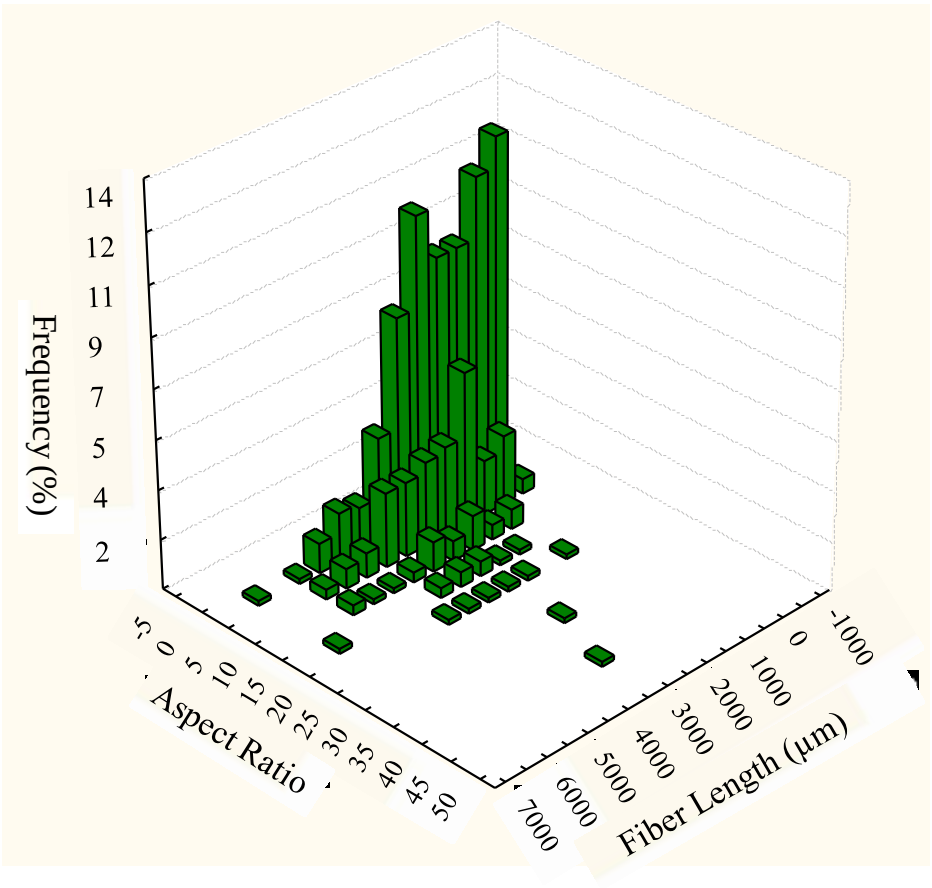

Figure 4-2 Blended Batch of Ground Wheat Straw: Aspect Ratio vs. Fiber Length vs. Frequency

PARTICLE SIZE ANALYSIS ON gWS FRACTIONS

Graphs for length distribution of fractions obtained from Large, Mid, and Fine batches are presented in Figure 4-3. It was found that particles that were collected by sieving through mesh numbers of 18, 25 and 35 as well as particles that passed through mesh size 100 all had very similar particle length distribution as shown in Figure 4-3 (a), (b), (c), and (f). The size distributions of particles found in these fractions were all similar to each other, however; the frequencies were found to be different.

The main difference between the three starting gWS batches (Large, Mid size, Fine size) was found mainly to be due to the differences in the particle lengths of fractions collected by sieves wish mesh sizes of 35 and 60 corresponding to fractions of 35-60 and 60-100. It was found that gWS particles in the 35-60 fraction of Large batch have their length distributions between 1,000 and 5,000 µm and between 1,500 to 6,000 µm for 60-100 fraction. Particle length for the Mid and Fine did not show any difference in these two fractions and stayed mainly between 1,000 and 4,000 µm and 100 to 3,000 µm for Mid and Fine batches respectively (Figure 4-3 (d) and (e)).

In order to identify the effects of length distribution difference on the aspect ratio of the fractions, aspect ratio distributions were evaluated and are shown in Figure 4-4 (a)-(f).

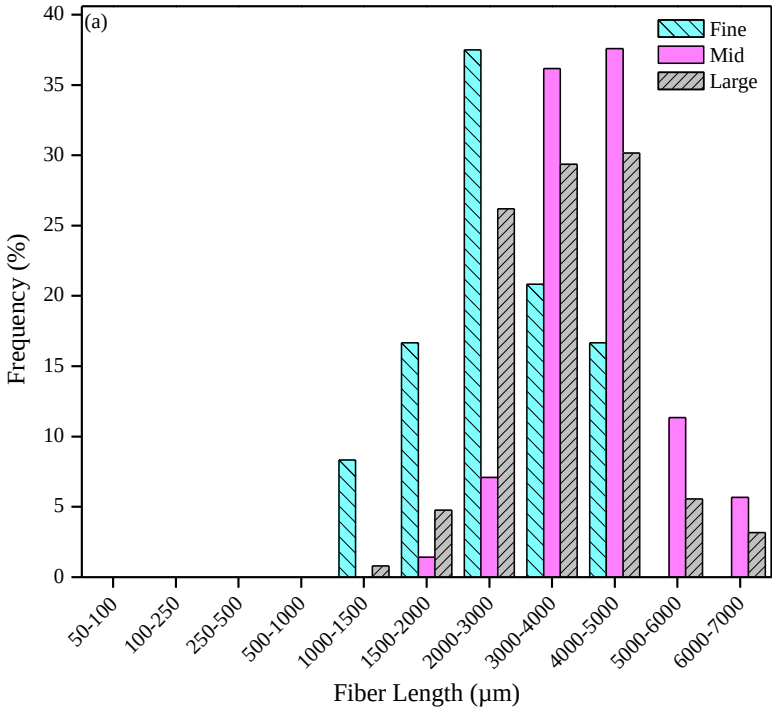
(a)
Fine
Mid
Large
Frequency (%)
0
5
10
15
20
25
30
35
40
50-100
100-250
250-500
500-1000
1000-1500
1500-2000
2000-3000
3000-4000
4000-5000
5000-6000
6000-7000
Fiber Length (µm)

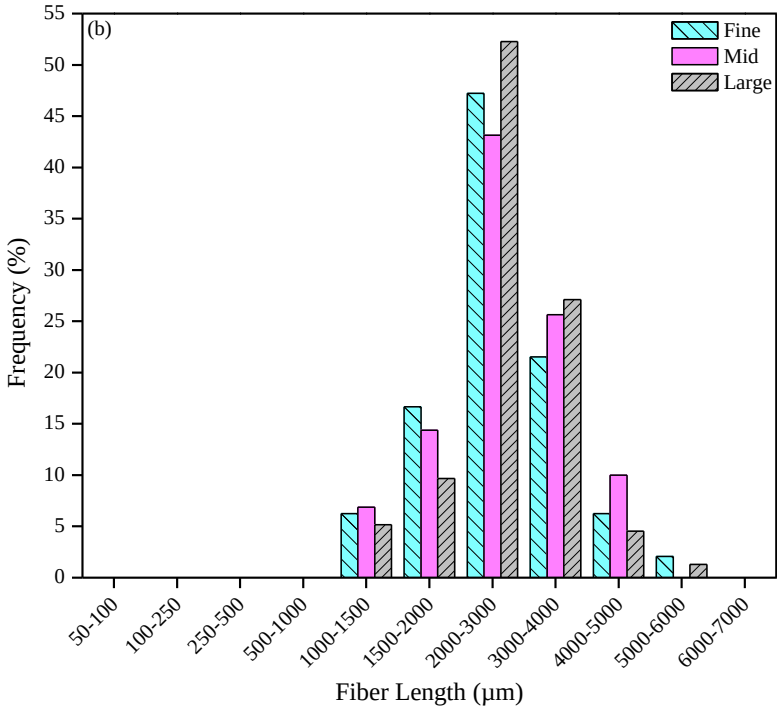
(b)
Fine
Mid
Large
Frequency (%)
0
5
10
15
20
25
30
35
40
45
50
55
50-100
100-250
250-500
500-1000
1000-1500
1500-2000
2000-3000
3000-4000
4000-5000
5000-6000
6000-7000
Fiber Length (µm)

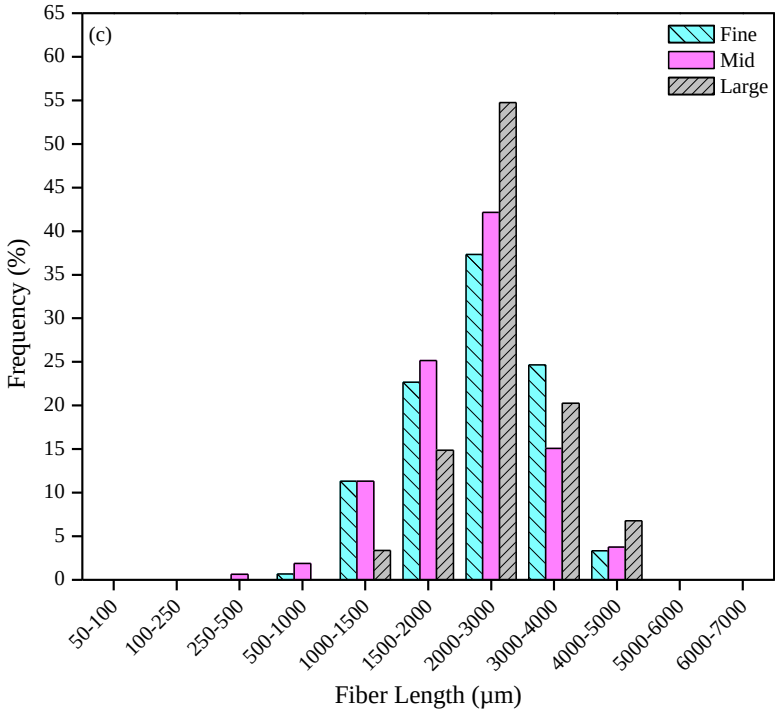
(c)
Fine
Mid
Large
Frequency (%)
0
5
10
15
20
25
30
35
40
45
50
55
60
65
50-100
100-250
250-500
500-1000
1000-1500
1500-2000
2000-3000
3000-4000
4000-5000
5000-6000
6000-7000
Fiber Length (μm)

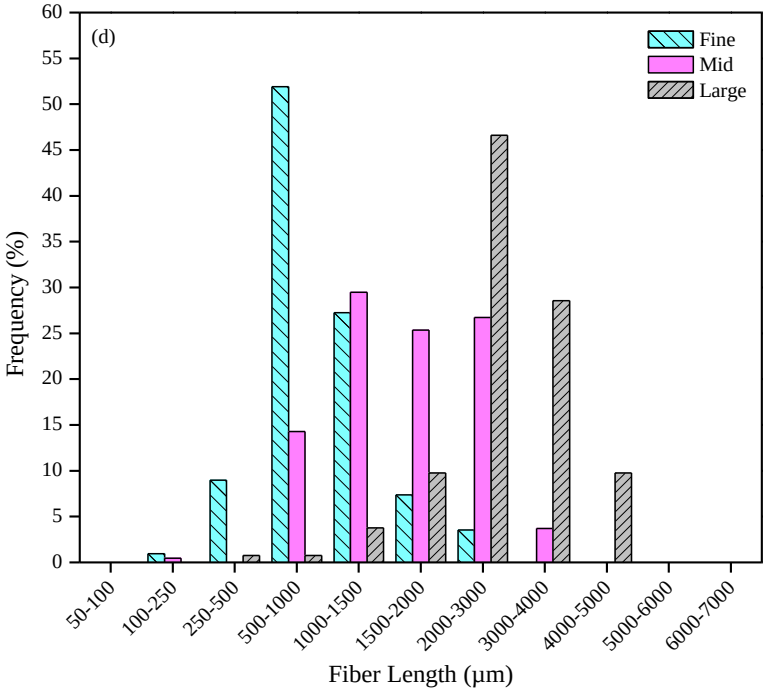
(d)
Fine
Mid
Large
Frequency (%)
0
5
10
15
20
25
30
35
40
45
50
55
60
50-100
100-250
250-500
500-1000
1000-1500
1500-2000
2000-3000
3000-4000
4000-5000
5000-6000
6000-7000
Fiber Length (μm)

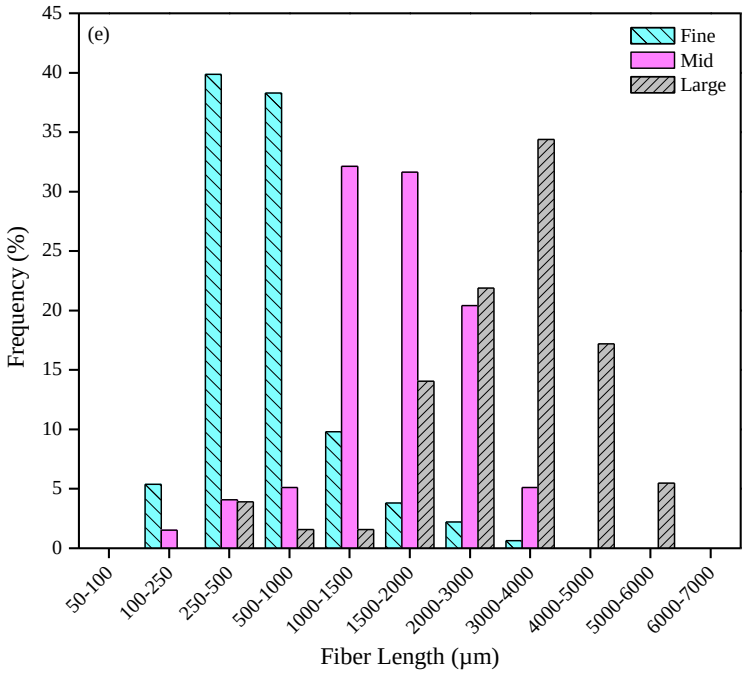

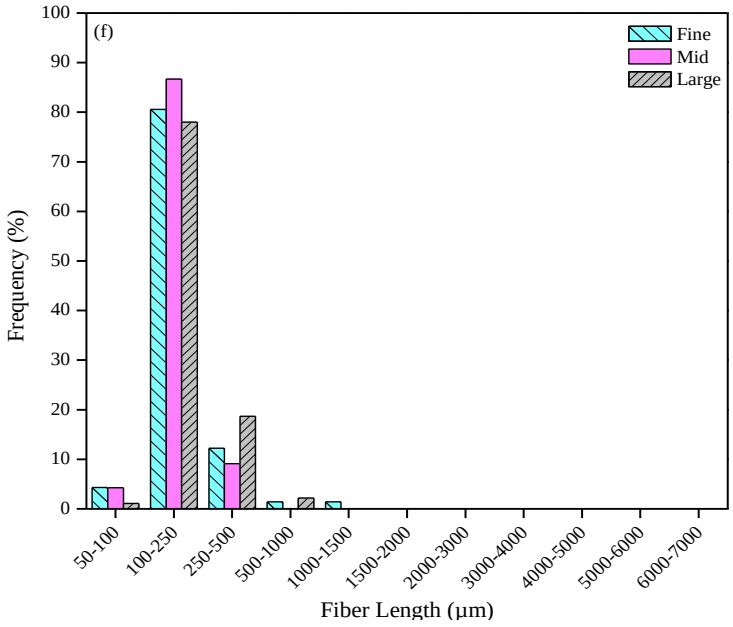

Figure 4-3 Wheat Straw Particle Length Distribution for Large-Size, Mid-Size, and Fine-Size at (a) Size<Mesh18 (b) Mesh18<Size<Mesh25 (c) Mesh25<Size<Mesh35 (d) Mesh35<Size<Mesh60 (e) Mesh60<Size<Mesh100 and (f) Size> Mesh100

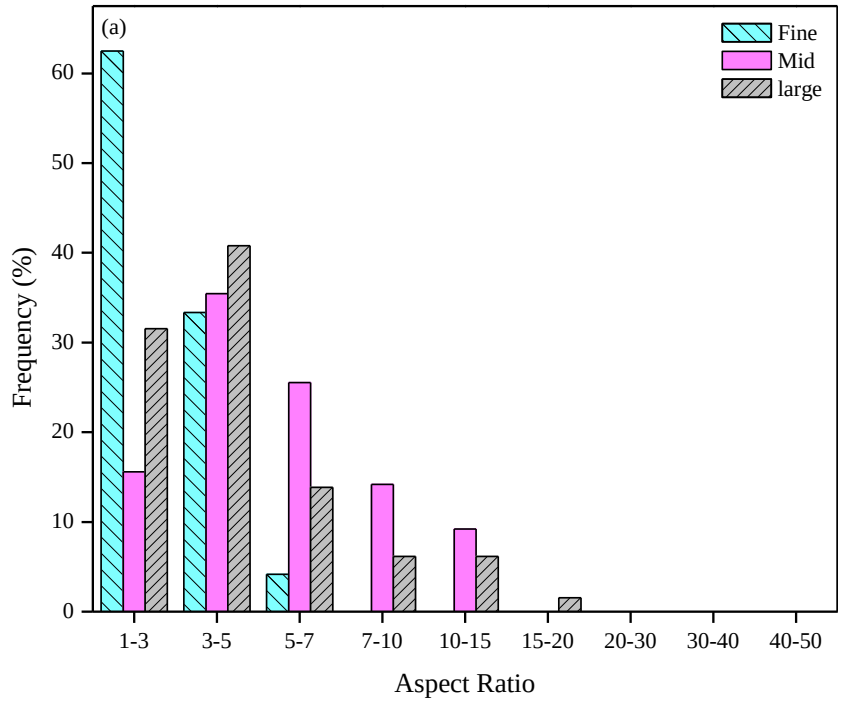
(a)
Fine
Mid
large
Frequency (%)
0
10
20
30
40
50
60
1-3
3-5
5-7
7-10
10-15
15-20
20-30
30-40
40-50
Aspect Ratio

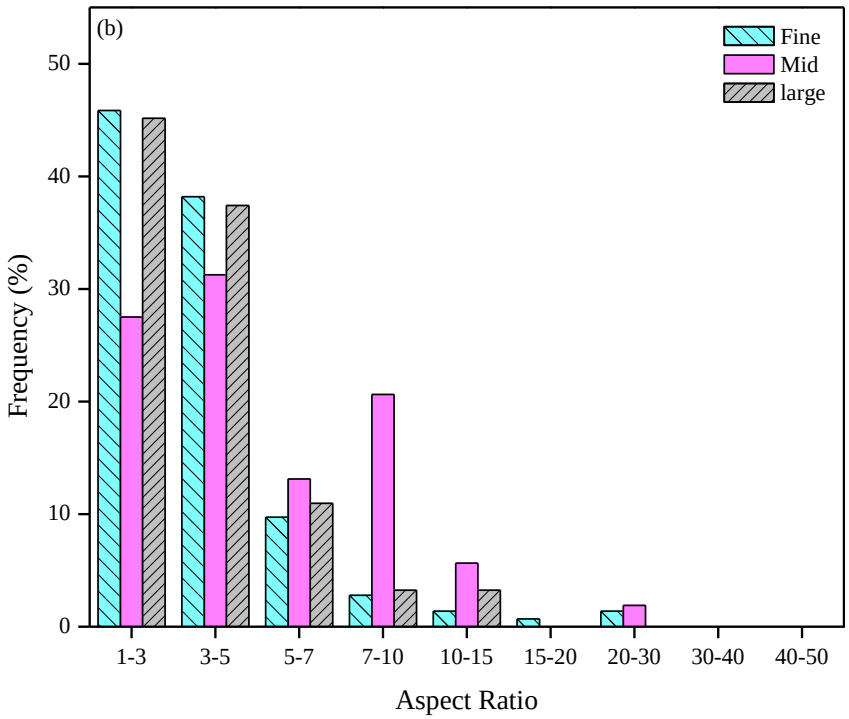
(b)
Fine
Mid
large
Frequency (%)
0
10
20
30
40
50
1-3
3-5
5-7
7-10
10-15
15-20
20-30
30-40
40-50
Aspect Ratio

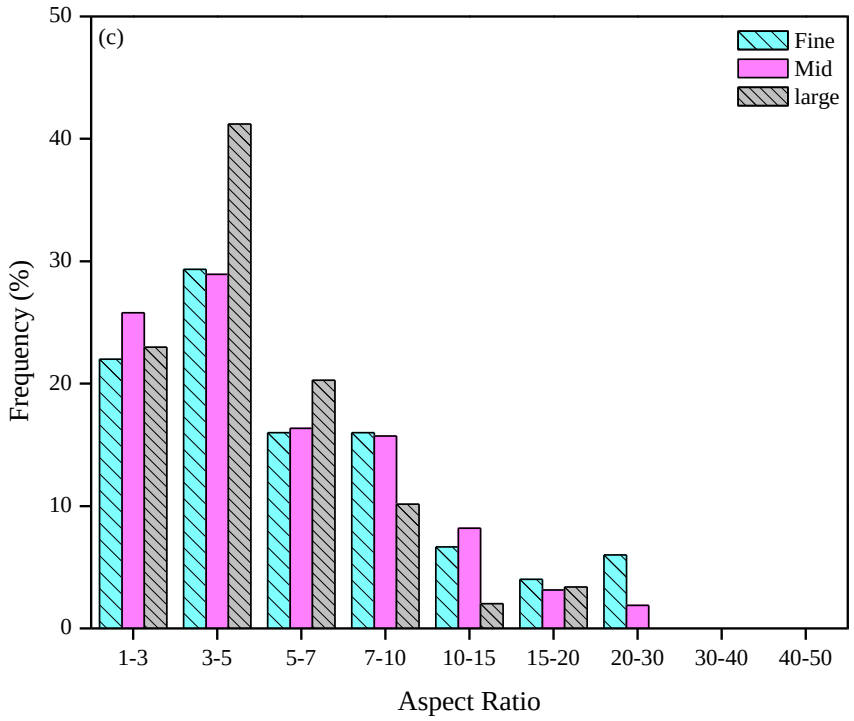
(c)
Fine
Mid
large
Frequency (%)
0
10
20
30
40
50
1-3
3-5
5-7
7-10
10-15
15-20
20-30
30-40
40-50
Aspect Ratio

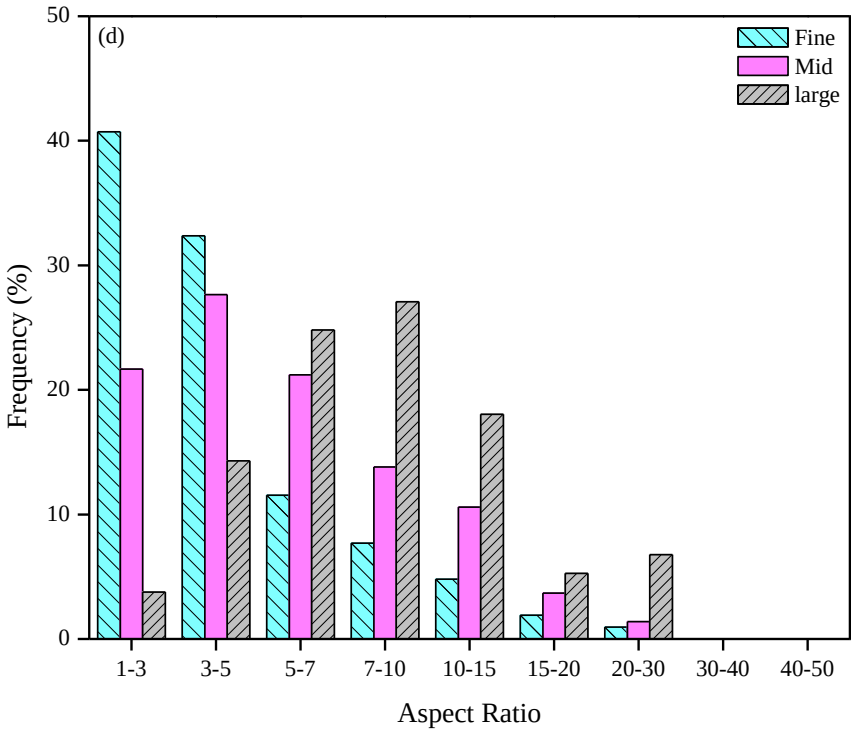
(d)
Fine
Mid
large
Frequency (%)
0
10
20
30
40
50
1-3
3-5
5-7
7-10
10-15
15-20
20-30
30-40
40-50
Aspect Ratio

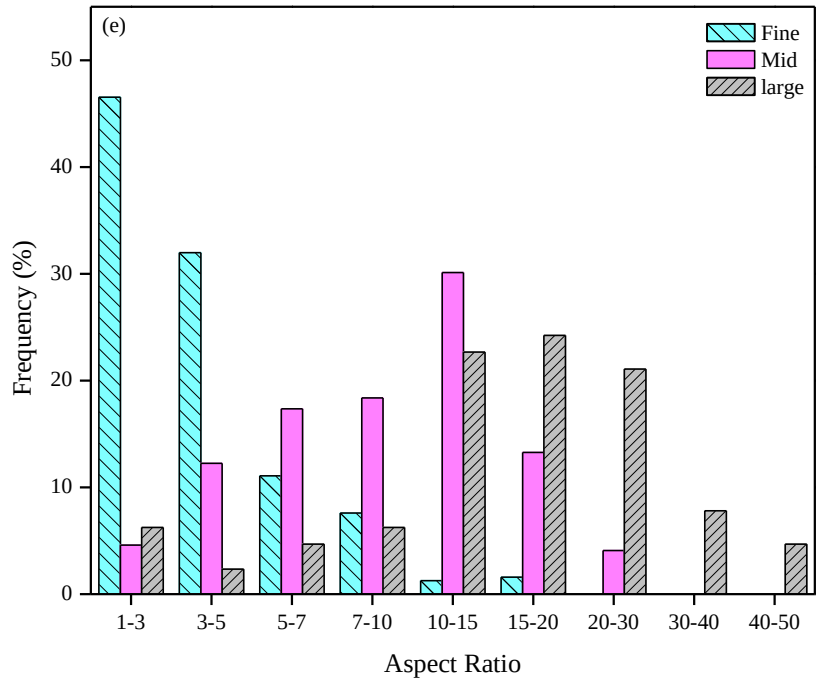

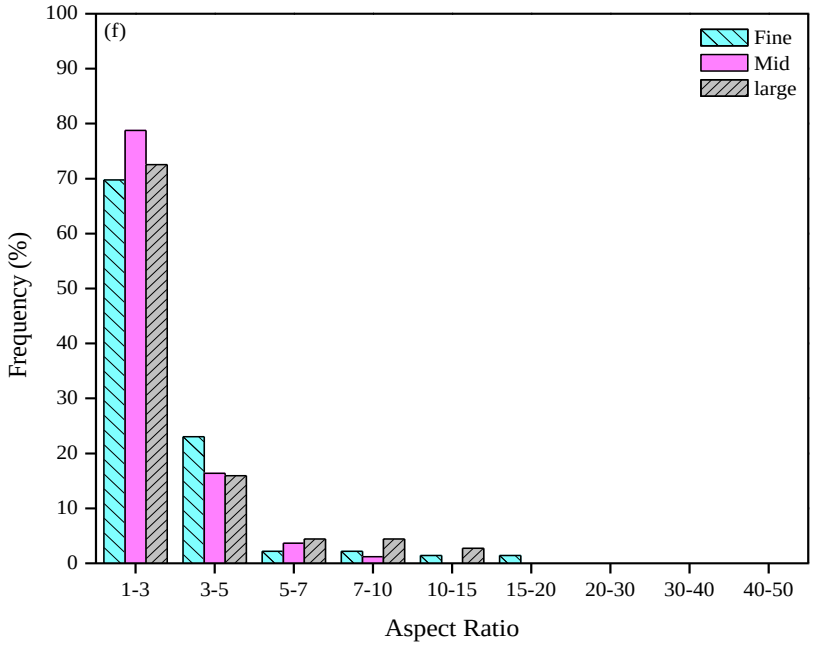

Figure 4-4 Wheat Straw Aspect Ratio Distribution for Large-Size, Mid-Size, and Fine-Size at (a) Size<Mesh18 (b) Mesh18<Size<Mesh25 (c) Mesh25<Size<Mesh35 (d) Mesh35<Size<Mesh60 (e) Mesh60<Size<Mesh100 and (f) Size> Mesh100

The main differences in the aspect ratios of particles were found to be in the fractions 35-60 and 60-100. One interesting point obtained was that the aspect ratios of Fine batch particles are mostly below 5 except in fraction 25-35 where close to 50 % of particles have aspect ratios above 5. This is the only fraction in the Fine batch that can compete with the Mid and Large fractions in terms of particle aspect ratio.

Another interesting observation obtained was the aspect ratios of particles for large and Mid size batches in fractions 35-60 and 60-100. It was found that close to 60 % of Mid size gWS and above 90 % of the Large gWS in fraction 35-60 have particle aspect ratio above 5. These values are even higher in fraction 60-100 where close to 85 % of Mid size particles and 93 % of Large particles show aspect ratio higher than 5. It should be noted that more than 70 % of the Large batch particles in fraction 60-100 have aspect ratios between 15 and 50 which is significantly high compared to other fractions.

Figure 4-5 (a)-(c) and Figure 4-6 (a)-(c) represent pictures from Large, Mid and Fine size ground wheat straw particles for fractions 35-60 and 60-100 are shown. The coexistence of fibers with relatively high aspect ratios and particles especially in finer fractions are obvious in these pictures.


1 mm
(a)


1 mm
(b)

Figure 4-5 Wheat Straw Particles in Fraction 35-60 (a) Large (b) Mid size (c) Fine


1 mm
(a)


1 mm
(b)

Figure 4-6 Wheat Straw Particles in Fraction 60-100 (a) Large (b) Mid size (c) Fine

4.1.4 PARTICLE MORPHOLOGY PRIOR TO COMPOUNDING

In order to investigate the structure of the gWS prior to compounding, scanning electron microscopy (SEM) was used to take micrographs of inner and outer surfaces of three batches of gWS. Moreover, gWS fractions were analyzed by SEM to identify potential structural differences according to particle sizes. Additional study of the structure of the wheat straw particles prior to compounding has been done by other members of our laboratory (Golbabaie 2008, Kapustan Krüger 2007).

SEM of Large, Mid, and Fine batches of gWS are shown in Figure 4-7. (a)-(c). It was found that due to the relatively harsh grinding process, gWS exhibit severe damage and surface

irregularities where the outer layer of the straw (epidermis) along with the inner layers are either peeled off or broken into smaller pieces. Also major cracks mainly along the length of the gWS in the larger batches (Mid and Large) were found as shown in Figure 4-7 (a)-(b).

Based on SEM micrographs it was concluded that layers of cellulose and hemicellulose are in coexistence with lignin and other waxy products. Due to this complex structure, it was not possible to identify the differences in composition of different gWS batches by using SEM. Golbabaie has reported that gWS particles contained a layer of epidermal tissue still attached to underling stem tissue including sclerenchyma and parenchyma (Golbabaie 2008). These stem tissues are fibrous materials that themselves are composite material, comprising from cellulose microfibrils bound within an amorphous matrix of lignin and hemicelluloses (Hornsby, Hinrichsen et al. 1997a). Therefore, it was concluded that grinding system does not provide enough energy to seperate the gWS layers and further no structural change was observed between different gWS batches. Sharma has reported that the straw constituents cannot be seperated without causing degradation or structural change (Sharma 1996).

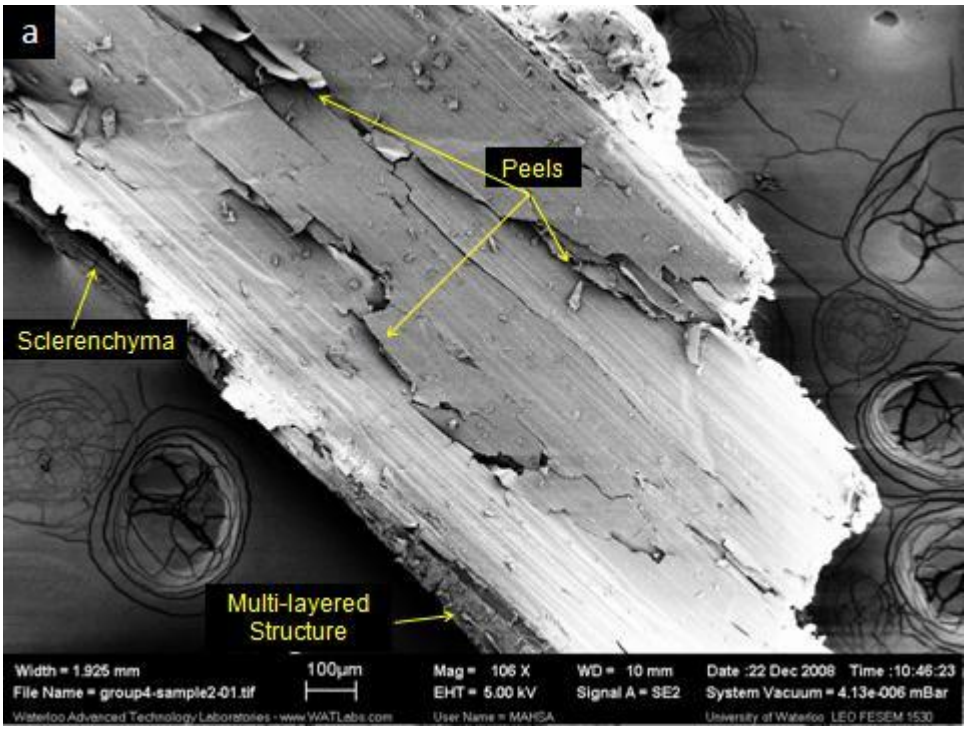
a
Peels
Sclerenchyma
Multi-layered
Structure
Width = 1.925 mm
File Name = group4-sample2-01.tif
100µm
Mag = 106 X
EHT = 5.00 kV
WD = 10 mm
Signal A = SE2
Date :22 Dec 2008 Time :10:46:23
System Vacuum = 4.13e-006 mBar
Waterloo Advanced Technology Laboratories - www.WATLabs.com
User Name = MAHSA
University of Waterloo LEO FESEM 1530

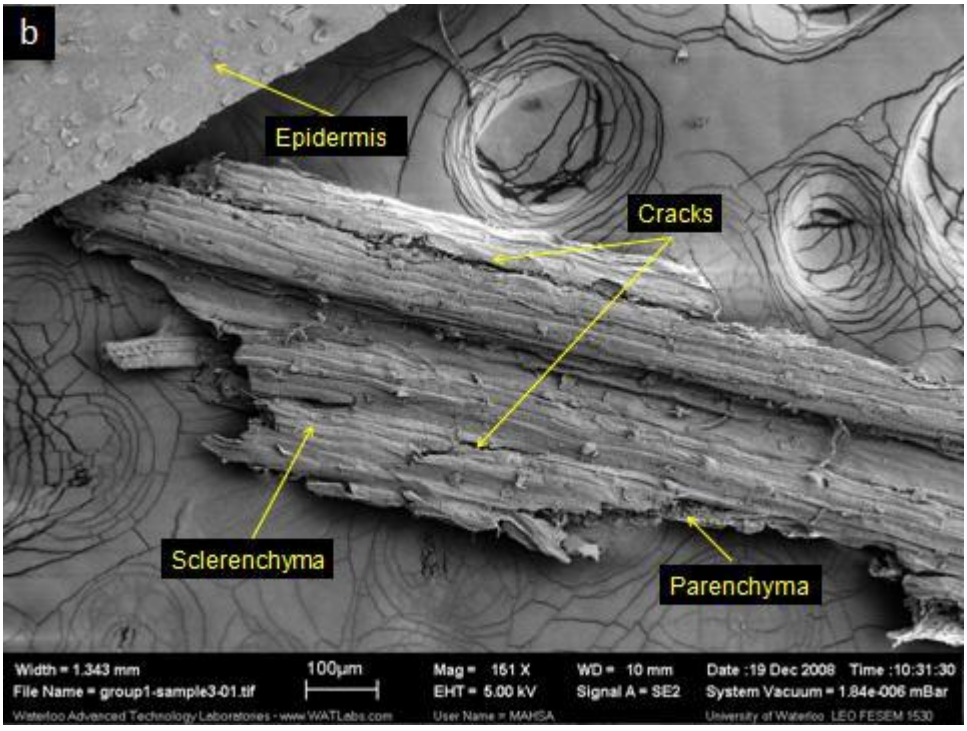
b
Epidermis
Cracks
Sclerenchyma
Parenchyma
Width = 1.343 mm
File Name = group1-sample3-01.tif
100µm
Mag = 151 X
EHT = 5.00 kV
WD = 10 mm
Signal A = SE2
Date :19 Dec 2008 Time :10:31:30
System Vacuum = 1.84e-006 mBar
Waterloo Advanced Technology Laboratories - www.WATLabs.com
User Name = MAHSA
University of Waterloo LEO FESEM 1530

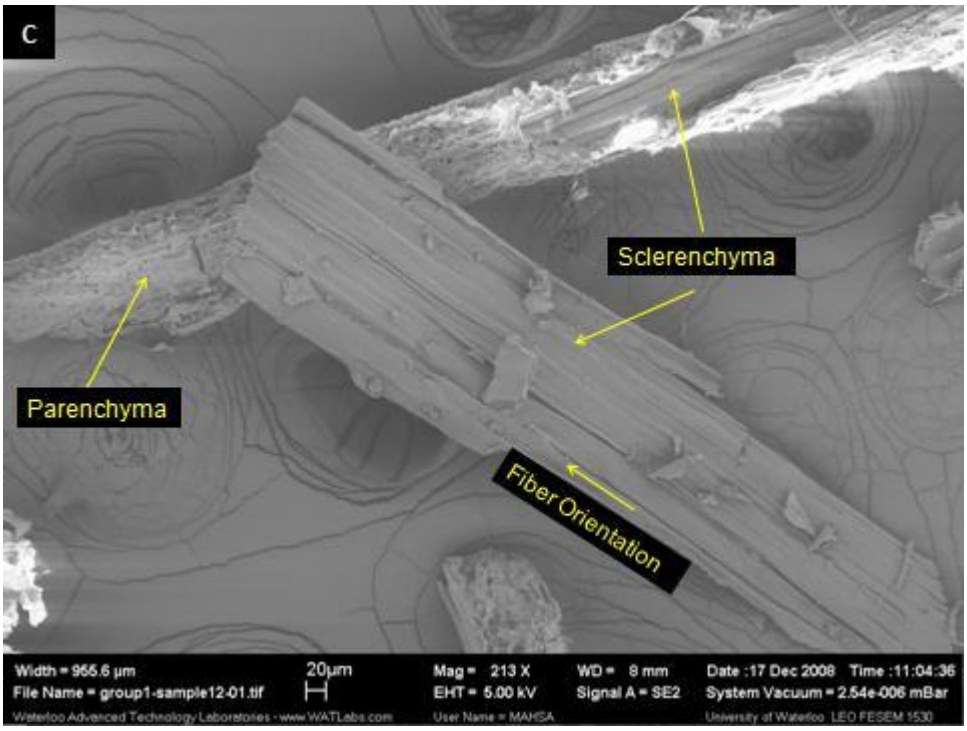

Figure 4-7 Scanning Electron Microscopy from (a) Large batch (b) Mid Batch and (c)Fine Batch Presenting Different Layers of gWS and Damages Caused by Processing

Similar results were obtained by analyzing the SEM micrographs of the fractions. In all fractions, it was found that the multi-layered structure was present and separation according to size does not necessarily create fractions with different cell structure or compositions.

Figure 4-8 (a) & (b) are obtained from Fractions of 36-60 and 60-100 from the Large batch. These particles showed the highest aspect ratio among all the other fractions (thin fibers). It was concluded that, although these fibers were found to be very thin in structure and potentially made from cellulose febrile, different WS structural layers were again in coexistence similar to other fractions. The degree of damage on these fractions caused by the grinding process was found to be similar to other fractions.

One interesting point obtained was the structure of the smallest fraction of the Fine batch. It was found that the gWS in this fraction were combination of short cylindrical particles and some irregular shaped particles (debris). Such debris can be a combination of the parenchyma and vascular bundles which were ground to smaller pieces along with leaf or grain tissue left with the WS during baling process. See Figure 4-9 (a)-(b).

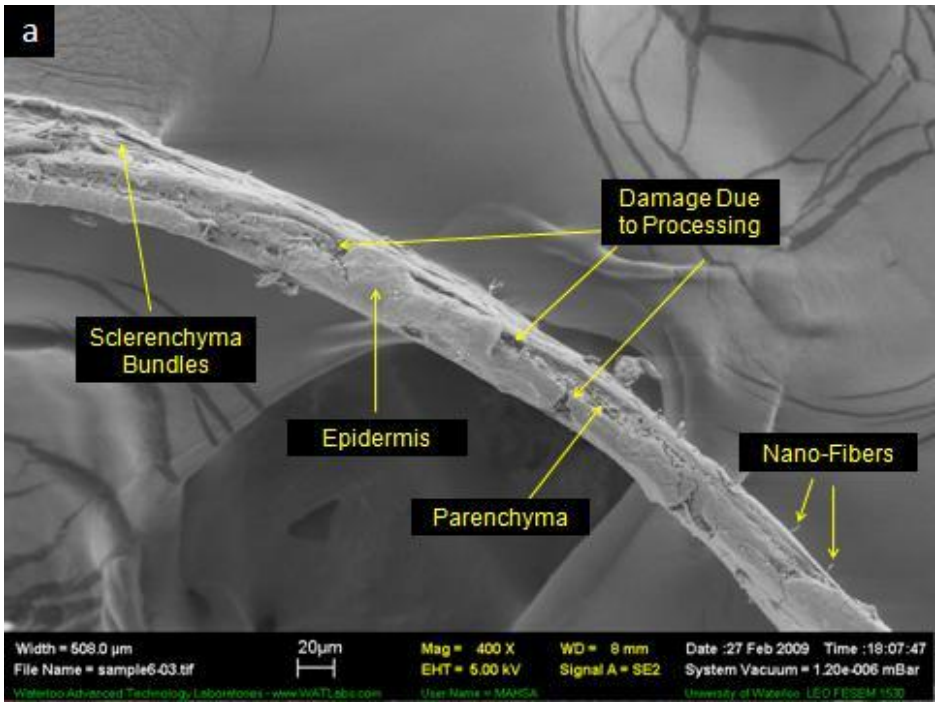

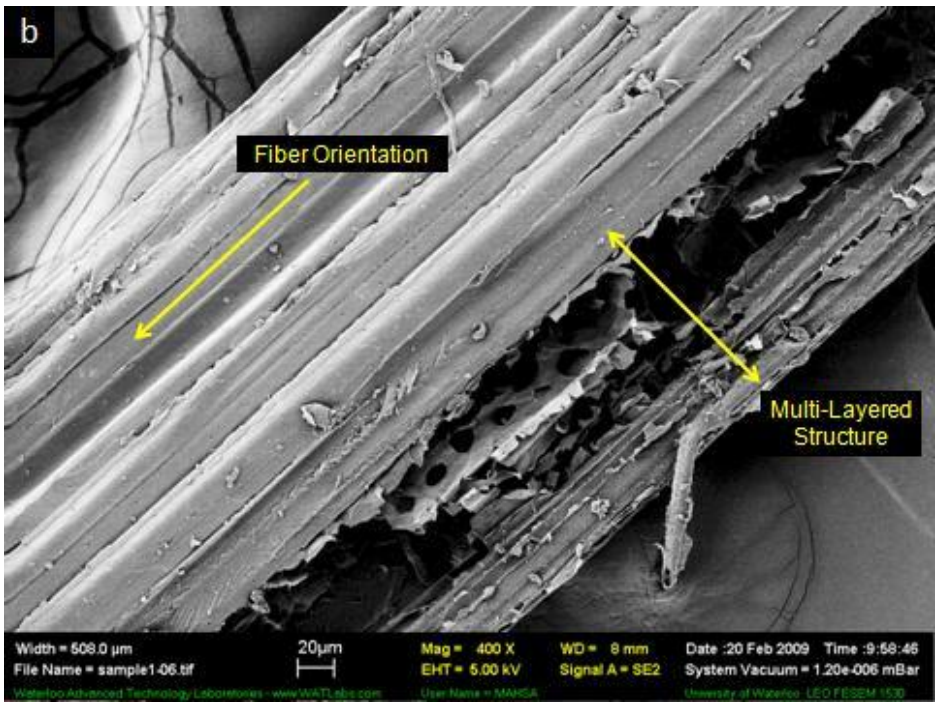

Figure 4-8 Scanning Electron Microscopy of Fractions (a)60-100 and (b) 35-60 from the Large Batch of gWS

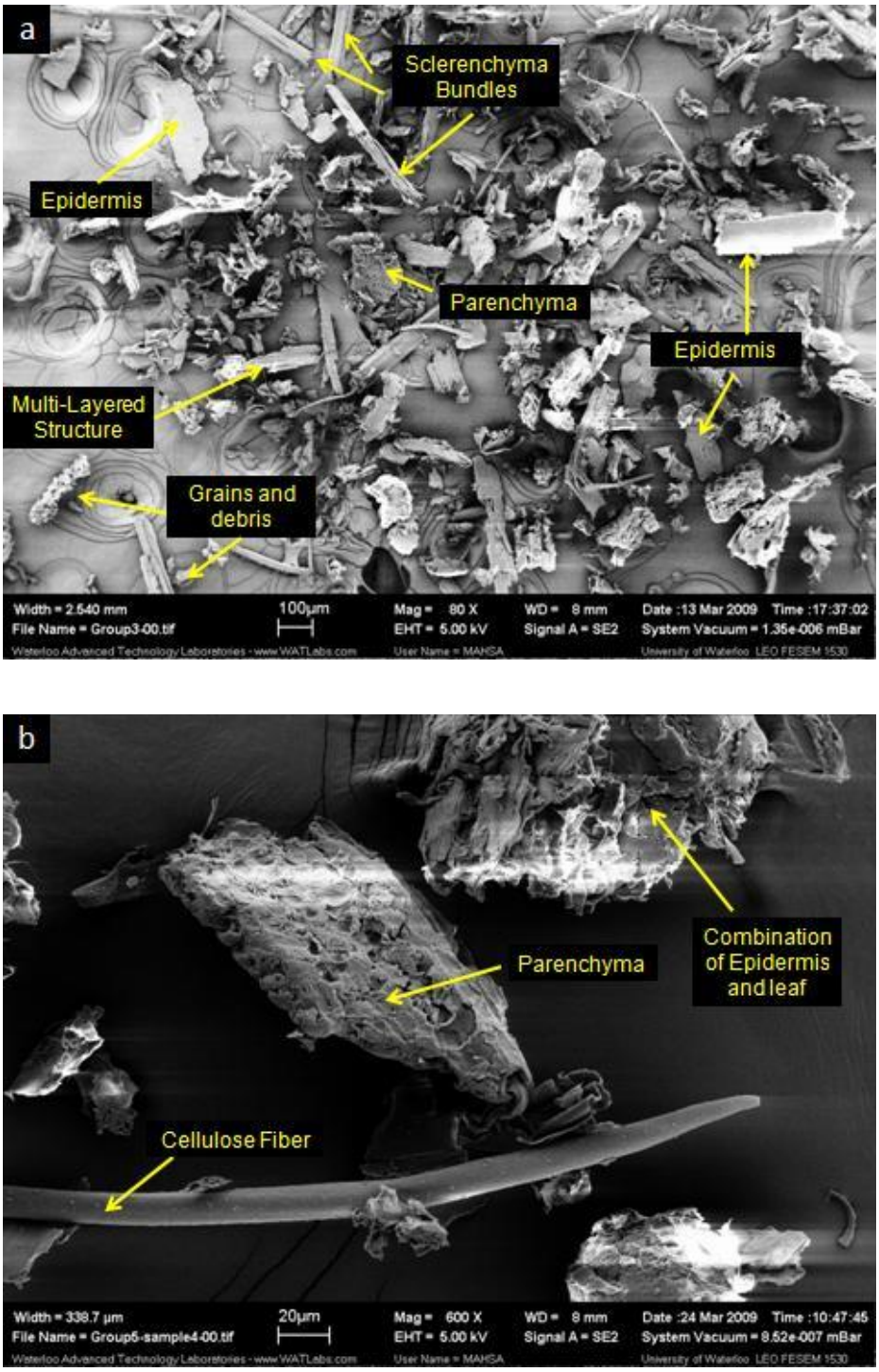

Figure 4-9 Scanning Electron Microscopy of the Smallest Fraction in the Fine Batch (a)80x Magnification (b) 600x Magnification

4.1.5 PARTICLE COMPOSITION

The wheat straw particles produced by grinding are made of plant cell walls, which in turn are made of mostly cellulose, hemicelluloses and lignin. In order to identify the main components of each wheat straw fraction and to make a correlation between the morphology, composition and thermal behavior of the particles, the chemical analysis was performed on selected particle fractions. Based on results from NDF and ADF tests, amount of hemicellulose in each fraction was obtained simply by subtracting the two values. NDF represents cellulose, hemicellulose and lignin fractions of the plant cell wall while ADF is characterized by the presence of cellulose and lignin (Sharma 1996). It should be mentioned that in this study any ash content correction on the NDF residual was not performed and the hemicellulose content was calculated based on the assumption that NDF values are free of ash. Hemicellulose content was calculated based on acid detergent fiber (ADF) and neutral detergent fiber (NDF) test values and the ash content data was obtained from TGA. The results obtained from these tests are presented in Table 4-3.

Table 4-3 Results Obtained from Feed Analysis of Fractions of gWS by AgriFood Laboratories

Large						
Size	<18	18-25	25-35	35-60	60-100	>100
ADF	56.40	54.60	52.70	52.3	51.5	46.2
NDF	84.02	82.74	82.29	79.92	79.61	70.3
Lignin (wt-%)	9.01	8.01	7.25	6.43	4.91	6.57
Hemicellulose (wt-%)	27.62	28.14	29.59	27.62	28.11	24.1
Mid						
Size	<18	18-25	25-35	35-60	60-100	>100
ADF	58.90	56.90	53.50	50.70	53.10	50.20
NDF	85.32	84.60	82.07	79.73	80.47	73.76
Lignin (wt-%)	9.04	8.47	6.89	6.12	5.78	5.75
Hemicellulose (wt-%)	26.42	27.70	28.57	29.03	27.37	23.56
Fine						
Size	<18	18-25	25-35	35-60	60-100	>100
ADF	58.9	54.20	51.90	47.5	46.20	46.40
NDF	85.32	81.62	79.76	77.00	75.29	70.79
Lignin (wt-%)	9.04	7.56	6.11	5.18	4.88	5.90
Hemicellulose (wt-%)	26.42	27.42	27.86	29.50	29.09	24.39

It was found that highest lignin content in all three batches was 9 wt-%. The lowest amount of lignin was seen in the Large and Fine fractions of 60-100 with lignin content of 4.9 wt-%. Lignin content of these two fractions in the Mid batch were found to be slightly higher (16 %). The lignin content was found to be related to the size of the ground wheat straw. Higher percentage of lignin was found to be more frequent in larger fractions of size<18 and 18-25 where the lignin content was limited to 8 to 9 wt-%. The lignin content of lower sizes showed a decrease as the size of wheat straw particles decreased with the exception of the finest fraction (size > 100).

Alemdar and co-workers have shown that untreated wheat straw had lignin content of 22±3 wt-%. (Alemdar, Sain 2008). In another work this content was found to be 19.5 wt-% (Ashori, Nourbakhsh 2009a). However, Mohanty et al. have reported that the lignin content in the wheat straw was close to 10 wt-% (Mohanty, Misra et al. 2005). This implies that the

composition of wheat straw component can be different according to factors such as wheat straw type, place where it is cultivated, or the cultivation season.

As shown in Figure 4-10 the amount of hemicellulose in each fraction is limited between 24 wt-% and 29 wt-%. These values were compared to literature values for hemicellulose content and are in the bottom end of the range (Ashori, Nourbakhsh 2009a, Ashori, Nourbakhsh 2009b). The lowest hemicellulose content is obtained from the finest particles in all three batches. An interesting point that was obtained from these values is that there is an increasing shift from left to right in the values of hemicellulose as the size of the fractions decreases replying that hemicellulose is also size dependent. This dependency however was found to be not as high as the case for lignin.

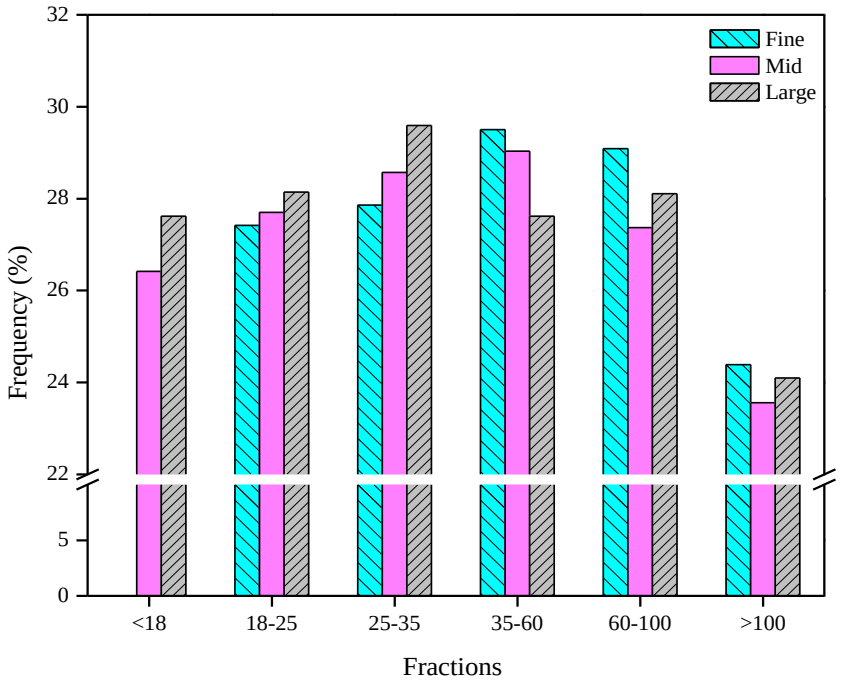

Figure 4-10 Hemicellulose Content Obtained from ADF and NDF Values from AgriFood Laboratories

4.1.6 THERMOGRAVIMETRIC ANALYSIS (TGA)

Thermal gravimetric analysis (TGA) was performed on selected fractions of wheat straw particles. Lignin and cellulose samples were purchased and used as external references to investigate the thermal stability and degradation onset temperatures under nitrogen. The thermogravimetric analysis of such lignin and cellulose was used to provide some basic knowledge in regards to the thermal stability of wheat straw.

The temperature range of interest is usually between 160 ^{o}C and 280 ^{o}C, which is the processing temperature for most thermoplastics. TGA and DTGA thermographs for lignin and cellulose references are shown in Figure 4-11. The thermographs indicated that lignin start to decompose at a relatively low temperature, close to 180 ^{o}C, and approximately 1 wt-% of the lignin decomposed at 213 ^{o}C. This indicated that lignin had the lowest onset of degradation temperature. Thermal degradation of lignin continued at high temperatures (above 500 ^{o}C) with multiple decomposition peaks.

Ramiah has reported that lignin is very thermally stable, cellulose is intermediate and hemicellulose is least stable (Ramiah 1970). Similarly, Mohanty et al. have reported that lignin is a thermoplastic polymer exhibiting a glass temperature of 90 ^{o}C and a melting temperature at which the polymer start to flow of around 170 ^{o}C (Mohanty, Misra et al. 2005). Further, in another study by Mengeloglu et al. the onset temperature degradation of wheat straw due to lignin was found to be around 178 ^{o}C (Mengeloglu, Karakus 2008).

Cellulose on the other hand starts to degrade at temperature close to 250 ^{o}C and 1wt-% of this material is decomposed at 290 ^{o}C indicating a higher thermal stability than lignin. Pure cellulose also showed a decompositions peak at 331 ^{o}C and was completely decomposed at temperatures close to 420 ^{o}C with almost no residue left due to complete thermal decomposition.

In a study on the thermal properties of wheat straw component it was found that lignin isolated from wheat straw compost exhibited a main decomposition peak at 500 ^{o}C which was preceded by a minor peak at 369 ^{o}C which shoulders near 320 ^{o}C (Sharma 1996). It should be noted that the thermal stability of the wheat straw components is not a constant factor and could vary based on parameters such as type of wheat and the place of cultivation.

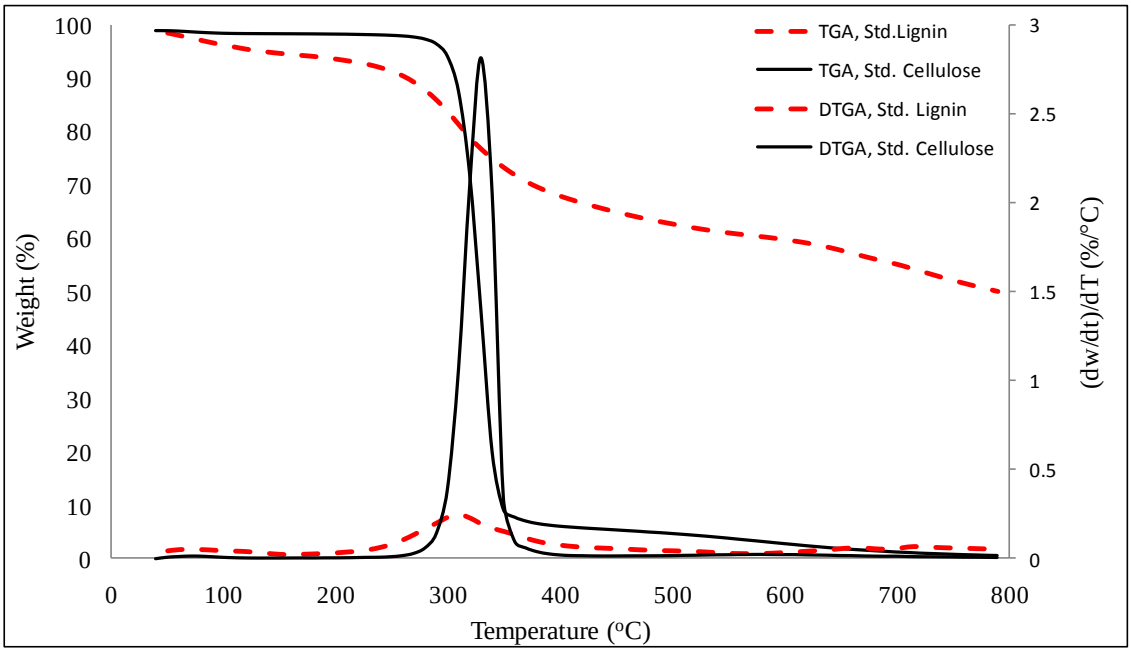

Figure 4-11 The TGA Curves of Standard Cellulose and Lignin at a Heating Rate of 10^{o}C/min in Nitrogen

TGA and DTGA curves for the fraction of Large, Mid, and Fine batches of gWS are presented in Figure 4-12 to Figure 4-13 illustrating three main weight loss peaks. The first stage of weight loss is attributed to the bonded and unbounded evaporation of water at temperature below 160 ^{o}C and the other two peaks are decomposition peaks representing chemical loss and structural bond breakage.

The main thermal degradation step of gWS was different in each fraction. This is mainly attributed to the size of the gWS particles. A minor difference in the value of temperature at 1 wt-% was seen from the largest fraction to the smallest fraction in the Large batch. This implies that the particles with smaller size distribution under go faster decomposition which can be attributed to their larger surface areas. A similar trend was also obtained in the other two batches Mid and Fine. It was also found that the Mid batch was the most thermally stable batch as indicated by the 1 wt-% decomposition values and the Fine batch was the least thermally stable batch. Another point made by this analysis was that the lignin content does not directly dictate the onset of decomposition point. As explained before, there is a decreasing trend in the amount of lignin by reducing the size; however, this reduction of lignin did not have any direct effect on the onset degradation of wheat straw particles and this property was mostly ruled by the size of the particles (See Figures Figure 4-14 to Figure 4-17).

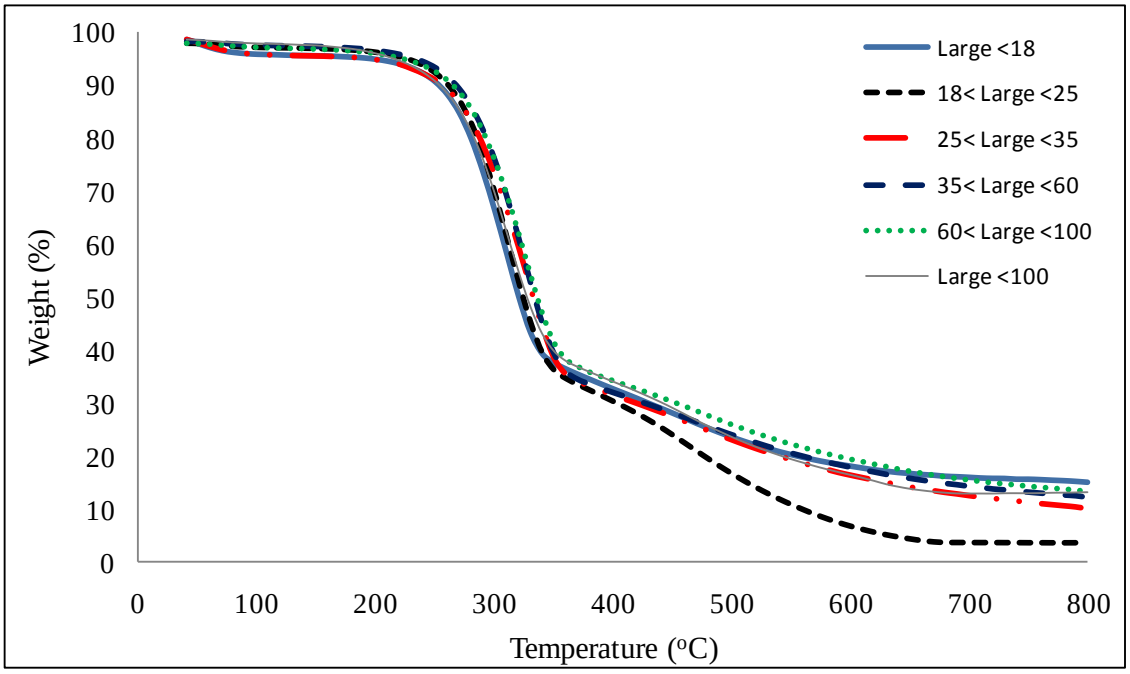

Figure 4-12 TGA Curves for Large gWS Fractions at a Heating Rate of 10°C/min in Nitrogen

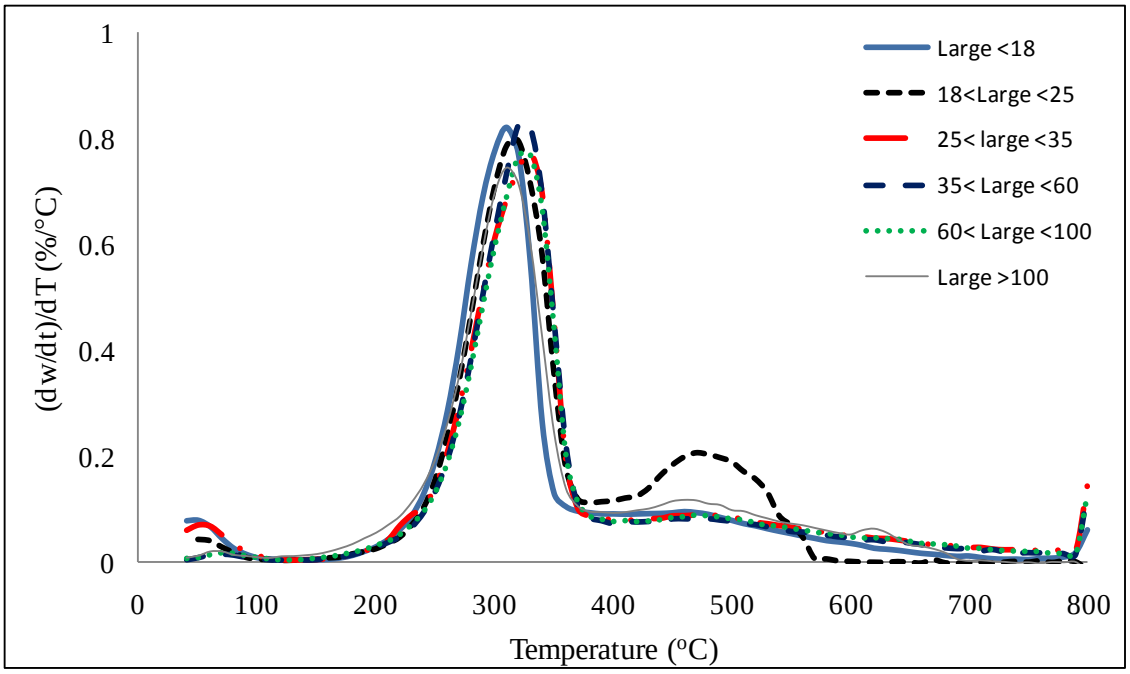

Figure 4-13 DTGA Curves for Large gWS Fractions at a Heating Rate of 10°C/min in Nitrogen

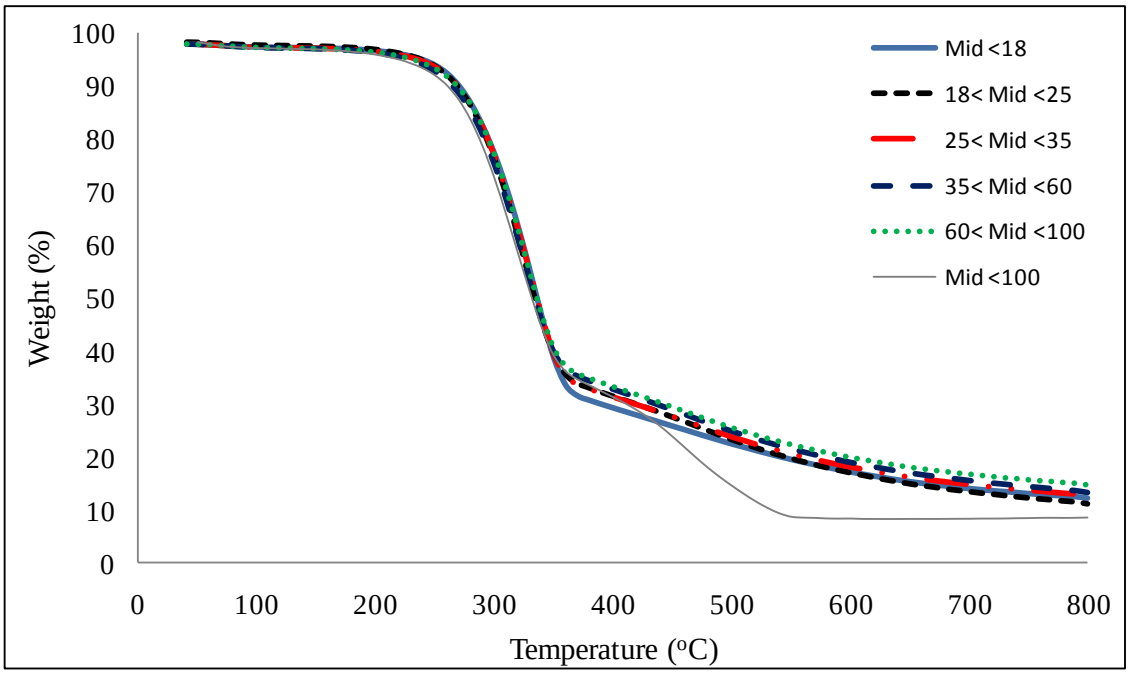

Figure 4-14 TGA curves for Mid gWS Fractions at a Heating Rate of 10°C/min in Nitrogen

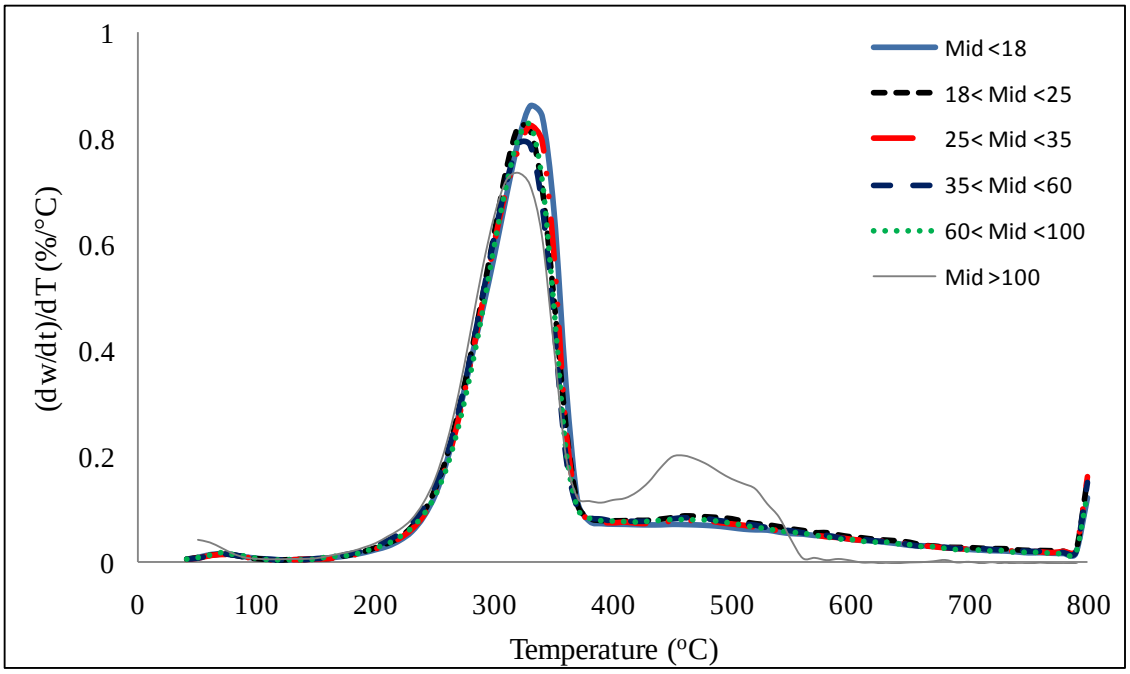

Figure 4-15 DTGA curves for Mid gWS Fractions at a Heating Rate of 10°C/min in Nitrogen

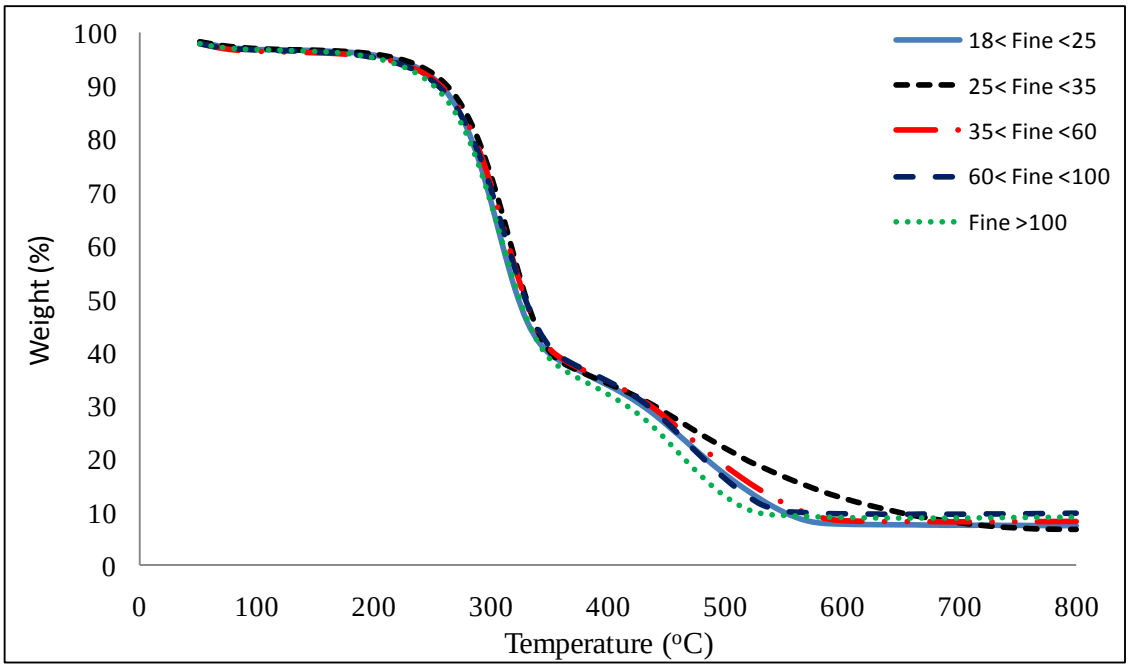

Figure 4-16 TGA curves for Fine gWS Fractions at a Heating Rate of 10°C/min in Nitrogen

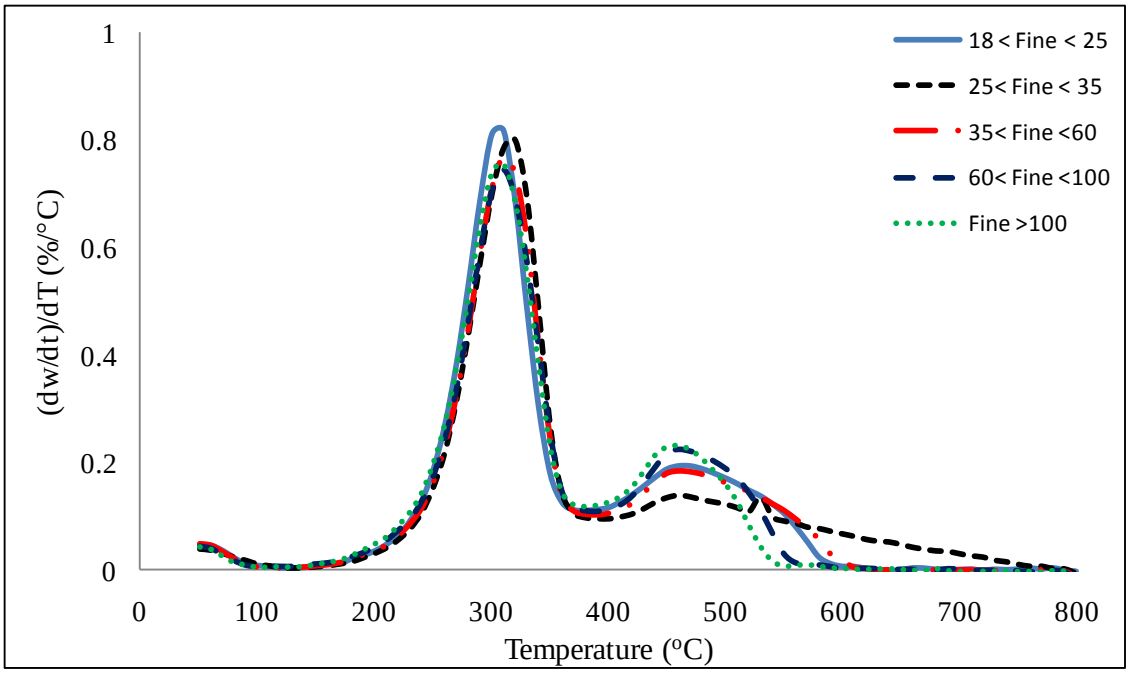

Figure 4-17 DTGA curves for Fine gWS Fractions at a Heating Rate of 10°C/min in Nitrogen

The properties taken from the thermograms are summarized in Table 4-4. Attention should be given to Large fractions (18< Size< 25) and Fine fraction (25< Size< 35). These two fractions had the lowest ash content among all fractions. The thermal stability of these fractions is also very similar to each other indicating that they are both mainly from the same part of the wheat straw. This implies that these particles were probably not obtained from the outer surface of the wheat straw where the content of the silica is higher (Hornsby, Hinrichsen et al. 1997).

The second degradation peak for all the batches took place at temperature higher than 450 °C. Comparing the TGA and DTGA thermograms of the Large and Mid batches with the Fine batch, it is clear that the Fine batch second degradation peaks are much more obvious. This can be related again to the fact that the smaller particles have higher surface areas for heat transport and thus a better thermogram is obtained. The thermal analysis was

not performed on the largest particles of the Fine batch since the amount of this fraction was very small compared to the other fractions.

Table 4-4 Decomposition Peaks and Weight Loss of Wheat Straw Fractions Obtained from TGA

Large						
	<18	18-25	25-35	35-60	60-100	>100
Temp. at 1wt-% Degradation (^{o}C)	207.73	206.18	206.18	203.87	201.55	183.02
Decomposition Peak 1 (^{o}C)	311.11	316.72	328.10	323.71	325.62	310.01
Weight Loss (wt-%)	63.12	66.71	64.264	66.28	62.73	63.60
Decomposition Peak 2 (^{o}C)	476.98	485.35	483.21	474.61	480.75	470.32
Weight Loss (wt-%)	14.68	24.74	15.13	14.05	14.79	17.63
Ash Content (wt-%)	15.37	6.79	10.54	13.96	15.16	14.35
Mid	<18	18-25	25-35	35-60	60-100	>100
Temp. at 1wt-% Degradation (^{o}C)	215.45	210.82	209.27	203.87	204.64	194.60
Decomposition Peak 1 (^{o}C)	333.69	325.45	332.61	324.68	327.00	316.07
Weight Loss (wt-%)	68.14	66.17	66.18	64.49	63.84	65.54
Decomposition Peak 2 (^{o}C)	475.81	483.00	473.9	482.39	479.39	462.36
Weight Loss (wt-%)	12.05	14.38	13.08	13.75	13.23	23.00
Ash Content (wt-%)	14.04	12.77	14.26	15.07	16.73	10.02
Fine	<18	18-25	25-35	35-60	60-100	>100
Temp. at 1wt-% Degradation (^{o}C)	--	201.55	203.09	196.92	192.28	189.2
Decomposition Peak 1 (^{o}C)	--	304.64	313.44	310.88	307.13	306.11
Weight Loss (wt-%)	--	62.78	64.22	61.86	62.01	64.55
Decomposition Peak 2 (^{o}C)	--	470.87	468.34	475.02	466.1	460.63
Weight Loss (wt-%)	--	26.16	29.66	26.28	24.98	23.16
Ash Content (wt-%)	--	8.72	5.64	9.67	11.33	10.61

Figure 4-18 is a representation of standard cellulose and lignin with a gWS sample from Large batch of fraction <18. It is apparent that gWS follows the thermal properties of cellulose between 240 ^{o}C and 350 ^{o}C and that of lignin for rest of the temperature range. Comparison of the thermograms of the gWS fractions and standards revealed that the filler constituents, cellulose and hemicellulose were thermally degraded first indicated by

primary weight loss peak whereas the secondary peaks represents the lignin loss as indicated by a minor shoulder to the peak at temperature close to 410 ^{o}C with a decomposition peak around 470 ^{o}C.

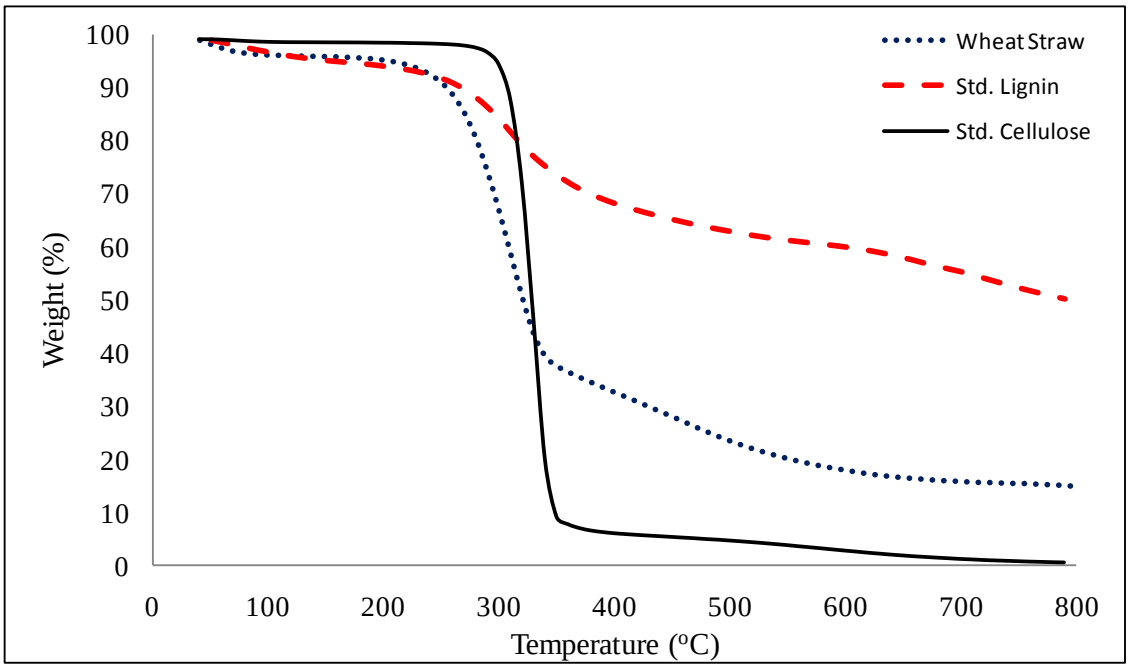

Figure 4-18 TGA of Standard Lignin and Cellulose with gWS from Large Size≤18

Based on the information obtained from TGA analysis, assuming that the second decomposition peak is mainly due to the existence of lignin, it was found that the lignin content of the wheat straw particles in all the fraction contribute to 12-30 wt-% of the total weight which is in contrary with the information obtained from the lignin test. Such a different result is believed to be due to the existence of structural hemicellulose which exists in close association with lignin which decomposes at temperatures higher than 410 ^{o}C. This deviation can also be due to the differences between the analyzing methods or due to the insensitivity of the TGA method (rate of 10^{o}C/min).

As it was mentioned before, the thermogravimetric analysis of the components of the wheat straw provide information about the thermal stability of it. In the same way, the thermal behavior of a batch of wheat straw is dictated by the thermal behavior of the most abundant components in the batch of straw. Table 4-5 was prepared from data presented earlier in Table 4-1 and Table 4-4. Thermal behavior of gWS batches and the whole ground bale of wheat straw (blend) are summarized in Table 4-5. It was found that the Mid and Large size ground wheat straws had similar thermal behaviour below 300 ^{o}C.

Table 4-5 Thermal Behavior of gWS Batches and a Blend of All Sizes

Sample ID	Large	Mid	Fine	Blend
Temp.* at 1 wt-% Degradation (^{o}C)	206.82	207.41	194.09	203.58
Decomposition Peak 1(^{o}C)	315.81	328.10	308.51	319.21
Weight Loss (wt-%)	64.78	65.48	62.45	64.45
Decomposition Peak 2	481.24	478.83	468.64	476.71
Weight Loss (wt-%)	25.46	13.62	25.40	20.23
Ash Content (wt-%)	11.34	14.36	10.20	12.35

* Temperature

4.2 CHARACTERIZATION OF WHEAT STRAW-CLAY-POLYPROPYLENE (WSCPP) COMPOSITES

4.2.1 COMPOUNDING

The components used in the formulation are: wheat straw, polypropylene, clay, coupling agent and anti-oxidants. The appropriate amounts for each composition were weighed, hand-blended, and fed into the extruder. Composition of components was varied according to Table 4-6 and Table 4-7. Ground wheat straw from the Fine batch was chosen as filler for composites presented in Table 4-6 to investigate the effects of coupling agent and clay mineral on the final properties of the composite. Composites formulation presented in Table 4-7 were prepared to investigate the effect of wheat straw particle size on the composite properties. Therefore, no clay was added to the formulation. Both anti-oxidants were used in equal amounts maintained at a total of 0.5 wt-% with respect to polypropylene content.

Table 4-6 Formulation of Wheat Straw-Clay-Polypropylene Composites Based on Different Amount of Components

ID	Polypropylene (wt-%)	Wheat Straw (wt-%)	Clay (wt-%)	PP-MA (wt-%)	Irganox 1010 (wt-%)	Irgafos 168 (wt-%)
Run #1	63	30	5	2	0.25 wt-% of PP	0.25 wt-% of PP
Run #2	53	40	5	2		
Run #3	43	50	5	2		
Run #4	65	30	5	0		
Run #5	61	30	5	4		
Run #6	66	30	2	2		
Run #7	68	30	0	2		
Run #8	93	0	5	2		
Run #9	100	0	0	0		

Table 4-7 Formulation of Wheat Straw-Polypropylene Composites Based on Particle Size

Run	Polypropylene (wt-%)	Wheat straw (wt-%)	Wheat straw (size)	PP-MA (wt-%)	Antioxidants (wt-%)
Run #10	98	0	--	2	Irganox 1010 0.25 wt-% of PP Irgafos 168 0.25 wt-% of PP
Run #11	70	30	Fine	2	
Run #12	70	30	Mid	2	
Run #13	70	30	Large	2	
Run #14	70	30	Blend	2	

4.2.2 PARTICLE SIZE ANALYSIS

Three batches of gWS obtained from the grinding process where individually analyzed for particle size before and after compounding process and the results are shown in Figure 4-19, Figure 4-20, and Figure 4-21 for Large, Mid, and Fine batches respectively. It should be noted that particles were extracted from matrix after compounding by xylene extraction for the particles size analysis.

The Large batch had its particle length mostly in a range of 1,000 to 7,000 µm prior to compounding with number average particle length equal to 3,272 µm. However, a drastic drop in the particle length was observed after compounding. Particle length dropped below 3,000 µm with number average of 635 µm. This trend can be attributed to the shear and temperature degradation during the compounding process. Similarly, Hornsby et al. have reported that wheat particles, examined after solvent extraction from moulded composites, undergo significant damage during processing and loses its fibrous identity, becoming much more plate-like in character (Hornsby, Hinrichsen et al. 1997b).

A similar trend was also observed for the Mid-size wheat straw particles. The length of the Mid size particles prior to compounding was found to be in the range of 100 to 6,000 µm. After compounding it was found that all particles had length of 2,000 µm or lower. Further,

the number average particle length decreased from 1,882 µm to 717 µm. From these data it was concluded that both the Large and Mid-size ground wheat straw had similar particle final length distributions after compounding with most of particles length in a range from 100 to 2,000 µm. It can be concluded that choosing either Large or Mid-size would result in similar final particle length and subsequently similar stiffness for the final composite.

Data obtained for Fine-size particles showed that processing did not affect the particle size distribution as much compared to Large and Mid-size ground wheat straws. Before compounding most particles in the Fine-size sample had particle length between 50 to 3,000 µm; after compounding their length were found to be between 50 and 200 µm. The number average particle length decreased from 515 to 437 µm.

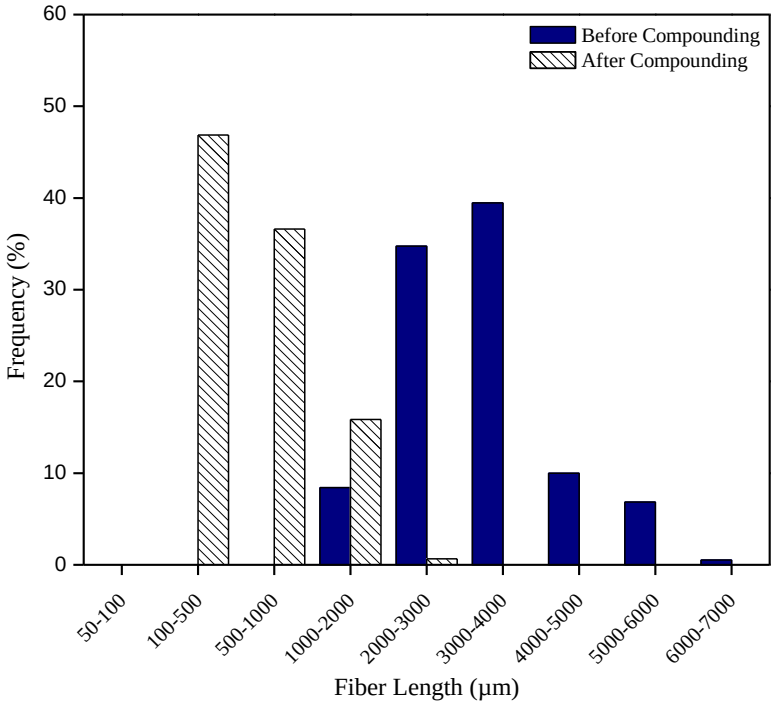

Figure 4-19 Particle Length Distribution for Large Batch Before and After Compounding

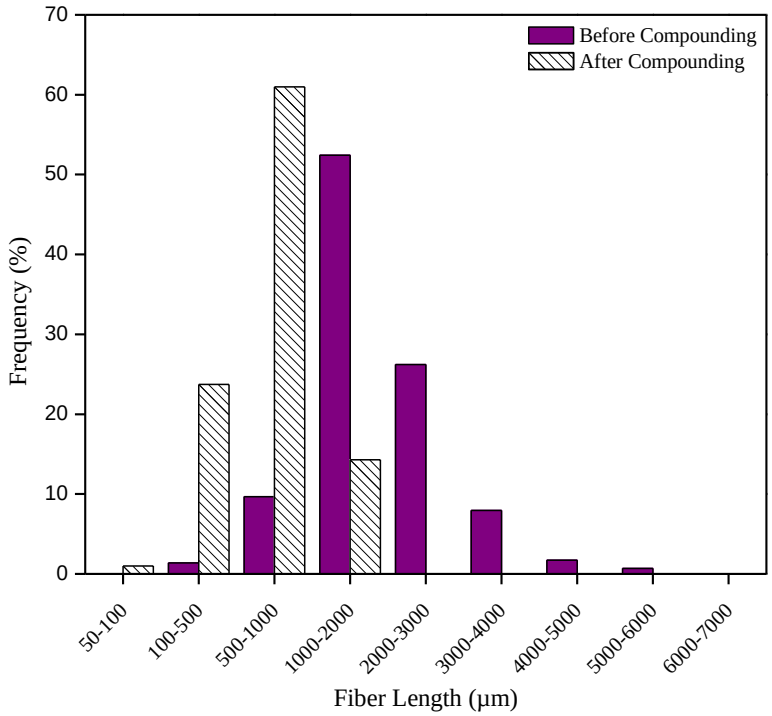

Figure 4-20 Particle Length Distribution for Mid Batch Before and After Compounding

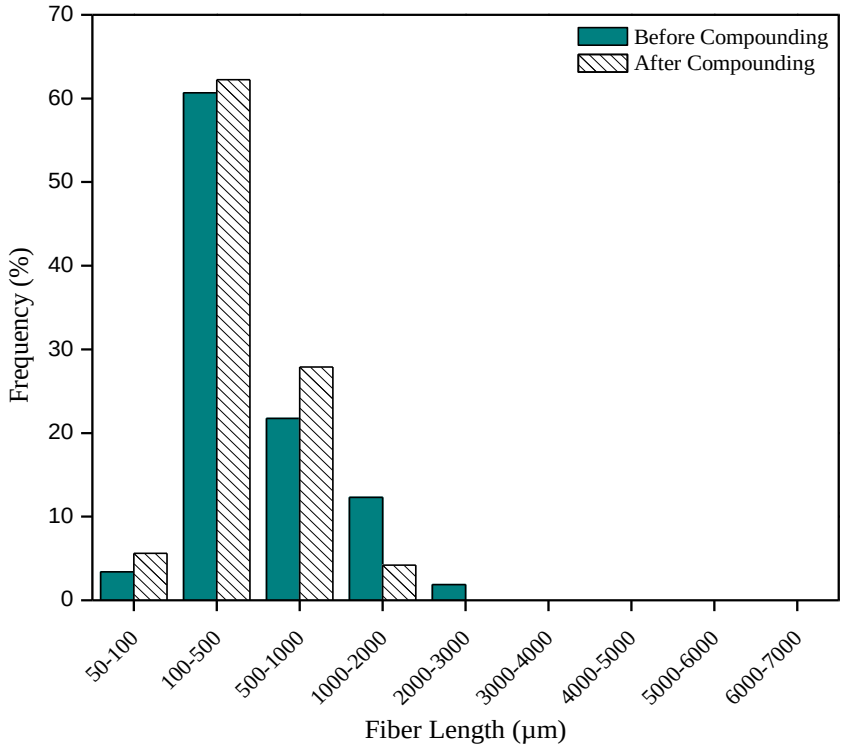

Figure 4-21 Particle Length Distribution for Fine Batch Before and After Compounding

The ground wheat straw presented a distribution of aspect ratios. It is well known that as the aspect ratio of the particle decreases, the efficiency of the particles in stiffening and reinforcing the matrix decreases (Kapustan Krüger 2007). The frequencies of aspect ratios observed for the wheat straw particles prior and after grinding are shown in Figure 4-22 to Figure 4-24. In general the maximum aspect ratio before compounding was limited to 30 for the Mid and Fine batches and to 20 for the Large batch. Surprisingly it was found that after compounding most particles in all three batches had aspect ratios between 1 and 10. Around 95 % of particles in the Large and Mid-size gWS had aspect ratios below 5 representing that most of the gWS used in this study after compounding is in the form of particulates as was found in earlier chapters of this work. In the case of the Fine batch, around 9 % of gWS showed aspect ratios higher than 5. Ground wheat straw in the Fine

batch is minimally affected by compounding process therefore; the values of aspect ratio are not much different from the AR value before compounding.

Based on this information it is concluded that the mechanism for particle size reduction during compounding is different for particles with different sizes. It is suggested that during the compounding stage the Large and Mid ground wheat straw particles were broken into smaller pieces which not only changed the average length but also the average width. It should be mentioned that the values of aspect ratio that were reported in earlier sections of this study (particle size analysis of gWS fractions) with high aspect ratio values (above 20 and higher) constituted a small amount (wt-%) of each batch.

Garcia et al. have reported that the higher aspect ratio of hemp fiber compared with the aspect ratio of wood fiber gave rise to better properties in PVC composites when hemp fiber was used as reinforcing agent (Garcia, Garmendia et al. 2008).

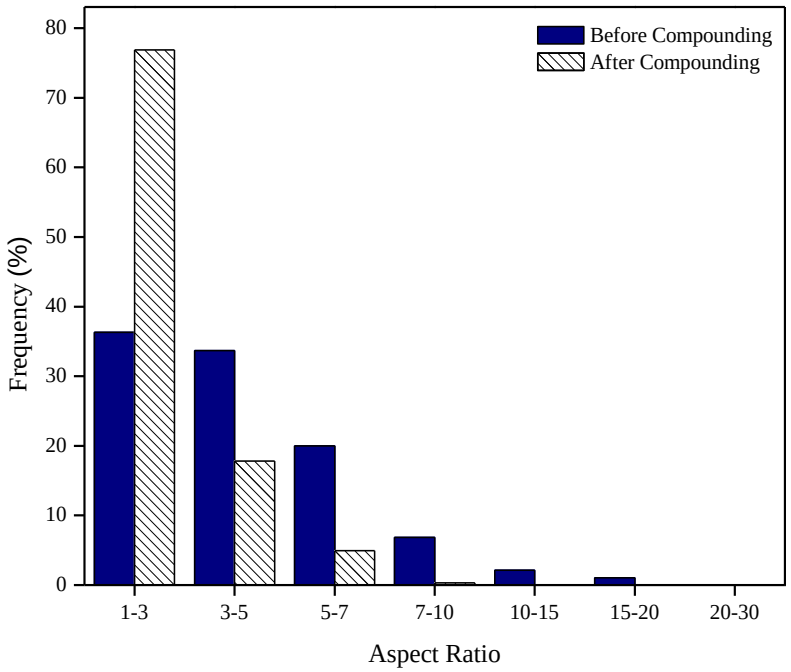

Figure 4-22 Aspect Ratio Distribution of Large Batch Before and After Compounding

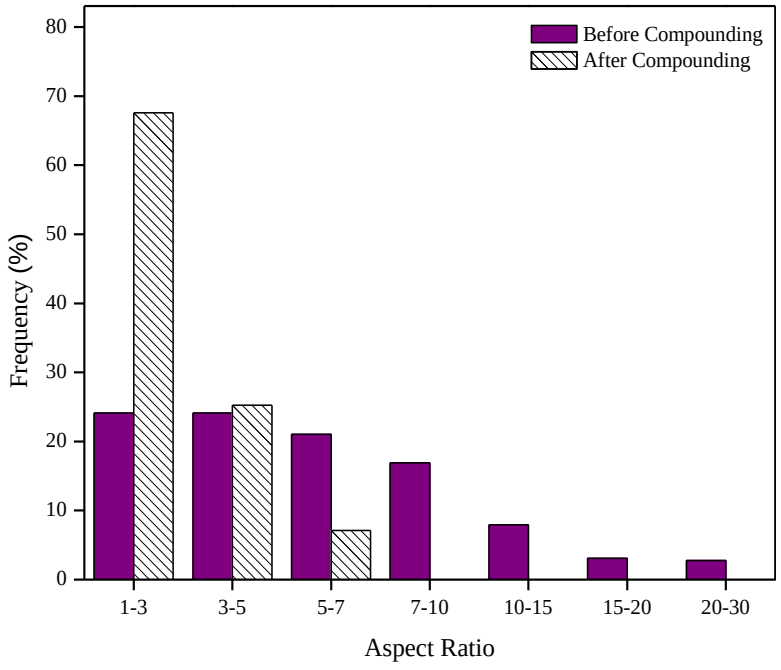

Figure 4-23 Aspect Ratio Distribution of Mid Batch Before and After Compounding

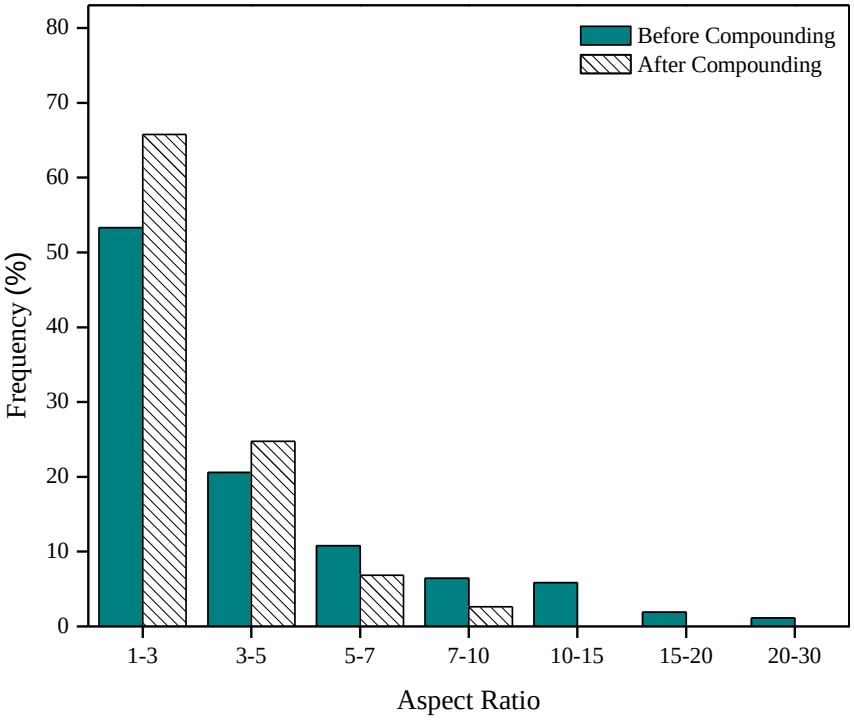

Figure 4-24 Aspect Ratio Distribution of Fine Batch Before and After Compounding

4.2.3 MORPHOLOGY

Morphology of the WSCPP composite samples obtained according to Table 4-6 were studied by scanning electron microscopy (SEM) analysis. Figure 4-25 (a)-(f) presents SEM micrographs of composite samples processed under similar conditions with different composition. The surface of freeze broken samples obtained after injection molding is used for SEM analysis. Figure 4-25 (a)-(c) show micrographs of composites containing 30, 40 and 50 wt% WS respectively (Run #1 to Run #3). It is evident from the micrographs that most particles are present in parallel to the surface of the composite sample indicating alignment of the particles during the injection molding (indicated by arrows) in 30 wt-% and 40 wt-% gWS composites, see Figure 4-25 (a)-(b). No particles alignment was obtained in the 50 wt-% gWS composite as shown in Figure 4-25(c). This is believed to be due to the high content of gWS which disturbs the tendency for alignment.

Although no particle alignment was found in the 50 wt-% gWS composite (Run#3), minimum number of fiber pullout was observed in these samples. Similar behavior was reported by Bledzki and coworkers where 50 wt-% natural fiber loading showed less fiber pullouts and debonding (Bledzki, Mamun et al. 2007). Further, in all these three samples, the particles is broken at the surface indicating that there is a good interfacial interaction between particles and polymer matrix.

Figure 4-25 (d)-(e) show the SEM micrographs of composite samples with 30 wt-% WS, 5 wt-% clay and 0 wt-% PP-MA (Run# 4). It is apparent from the micrograph that the interfacial interaction between the polymer matrix and the natural fiber is weak, as observed by the fiber pull-outs shown in circles. On the other hand, Figure 4-25 (f) shows the micrograph of composites sample having 30 wt-% WS, 5 wt-% clay and 4 wt-% PP-MA. The micrograph shows that there is a good interfacial adhesion between polymer matrix and WS. The good interfacial adhesion is due to the chemical linkage between the hydroxyl groups of natural fiber surface with maleic anhydride of PP-MA which in turn facilitate a better stress transfer from the polymer to the fiber. Bledzki et al. similarly found that the fiber pullout and debonding was reduced significantly and the adhesion between natural fiber and matrix were improved strongly due to addition of PP-MA for every fiber loading (Bledzki, Mamun et al. 2007).

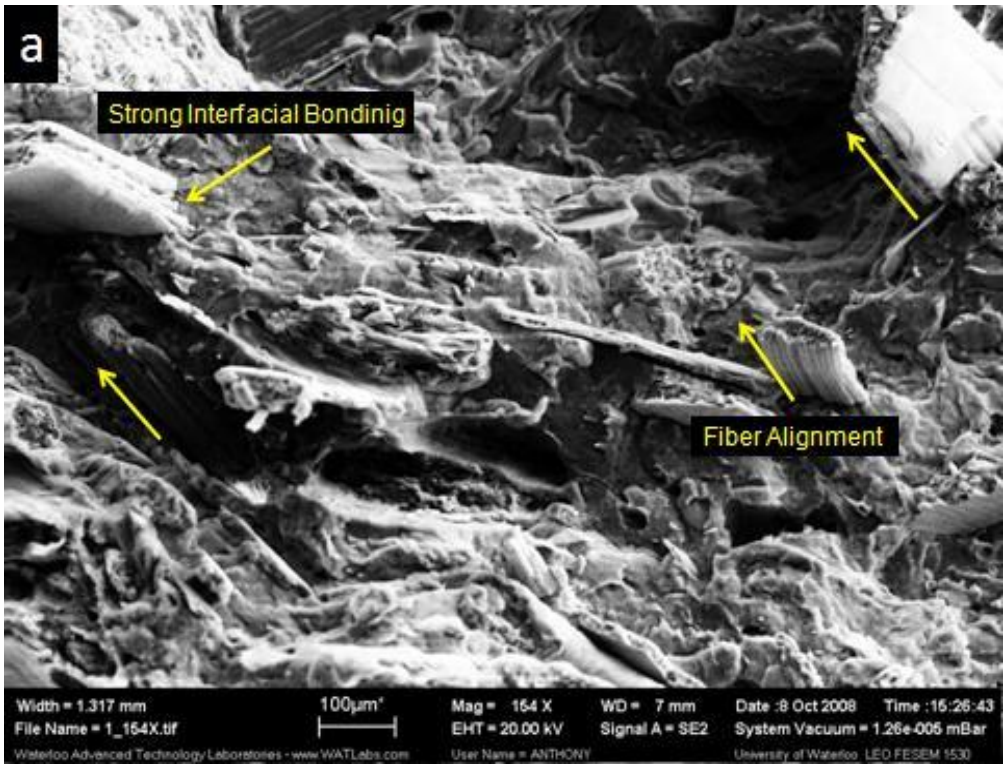
a
Strong Interfacial Bondinig
Fiber Alignment
Width = 1.317 mm
File Name = 1_154X.tif
100µm
Mag = 154 X
EHT = 20.00 kV
WD = 7 mm
Signal A = SE2
Date :8 Oct 2008
Time :15:26:43
System Vacuum = 1.26e-005 mBar
Waterloo Advanced Technology Laboratories - www.WATLabs.com
User Name = ANTHONY
University of Waterloo LEO FESEM 1530

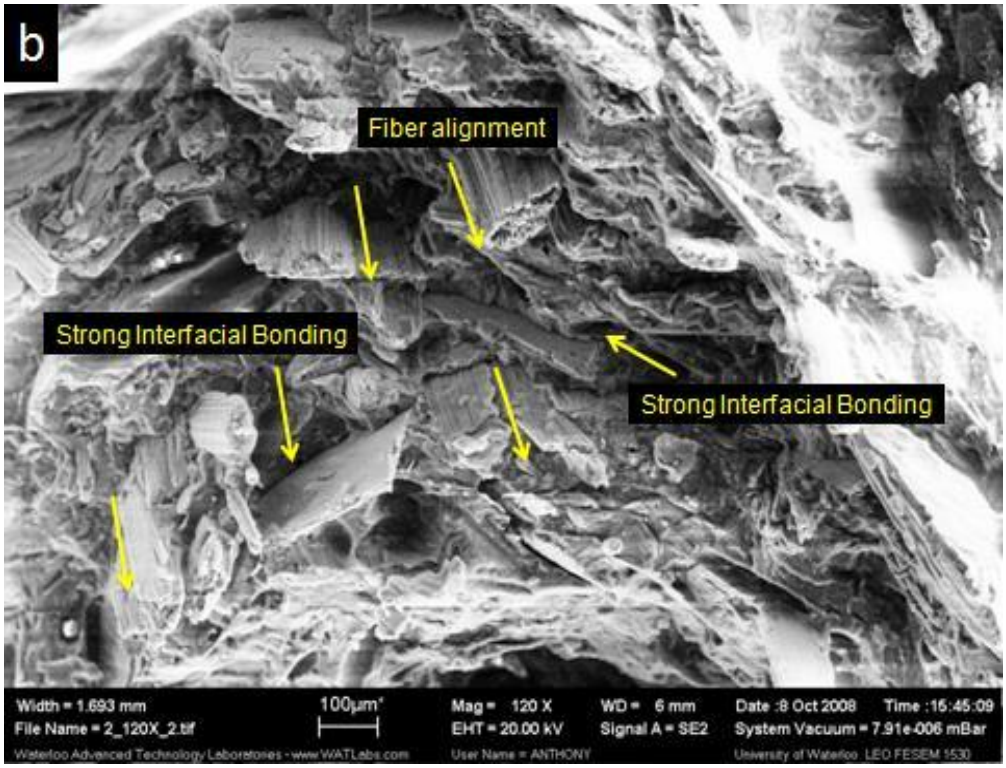
b
Fiber alignment
Strong Interfacial Bonding
Strong Interfacial Bonding
Width = 1.693 mm
File Name = 2_120X_2.tif
100µm
Mag = 120 X
EHT = 20.00 kV
WD = 6 mm
Signal A = SE2
Date :8 Oct 2008
Time :15:45:09
System Vacuum = 7.91e-006 mBar
Waterloo Advanced Technology Laboratories - www.WATLabs.com
User Name = ANTHONY
University of Waterloo LEO FESEM 1530

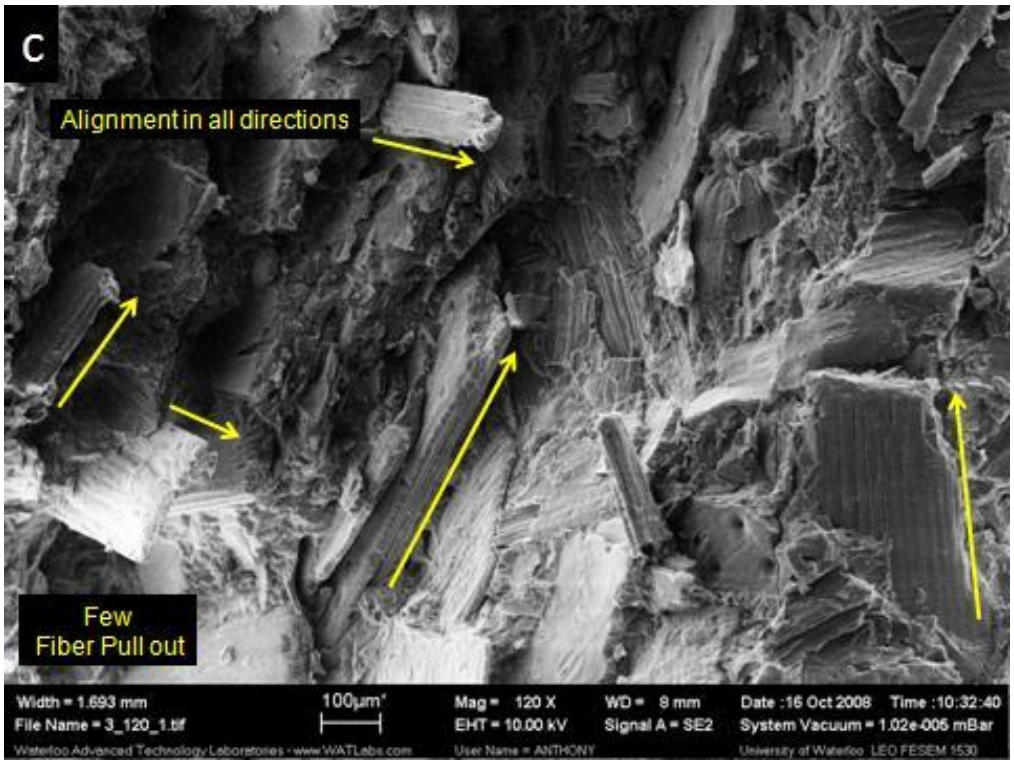
c
Alignment in all directions
Few
Fiber Pull out
Width = 1.693 mm
File Name = 3_120_1.tif
100µm
Mag = 120 X
EHT = 10.00 kV
WD = 8 mm
Signal A = SE2
Date :16 Oct 2008 Time :10:32:40
System Vacuum = 1.02e-005 mBar
Waterloo Advanced Technology Laboratories - www.WATLabs.com
User Name = ANTHONY
University of Waterloo LEO FESEM 1530

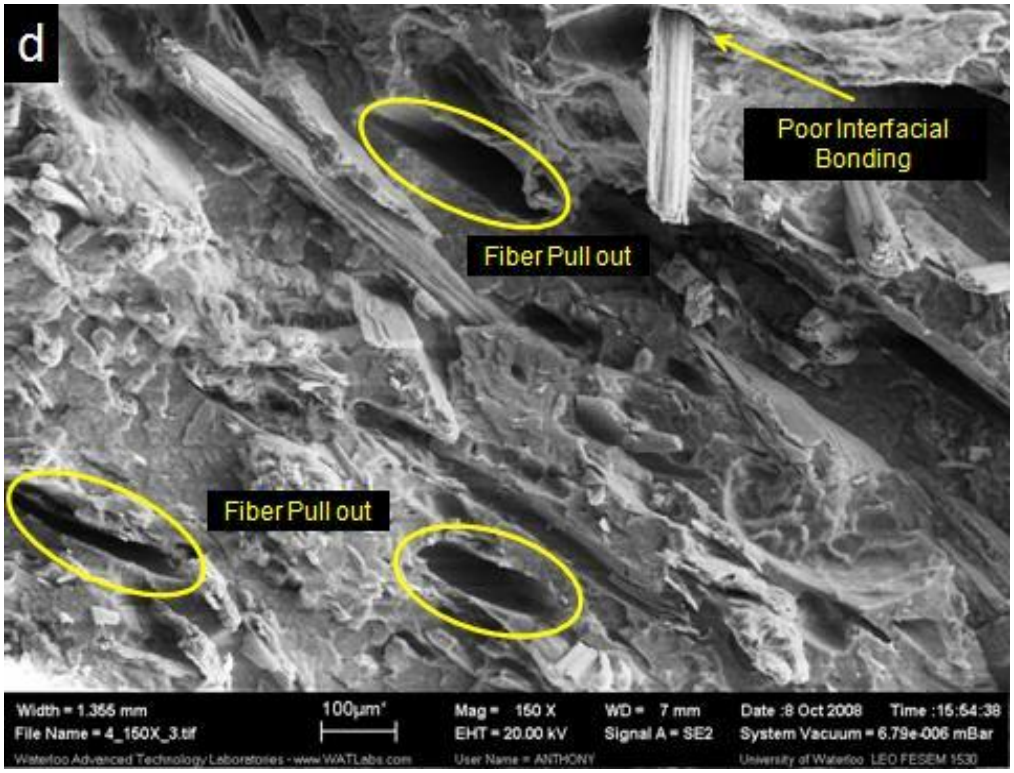
d
Poor Interfacial
Bonding
Fiber Pull out
Fiber Pull out
Width = 1.355 mm
File Name = 4_150X_3.tif
100µm
Mag = 150 X
EHT = 20.00 kV
WD = 7 mm
Signal A = SE2
Date :8 Oct 2008 Time :15:54:38
System Vacuum = 6.79e-006 mBar
Waterloo Advanced Technology Laboratories - www.WATLabs.com
User Name = ANTHONY
University of Waterloo LEO FESEM 1530

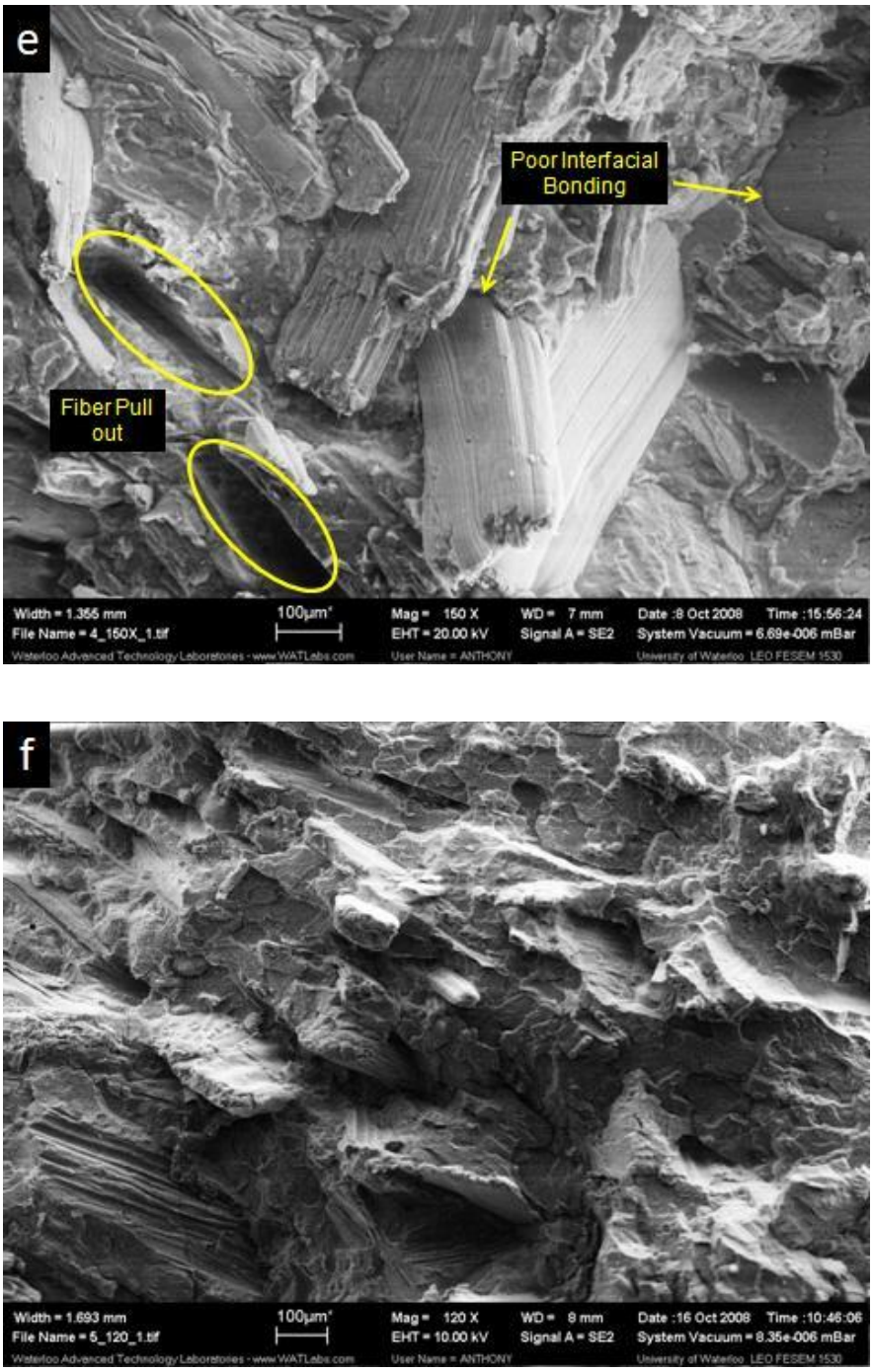

Figure 4-25 SEM of (a) 30wt-%WS 5wt-%Clay PP Composite with 2wt-% PP-MA, (b) 40wt-%WS 5wt-%Clay PP Composite with 2wt-% PP-MA, (c) 50wt-%WS 5wt-%Clay PP composite with 2wt-% PP-MA, (d) and (e) 30wt-%WS 5wt-%Clay PP Composite with 0wt-% PP-MA and (f) 30wt-%WS 5wt-%Clay PP Composite with 5wt-% PP-MA.

Figure 4-26 is a micrograph obtained from a composite of polypropylene and organo-clay. The mixing process must be capable to open the basal plane of the clay in order to intercalate some polymer chains in the matrix and even to break the crystal structure of the clay to ensure maximum specific surface contact between the organic modifier of the clay and some intercalated polymer chains (Pascual, Fages et al. 2009). However, melt mixing at our operating conditions was not sufficient to ensure intercalation or exfoliation of the clay particles and therefore the product obtained is a conventional composite (explained further in the Secion on X-ray diffraction). This was also observed in the micrograph where most of the clay particles were clumped together, thus acting as micron size fillers (indicated by the arrows). It was found that most of the clay particles are uniformly distributed in the polymer phase; however clay particles were also found to be also on the surface of the wheat straw.

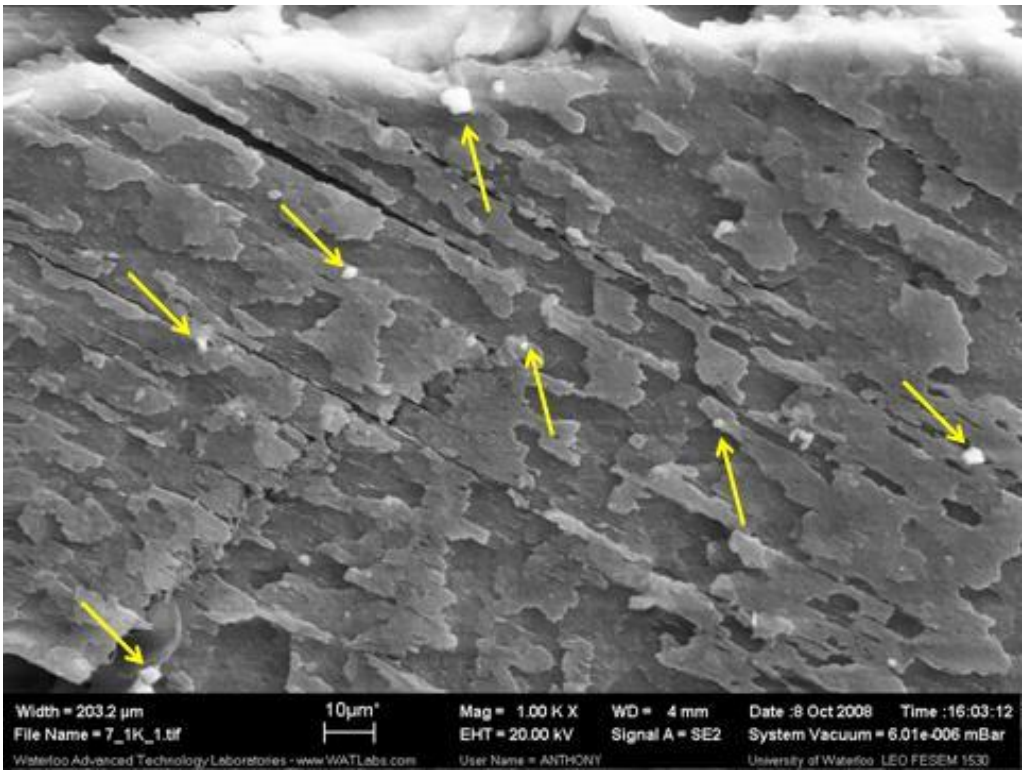

Figure 4-26 SEM of Polypropylene Organo-Clay Composite (Run#8). Arrows Indicate Clumped Clay Particles in Micron Size.

4.2.4 X-RAY DIFFRACTION (XRD)

The clay mineral has a layered structure. When the polymer chains enter the layered structure without destroying the layered hierarchy, the process is called intercalation. When the polymer chains separate and disperse the layered structure in individual layers within the polymer matrix the process is called exfoliation. The XRD analysis helped to identify intercalation and/or exfoliation levels by identifying the main diffraction peaks in the crystalline clay structure (Kádár, Százdi et al. 2006).

The clay mineral intercalation and exfoliation were studied by XRD. The XRD curves are shown in Figure 4-27. The WSCPP composites prepared with 0, 2 and 5 wt-% clay (Run #7, Run #6, Run #1) were investigated with XRD and were compared with pure PP and pure clay powder (Cloisite® 15A). XRD pattern of the organo-clay showed a diffraction peak at 2.65^{o} corresponding to (001) plane (Mandalia, Bergaya 2006). This peak position is representative of an interplanar d-spacing of 3.33 nm.

The XRD pattern of WSCPPCs with different clay content showed a decrease in the peak intensity as a consequence of lower amount of clay in the composites compared to pure clay powder. It was found that there is a minor shift towards lower values of 2θ which corresponds to a low level of intercalation by compounding. Composites of Run#1 and Run#6 had their diffraction peaks at 2.45^{o} and 2.40^{o} (d-spacing of 3.6 and 3.7 nm respectively) which shows a 10 % special increase in organo clay galleries compared to pure clay powder. It should be mentioned that such an increase is not an indication of any exfoliation and only low intercalation is expected.

In agreement with this result, Pacual et al. have reported that the interplanar distances over 70 Å are representative for total exfoliation which corresponds to 2θ values close to 0^{o}(Pascual, Fages et al. 2009). In order to quantify the level of intercalation or any minor

exfoliation of the clay particles, it is recommended to use transmission electron microscopy (TEM) (Zhang, Jiang et al. 2005). However, TEM was not performed on the samples in this study and no proof of intercalation or minor exfoliations are proposed.

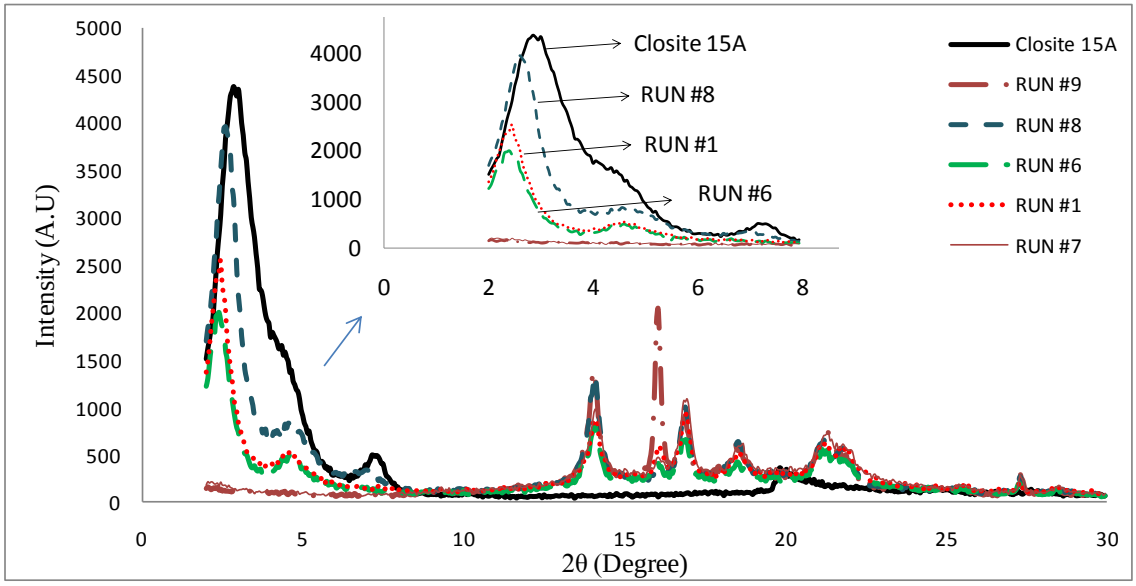

Figure 4-27 XRD Pattern of Different WSCPPCs, Pure PP, and Organo-Clay

4.2.5 THERMAL PROPERTIES

CRYSTALLINITY, MELTING AND CRYSTALLIZATION TEMPERATURES

Differential scanning calorimetry (DSC) analysis was performed in order to identify the thermal and structural properties of the WSCPPCs. Information in regards to crystallinity of the composites are critical as crystallinity can directly affect the mechanical properties of the material. Crystallinity is obtained by quantifying the heat required to melt the composite and normalizing this value to that of a 100 % crystalline polypropylene (209 J/g) according to the following equation (Le Digabel, Boquillon et al. 2004):

$$Crystallinity\ (\%) = \frac{\Delta H}{\Delta H^{\circ}} \times \frac{100}{w} \qquad \text{Equation 4-1}$$

Where ΔH is the heat of fusion of the WSCPP composite, ΔH° is the heat of fusion of the 100 % crystalline polypropylene, and w is the weight fraction percentage of the polymer in the composite.

Table 4-8 summarizes the information obtained from DSC analysis for WSCPP. It was found that the addition of gWS to the polymer increased the crystallinity of the composites; however, this increase was not proportional to the amount of gWS. This trend suggested that the gWS particles act as nucleating agents hence promoting the creation of more crystalline spherullites and a higher crystallinity. Similar results have been shown by Ng in which the degree of crystallinity was increased by the addition of gWS (Ng 2008).

The crystallization temperature was increased with the addition of gWS, however the increase was found not to be proportional to the amount of gWS. Similar results have been showed by Kruger where addition of natural fibers increased the crystallization temperature of polypropylene disproportionally (Kapustan Krüger 2007). On the other hand, Averous et al. have argued that the crystallization temperature and the heat of fusion of the polymer matrix reduce with higher content of filler because filler act as diluents to the PP matrix (Avérous, Le Digabel 2006). It is important to mention that the DSC results shown in this work have been replicated and the reproducibility of these data has been considered. Therefore, results presented by DSC analysis are not in agreement with Averous.

The effect of the PP-MA on the crystallization of the composites was studied. It was found that the degree of crystallinity and the temperature of the crystallization are lowered by the addition of PP-MA. The reduction in crystallinity can be explained by the increase in the amorphous domain of the composite by addition of low molecular weight and mainly amorphous coupling agent. Mandacho et al. reported that in PP/EPDM/Flax fiber composites the use of PP-MA as coupling agent hindered the transcrystallinity (Manchado, Arroyo et al. 2003). In agreement with Mandacho, Avella has reported that the low degree

of crystallinity observed in samples containing coupling agents can be attributed to the PP-MA/ET-MA nucleating action, which produces a smaller size of spherulites and consequently a more pronounced presence of amorphous phase in the system (Avella, Bozzi et al. 1995).

Studies on crystallization behaviour of PP composites filled with calcium carbonate ($CaCO_3$) of different particle sizes showed that $CaCO_3$ of smaller particle sizes resulted in lower composite crystallinity (Zhang, Jiang et al. 2006). Similar trend was seen for the composites with organo-clay. Comparing the crystallinity values of Run#9 (Pure PP) with Run#8 (PP + clay) showed 18 % decrease in the value of crystallinity as organo-clay was added to the polymer. This is believed to be due to disturbance of the polymer matrix crystalline structure by the clay particles.

Table 4-8 DSC Analysis of WSCPPCs Based on WS, PP-MA, and Clay Content

Sample ID	Crystalization Onset Temp.* (°C)	Crystaization Temp.* (°C)	ΔHc (J/g)	Melt Onset Temp.* (°C)	Melt Temp.* (°C)	ΔHm (J/g)	Crystalinity (%)
Run #1	121.66	116.85	60.01	153.57	163.61	55.25	41.02
Run #2	120.60	114.24	68.40	153.37	165.48	62.20	49.60
Run #3	123.49	119.45	48.28	155.23	160.71	45.60	43.64
Run #4	122.80	118.13	65.80	154.51	164.01	61.60	42.11
Run #5	121.36	115.67	60.41	153.13	164.26	55.08	37.65
Run #6	122.13	116.88	61.64	153.43	163.71	55.86	38.18
Run #7	122.69	117.39	66.82	153.69	163.65	62.48	42.71
Run #8	116.56	112.56	88.19	150.80	169.55	70.67	33.81
Run #9	117.81	114.69	91.09	152.70	165.57	83.59	40.00

* Temperature; DSC curved available in the Appendix.

THERMAL DEGRADATION AND STABILITY

Thermal gravimetric analysis was performed on composite samples presented in Table 4-6. It was found that all the samples have two main decomposition peaks. The first decomposition peak represents the degradation of the wheat straw at temperatures around 320 ^{o}C (close to the main degradation of cellulose) and the second peak representing polypropylene degradation around 420^{o}C (Zhang, Jiang et al. 2006) as indicated in Table 4-9.

Mengeloglu et al. have reported on thermal stability of the wheat straw flour-recycled thermoplastic composites. Similar to the results presented in this work, the filler's decomposition peak was found to be at 330 ^{o}C while the polymers decomposition peaks were at 470 ^{o}C and 420 ^{o}C for HDPE and PP composites respectively (Mengeloglu, Karakus 2008).

Table 4-9 TGA Analysis of WSCPPCs under Nitrogen at 10°C/min

Sample Id	Temp.* at 1 wt-% Degradation (°C)	Decomposition Peak 1 (°C)	Weight Loss (wt-%)	Decomposition Peak 2 (°C)	Weight Loss (wt-%)	Ash (wt-%)
Run #1	244.76	320.77	18.32	451.1	70.83	8.95
Run #2	233.08	321.04	25.46	450.26	60.53	7.08
Run #3	228.78	322.02	32.65	452.99	49.48	10.88
Run #4	242.30	322.61	18.06	448.24	71.57	5.63
Run #5	240.46	322.18	20.59	450.98	66.88	6.61
Run #6	242.92	323.51	17.84	450.38	73.25	3.15
Run #7	239.23	320.68	18.34	419.70	73.83	1.96
Run #8	292.10	0.00	0.00	423.19	97.15	2.80
Run #9	309.39	0.00	0.00	399.69	99.70	0.17

* Temperature

Figure 4-28 (a)-(b) show the TGA and derivative thermogravimetric analysis (DTGA) graphs obtained from the TGA analysis to investigate the effect of the filler loading on the thermal properties of the composite. No difference was observed in the thermal properties of the composites except in the onset temperature of degradation. The composite with the highest amount of gWS (Run #3) had the lowest onset temperature of degradation. This observation could be related to the amount of lignin which becomes more significant as the filler loading is increased.

Figure 4-29 (a)-(b) show the TGA and DTGA graphs obtained to investigate the effect of PP-MA on the thermal properties of the composites. It was expected that a better impregnation of the filler by polypropylene matrix would increase the thermal stability of the composites. However, in this study such a result was not obtained. Similar to this observation Araujo et al. have reported that composites compatibilized with PP-MA are less stable, while composites with no compatibilization are more stable (Araujo, Waldman et al. 2008). One possible explanation is that the composites with compatibilizers present

more interfacial interaction due to reaction between the hydroxyl groups of the natural fiber surface and the maleic anhydride. This contact promotes more interaction between the degradation processes of the two components. In other words, degradation of one component may be accelerating the degradation of the other component. Another explanation for such behaviour could be due to the presence of peroxides residues used to graft maleic anhydride to the polymer (Araujo, Waldman et al. 2008).

The addition of organo-clay has increased the thermal stability of the composites as shown in Figure 4-30 (a)-(b). It was found that addition of clay improved the onset of the degradation of the composites (slightly). It is possible that clay particles are well dispersed on the surface of the gWS or inside the polypropylene matrix. Based on these thermographs, it was concluded that clay has higher effects on the thermal stability of the polymer than the gWS particles indicated by the shift in the second decomposition peak.

In agreement which this work, Zhang et al. have observed a 20 ^{o}C increase in the onset degradation of polyethylene upon addition of 3 wt-% and 8 wt-% tricaly II (Zhang, Jiang et al. 2006, Zhang, Jiang et al. 2005).

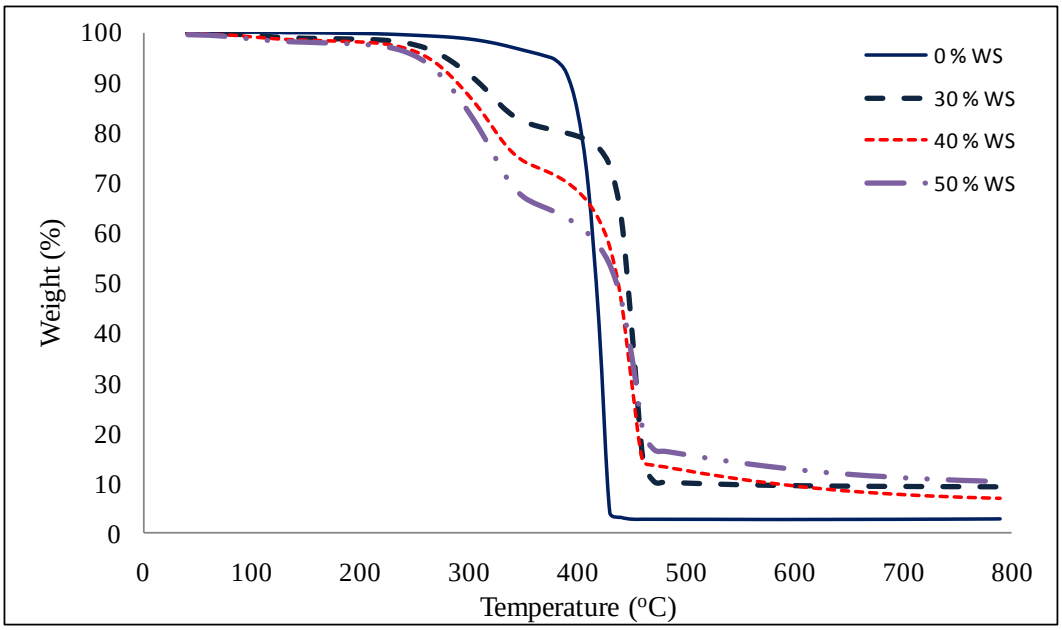

(a)

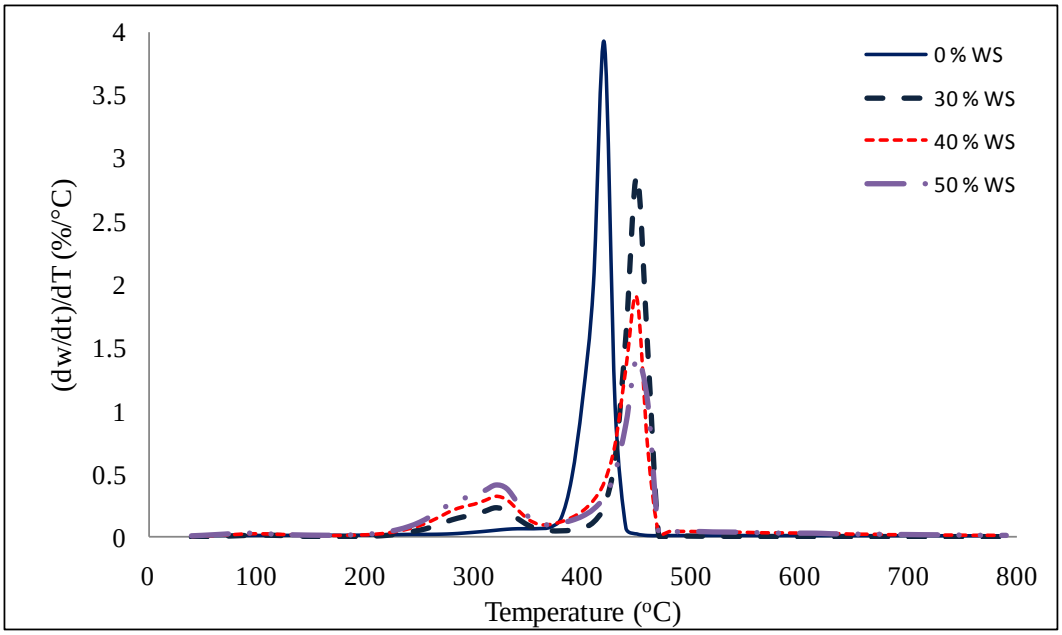

(b)

Figure 4-28 TGA (a) and DTGA (b) Curves for WSCPPCs at a Heating Rate of 10°C/min in Nitrogen Based on gWS Loading in Polypropylene

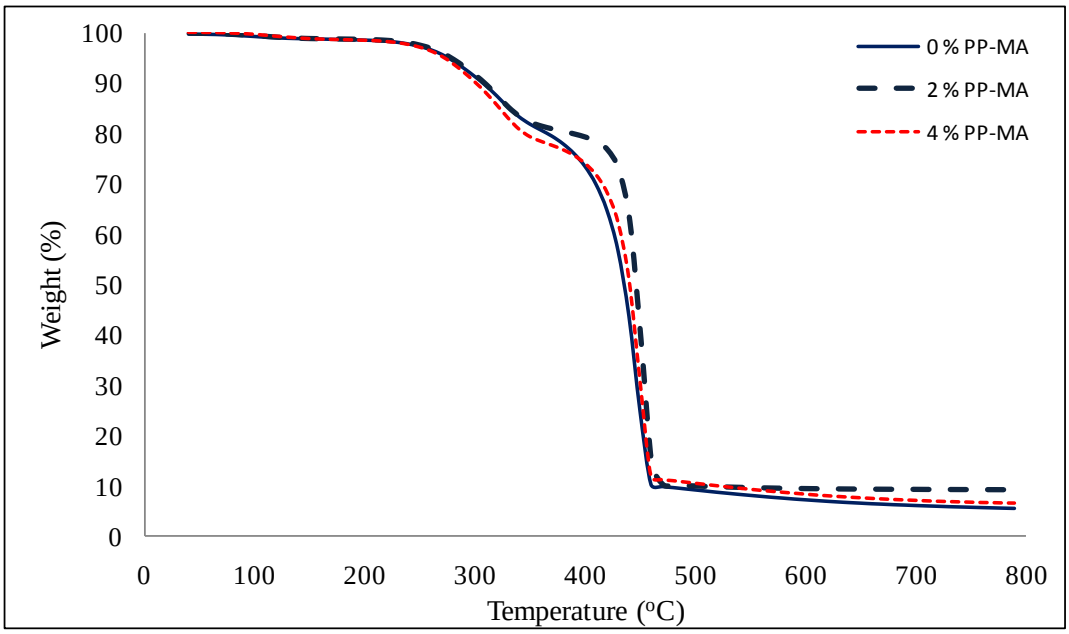

(a)

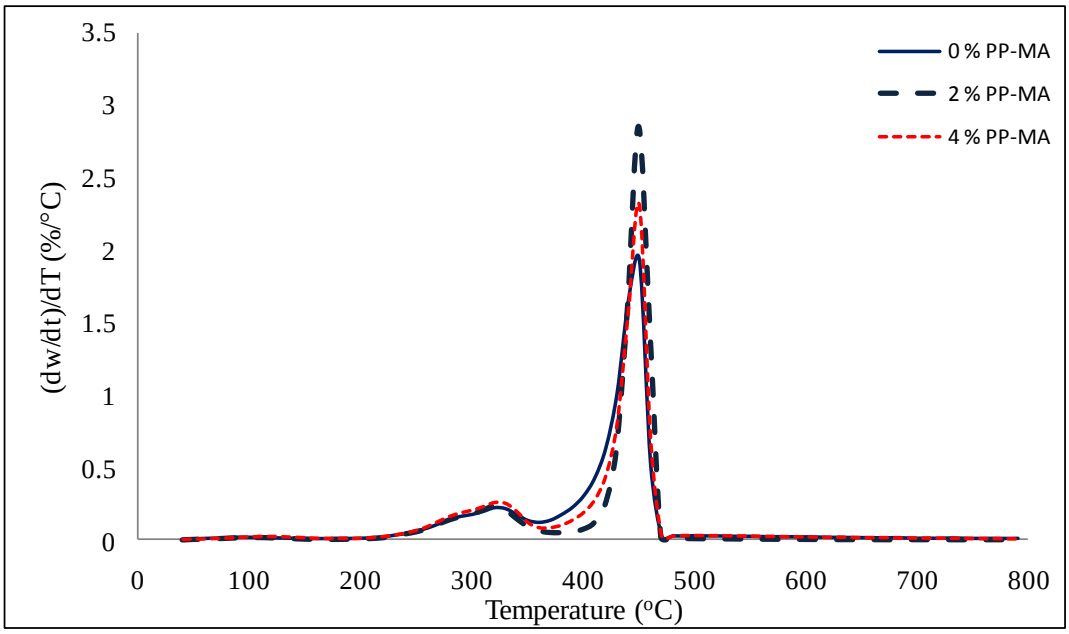

(b)

Figure 4-29 TGA (a) and DTGA (b) Curves for WSCPPCs at a Heating Rate of 10°C/min in Nitrogen Based on PP-MA Loading in Polypropylene

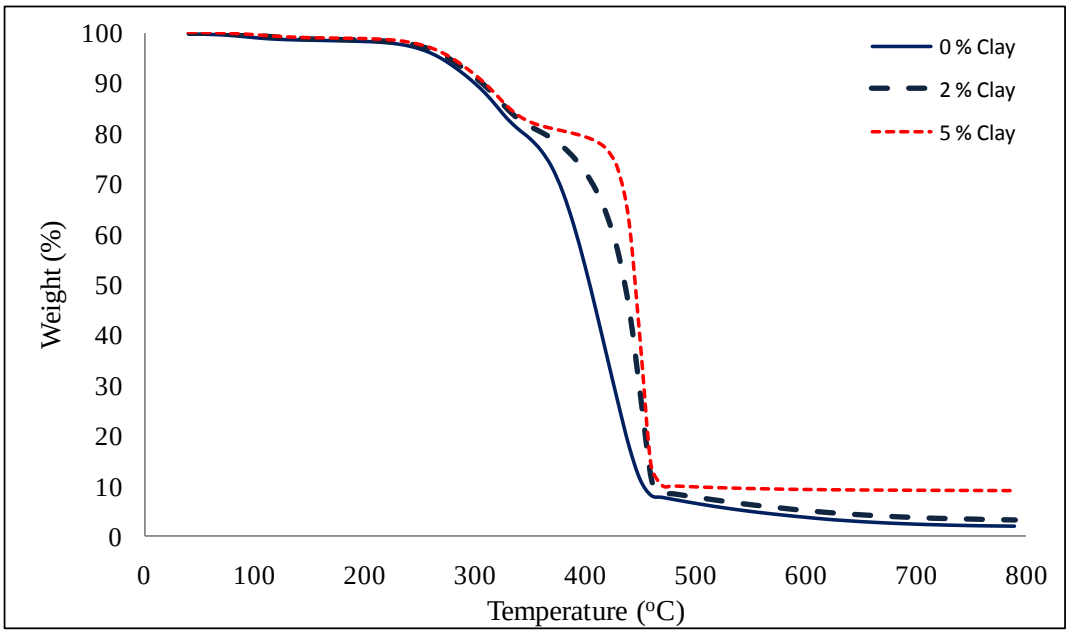

(a)

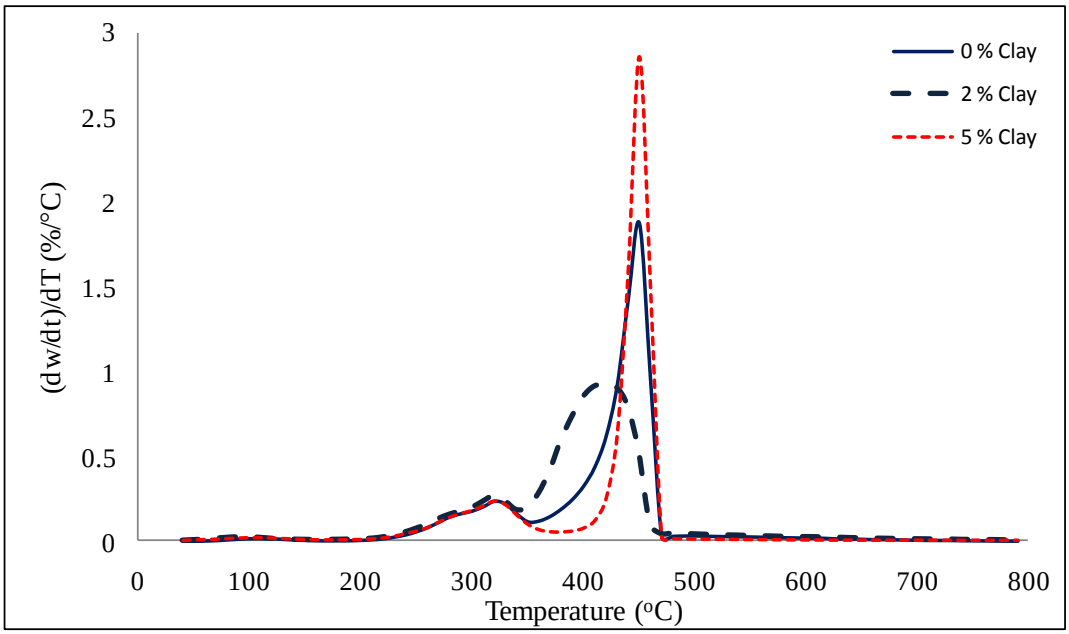

(b)

Figure 4-30 TGA (a) and DTGA (b) Curves for WSCPPCs at a Heating Rate of 10°C/min in Nitrogen Based on Organo-Clay Loading in Polypropylene

4.2.6 WATER ABSORPTION

The water absorption plots are presented in Figure 4-31 (a)-(c). The increase in weight of composite samples was due to water absorption. In order to study the effect of WS in a composite on water absorption properties, the composition of WS was varied between 0-50 wt-% keeping other components constant during the preparation of the composite.

Figure 4-31 (a) presents the characteristic water absorption plot for different quantity of WS. It was found that the sample having 0 wt-% WS did not absorb any significant amount of water even after exposing the sample to water for about 4 months. This observation suggests that moisture only penetrates into composites through the gWS. The composite sample having 30 wt-% WS (Run #1) absorbed about 10.2 wt-% of water and got saturated in about 90 days. Composite samples having 40 wt-% WS (Run #2) absorbed about 12.0 wt-% water and reached saturation in 70 days and the composite sample having 50 wt-% WS (Run #3) absorbed about 17 wt-% water and reached saturation in a period of only 40 days. The higher water absorption in the samples having WS are due to the good water absorption property of WS. Further, the results of the present study indicated that, the higher the WS content, the higher the water absorption.

Thomas et al. in their study on moisture absorption properties of pineapple-leaf fiber and LDPE have reported that the moisture absorption increased almost linearly with the natural fiber loading (Thomas, George et al. 1998). Similar observations are made in literature on wood based polypropylene composites (Tajvidi, Najafi et al. 2006). The reason for these observations is because of the affinity of water molecules and the hydrophilic hydroxyl groups on the surface of gWS.

The effect of PP-MA on water absorption was studied by varying the PP-MA content at 0, 2 and 4 wt-% and keeping other components constant. The water absorption behaviour of

these samples is presented in Figure 4-31(b). The composite sample having no (Run #4) showed higher water absorption during the initial period (within 40 days) of exposure of samples to water. However, the rate of water absorption was reduced slowly and reached a maximum of 9 wt-% and reached saturation in about 90 days.

The composite sample which had 2 wt-% of PP-MA (Run #1) showed slightly slower water absorption properties during initial stages and reached a maximum of 10.2 wt-% and was saturated in 90 days. The composite sample having 2 wt-% of PP-MA absorbed more water before reaching the saturation point compared to composite sample having 0 wt% PP-MA. However, this behaviour was not predicted since the presence of PP-MA in sample should reduce the hydrophilic nature of the composite. The reason for the low weight gain, for the composite sample having no PP-MA after 40 days, may be due to leaching of some low molecular weight components of natural fiber. The sample having 5 wt-% PP-MA (Run #5) showed reduced water absorption about 8 wt-% and reached saturation in 90 days.

In order to investigate the effect of clay on water absorption, the amount of clay during compounding was varied at 0, 2 and 5 wt-% keeping other components constant. The characteristic water absorption plots for the samples are presented in Figure 4-31(c). In all three samples saturation point was reached at almost in 90 days. However, the percentage of water absorbed before the saturation was different. The composite sample having no clay (Run #7) absorbed around 7.5 wt-% water, composite having 2 wt-% of clay (Run #6) absorbed slightly more water of around 8 wt-% and the composite with 5 wt-% of clay showed highest amount of water absorption about 10.2 wt-% (Run #1).

The water absorption behaviour of these composites indicated that the organically modified clay had a tendency towards water absorption, hence the amount of water absorption increased with increasing the clay content.

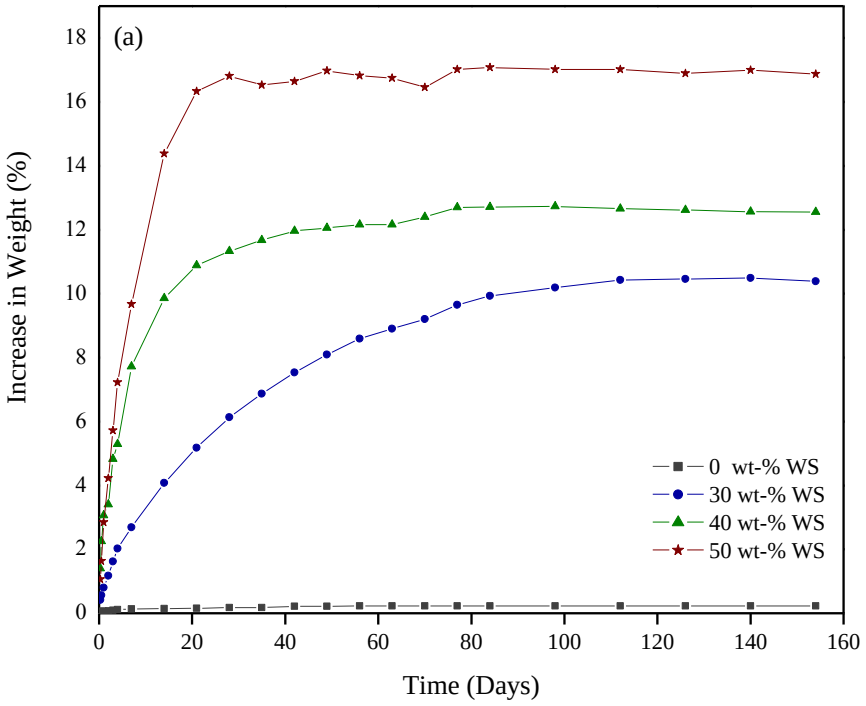
(a)
Increase in Weight (%)
Time (Days)
0 wt-% WS
30 wt-% WS
40 wt-% WS
50 wt-% WS

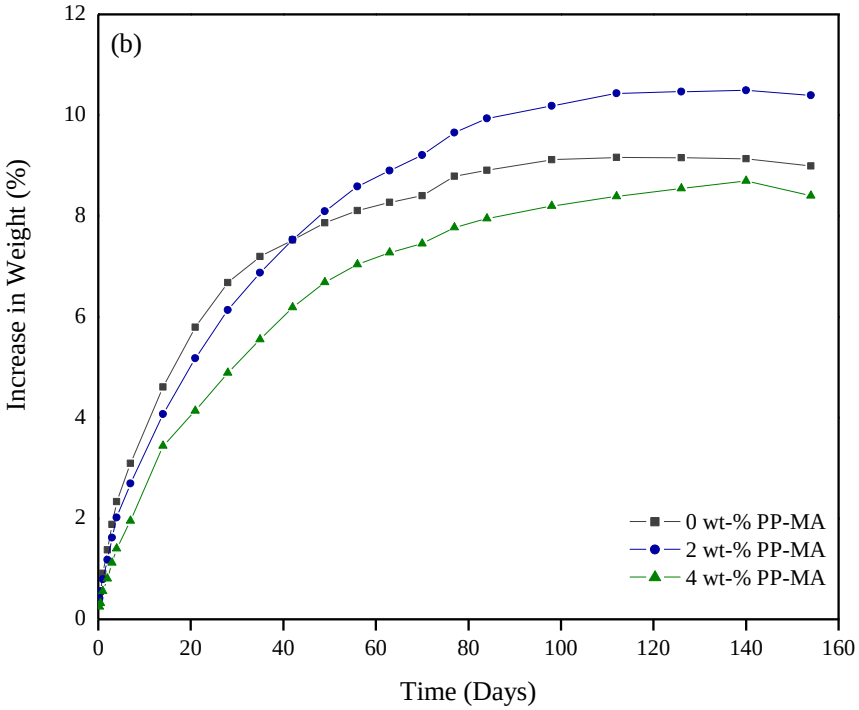
(b)
Increase in Weight (%)
Time (Days)
0 wt-% PP-MA
2 wt-% PP-MA
4 wt-% PP-MA

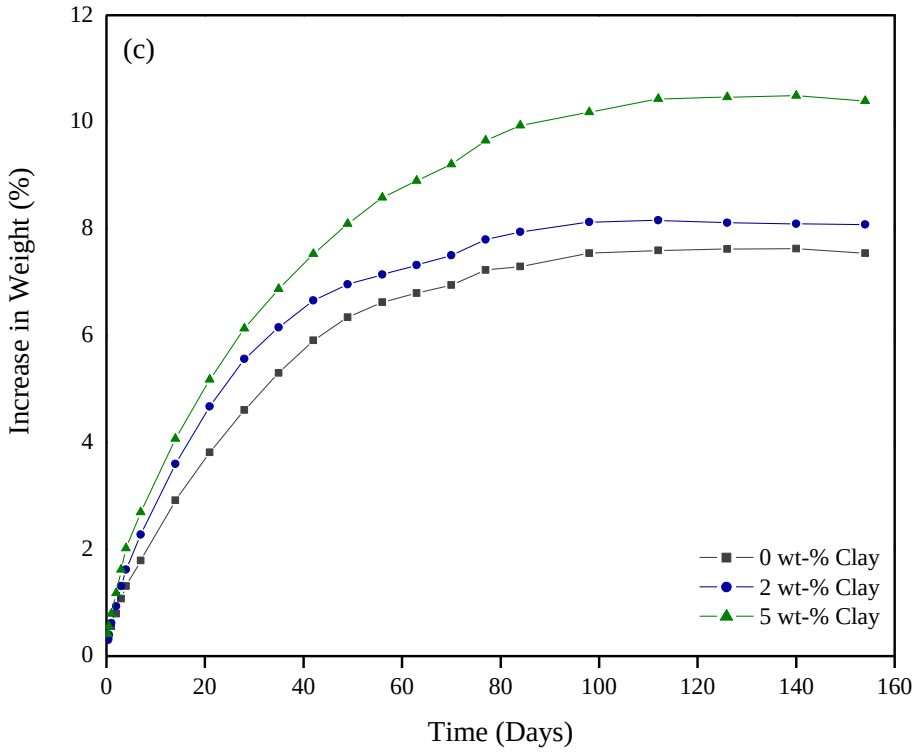

Figure 4-31 Water Absorption Properties of WS-PP-Clay Composites with Respect to (a) WS Content, (b) PP-MA Content, (c) Organo-Clay Content.

Similar study was performed on composite samples listed in

Table 4-7 to investigate the effect of WS size on the water absorption properties of the composites. Composites of WSPP with different sizes of gWS (Run #11 to Run #14) were prepared and submerged in water for four months. The water absorption results obtained from these composites are shown in Figure 4-32.

It was found that the particle size of gWS is not affecting the water absorption properties significantly. All batches except the Large size batch had a very similar water absorption trend to each other for the first 60 days after which the Blend batch started to deviate from the rest. The Fine and the Mid batches reached saturation in 100 days with 9.3 % and 9.4 %

increase in the composite weight respectively. The Large and Blend batches also reached saturation in around 100 days with maximum water absorption values of 10.3 % and 10.0 % respectively. From these values it was concluded that the particle size of gWS is not the main factor which dictates the water absorption properties of the composite. Rather it was the amount of the gWS and the coupling agent that were mostly affecting this property.

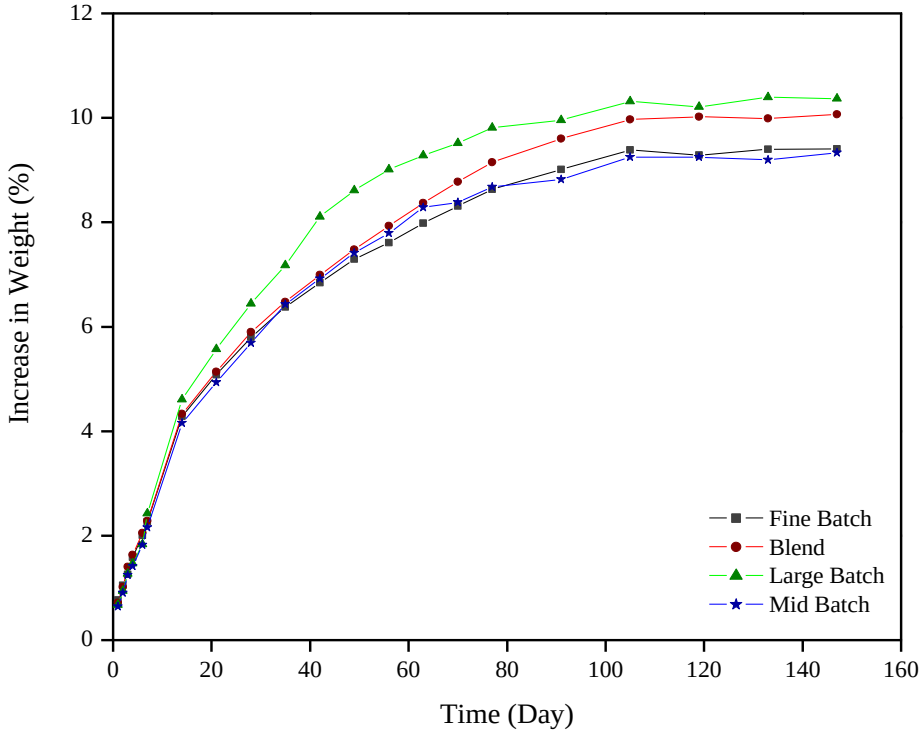

Figure 4-32 Water Absorption Properties of WSPP Composites with Respect to gWS Size

It has been reported that moisture absorption into the composite materials consists of three mechanisms: (i) diffusion of water molecules inside the microgaps between polymer chains; (ii) capillary transport of water molecules into the gaps and flaws at the interface between fibers and the polymer due to the incomplete wettability and impregnation; and (iii) transport of water molecules by micro cracks in the matrix, formed during the compounding process (Espert, Vilaplana et al. 2004). To model the absorption process, the diffusion mechanism was used. Knowledge of diffusivity coefficient and transport

properties is critical for predicting the water absorption behaviour of the composite and their physical and mechanical properties. The diffusivities along with n and k constants of all the composite samples were calculated and are represented in Table 4-10.

From Table 4-10 it was found that the value of n for most of the composite samples is slightly higher than 0.5, indicating that the process of water absorption is non-Fickian. The deviation from Fickian diffusion could be due to the active participation of other two mechanisms during the immersion period of composites in water. It is reported that deviation from the Fickian diffusion could be a result of the natural fiber swelling, natural fiber matrix interface weakening, micro-cracking, and leaching (Espert, Vilaplana et al. 2004). Pure polypropylene (Run #8) and polypropylene with 5 wt% clay (Run #9) did not absorb much water which was indicated by their corresponding low n values. The value of k was the same for most of the composite samples which is indicative of similar kind of interaction between water and composites.

The diffusivity (D) values for composite samples are presented in Table 4-10. The value of D is a measure of how fast the water molecules enter into the composite samples. The value of D observed to be increasing for composite samples with increase in WS content (Run #1, Run #2, and Run #3). The diffusivity values were observed to be high for composites without any coupling agent compared to that of samples with coupling agent. Furthermore, the diffusivity for samples with clay was higher than for those samples without clay indicating that the presence of clay enhances the water absorption. It should be mentioned that the D values have been compared with literature values and are in the correct range (Gouanve, Marais et al. 2007).

Table 4-10 Diffusivity Values (D) and Moisture Constants (n, k) of WSCPPCs

ID	Wheat straw (wt%)	Clay (wt%)	PP-g-MA (wt%)	D x 10^{-8} (cm^2/sec)	n	k
Run #1	30	5	2	0.307	0.577	0.01
Run #2	40	5	2	1.037	0.742	0.01
Run #3	50	5	2	1.367	0.689	0.02
Run #4	30	5	0	0.472	0.635	0.01
Run #5	30	5	4	0.322	0.637	0.01
Run #6	30	2	2	0.412	0.626	0.01
Run #7	30	0	2	0.297	0.617	0.01
Run #8	0	5	2	0.084	0.315	0.08
Run #9	0	0	0	0.014	0.101	0.41

Similar analyses were performed on samples listed in Table 4-7 (last four) and results are shown in Table 4-11. The constant n for all composites were higher than 0.5 representing a non Fickian process. The k values were almost constant for all four composites since all experiments were performed at the same temperature. Based on diffusion coefficients it was found that the particles which are smaller in size absorb water faster. This trend was expected since smaller particles provide larger surface areas to water and hence have higher diffusion coefficient.

Table 4-11 Diffusivity Values (D) and Moisture Constants (n, k) of WSCPPC

Sample ID	Wheat straw (wt-%)	Clay (wt-%)	PP-g-MA (wt-%)	D x 10^{-8} (cm^2/sec)	n	k
Run#11	30	0	2	0.29	0.61	0.01
Run#12	30	0	2	0.18	0.68	0.01
Run#13	30	0	2	0.14	0.68	0.01
Run#14	30	0	2	0.21	0.64	0.01

4.2.7 MELT FLOW INDEX (MFI)

MFI of different formulations of WSCPPCs (Table 4-6 and Table 4-7) were measured in order to investigate the effect of gWS content, PP-MA %, Clay % and filler size on the flow properties of the composites. The results are summarized in Table 4-12.

The addition of 30 wt-% gWS to polypropylene drastically reduced the MFI. Increasing the amount of wheat straw further reduced the MFI. Addition of PP-MA to the polypropylene increased the MFI which is due to the low molecular weight of the anhydride grafted polymer. Addition of clay further reduced the flow properties. MFI did not change significantly with the size of the wheat straw which is an indication that the MFI of the composites is mainly governed by the amount of the WS and not the size of the WS particles. Similar MFI values obtained for Run #12-14 indicated that the gWS particles size distribution of the composites after compounding are very similar to each other as shown previously in this work.

Table 4-12 MFI Values of WSCPP Based on gWS Content, PP-MA wt-%, Clay wt-% and gWS Size.

Sample ID	MFI (g/ 10min)	Std. Dev (%)
Run #1	4.20	0.21
Run #2	2.25	0.16
Run #3	0.68	0.10
Run #4	4.08	0.13
Run #5	4.20	0.21
Run #6	4.44	0.16
Run #7	5.28	0.27
Run #8	11.5	0.15
Run #9	13.02	0.35
Run #10	14.4	0.02
Run #11	5.55	0.39
Run #12	5.30	0.12
Run #13	5.00	0.20
Run #14	5.28	0.02

4.2.8 MECHANICAL PROPERTIES

FLEXURAL PROPERTIES

The effect of wheat straw, coupling agent and clay contents on flexural properties of the composites was studied and the results are presented in Figure 4-33 (a)-(c). The amount of wheat straw on flexural modulus was studied by keeping the composition of the other constituents constant. Composite sample containing no wheat straw showed modulus of 1,215 MPa. The addition of 30 wt-% WS into the polymer matrix increased the flexural modulus to 2,000 MPa that is an increment of 64 %. Increasing the content of WS further increased the flexural modulus of the composite. The increase in flexural modulus by increasing WS content is expected as the addition of fillers with higher stiffness in polypropylene increases the flexural properties of the composite.

Similar behaviour has been reported elsewhere. Qiao et al. reported on a study that waste paper sludge flour had a 31 % increase in flexural modulus by adding 30 wt-% of that filler (Qiao, Zhang et al. 2004). Penthapulakkal and the coworkers in a study on wheat straw fibers for reinforcing applications found that the addition of wheat straw fibers significantly enhanced the flexural modulus of polypropylene indicating the suitability of the wheat straw fibers as reinforcing fibers (Panthapulakkal, Sain 2006). Further, it was reported that the flexural modulus in general depends on the filler concentration (Cao, Shibata et al. 2006). Ashori et al. also reported that because of high modulus of lignocellulosic fibers, they can reinforce the PP matrix (Ashori, Nourbakhsh 2009b).

The effect of addition of the coupling agent on the flexural modulus was studied by varying the PP-MA content at 0 wt-%, 2 wt-% and 4 wt-% while keeping the other components constant. It was observed that the composite with no coupling agent (Run #4) showed the lowest value of flexural modulus. Addition of 2 % PP-MA increased the flexural modulus

by 11 %. However, further addition of the coupling agent was found not to have a significant effect on the modulus.

Similar results reported elsewhere indicated that addition of PP-MA increased the stiffness of the composites (Qiao, Zhang et al. 2004). Addition of coupling agent in a composite effectively improves the interfacial bonding due to the formation of covalent linkage and the hydrogen bonding between the maleic anhydride and hydroxyl groups of the natural fiber which in return create a stiffer material with higher resistance to deformation. In agreement with this argument, it was also reported in the literature that the addition of coupling agents like PP-MA leads to chemical interaction between the hydroxyl groups of filler and maleic anhydride functionality of PP-MA (Cao, Shibata et al. 2006).

The effect of addition of organo-clay on the flexural modulus of the composite was studied by keeping the other constituents constant. The samples were prepared with different amounts of organo-clay at 0, 2 and 5 wt-%. Composites with 2 wt-% and 5 wt-% organo-clay only showed a minor increase of 2.3 % and 6.0 % in flexural modulus, respectively. However it was reported that presence of very small quantity of clay in intercalated or exfoliated form enhances the properties of composite to the greater extent (Ray, Okamoto 2003).

The increase in properties of composite with clay reported here was not as high as other results in the literature indicating that there is no intercalation or exfoliation of clay in the composite. Furthermore, the microscopy results showed that the clay particles are acting as a conventional micro-filler in the composite. The slight increase in flexural modulus with increase in clay content supports the prior discussion on flexural modulus being a linear function of filler concentration.

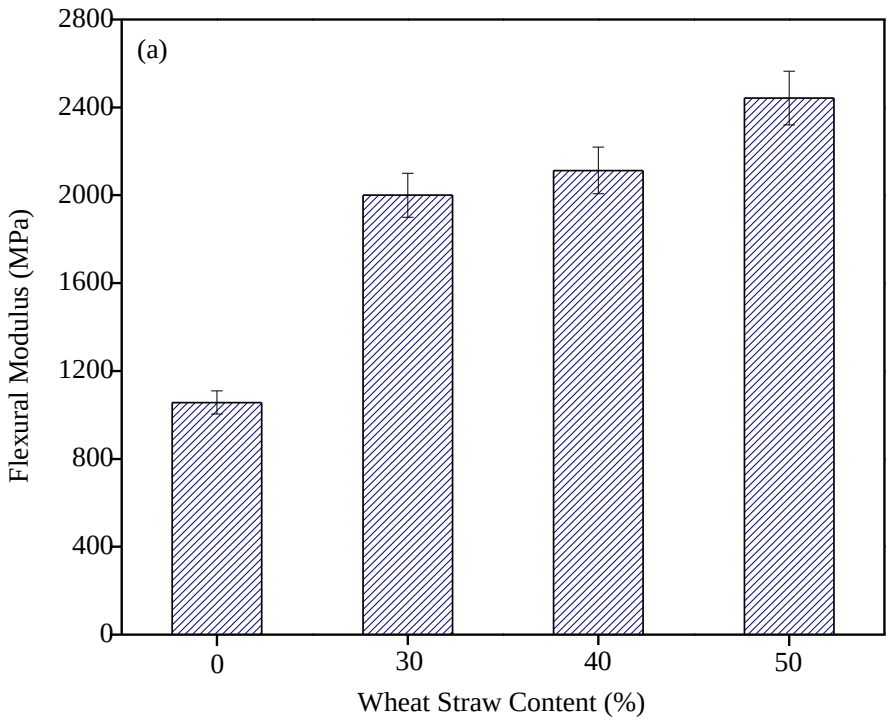
(a)
Flexural Modulus (MPa)
2800
2400
2000
1600
1200
800
400
0
0
30
40
50
Wheat Straw Content (%)

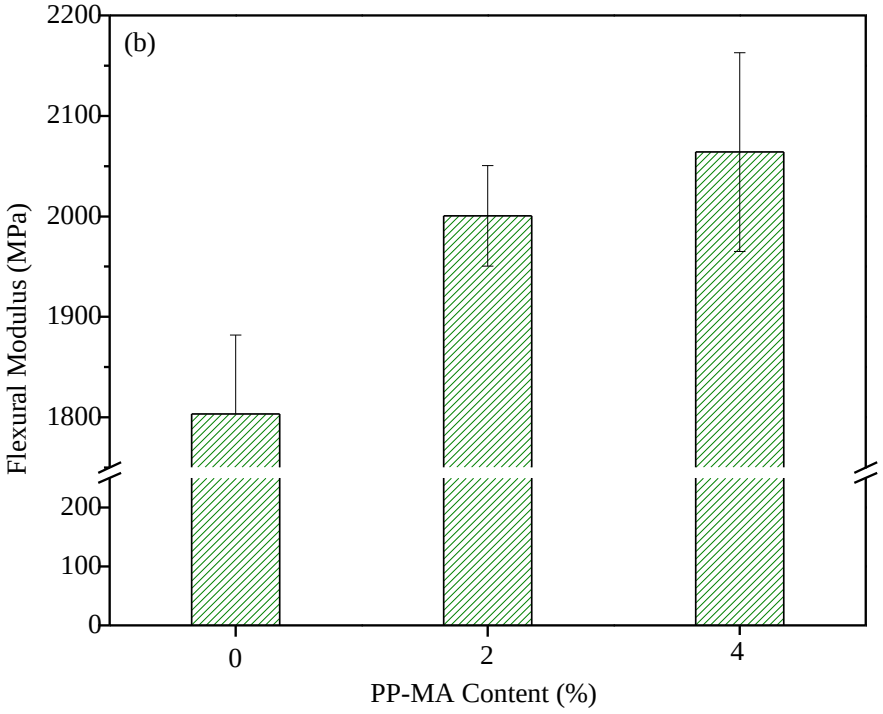
(b)
Flexural Modulus (MPa)
2200
2100
2000
1900
1800
200
100
0
0
2
4
PP-MA Content (%)

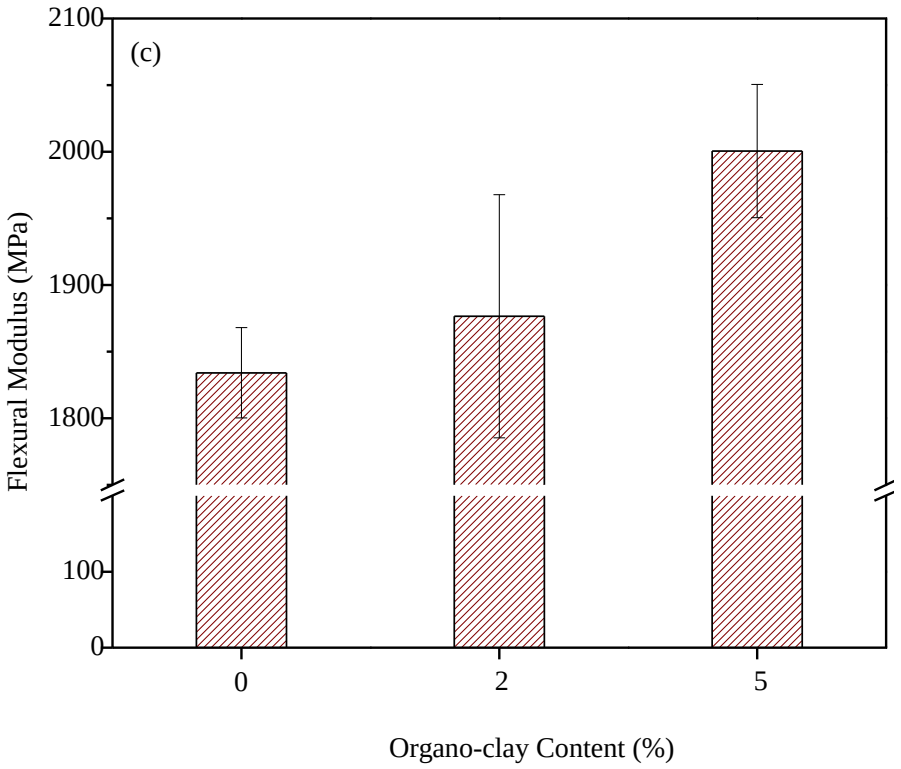

Figure 4-33 Flexural Modulus of WSPPC Composites with Respect to (a) WS Content, (b) PP-MA Content, (c) Organo-Clay Content

Studies were conducted in order to obtain the effect of the different gWS particle size on the flexural properties of the composites. For this reason, composites from Fine, Mid and Large gWS batches along with a blend of all sizes according to Table 4-7 were prepared and the results are shown in Figure 4-34. It was found that the flexural modulus of the composite prepared from the Large batch of gWS was the highest. Composites made from the Mid and Blend batches showed similar flexural modulus values, only 6 % lower than that of Large batch. As it was shown before in the particle size analysis of the Large batch of gWS, the particle sizes of the Large batch are very similar to that of Mid batch after extrusion. This similarity between the particle sizes is the main reason that flexural modulus made from both gWS batches are almost the same.

Flexural modulus of the composites made from the Fine batch particles however, showed a 15 % drop compared to Large batch indicating that the larger the size of the particles, the higher will be the flexural modulus of the composites made from those particles. This conclusion is also in line with the previously mentioned observation that the particles with higher aspect ratio tend to have higher reinforcement properties.

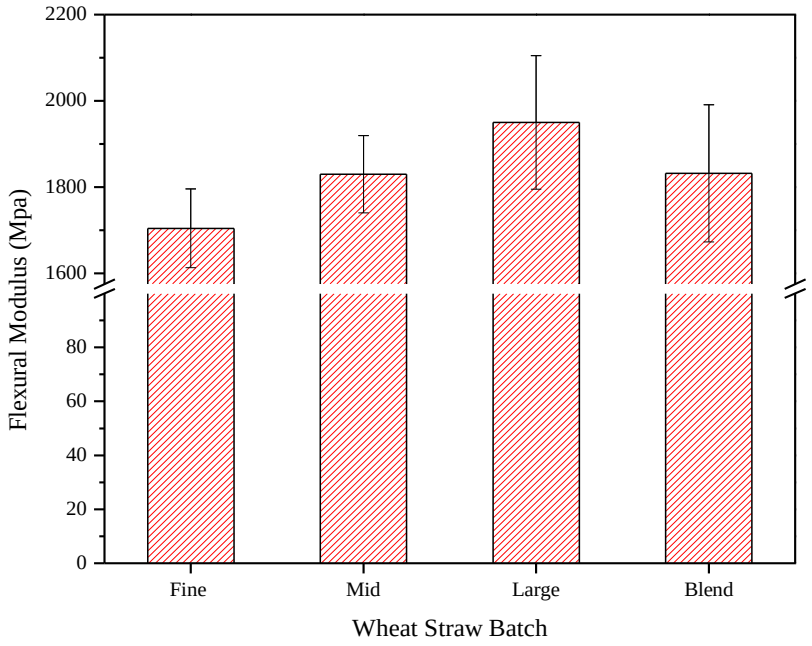

Figure 4-34 Flexural Modulus of WSPP Composites with Respect to Particle Size Distribution

FLEXURAL STRENGTH

Effect of wheat straw, coupling agent and clay contents on flexural strength of the composites was studied and the results are presented in Figure 4-35 (a)-(c). It was found that the addition of gWS to the polypropylene reduced the flexural strength. The decreasing strength obtained by addition of WS is mainly attributed to the weak interfacial bonding

between the filler and the matrix. It becomes more significant as higher amounts of filler are introduced to the polymer. These weak interactions do not contribute to transfer of stress from the filler to the matrix at high stress levels. The result found for the flexural strength here are in agreement with those reported by Kruger and Ng (Ng 2008, Kapustan Krüger 2007).

The effect of addition of the coupling agent on the flexural strength was studied by varying the PP-MA content at 0wt-%, 2wt-% and 4wt-%. It was observed that the addition of the coupling agent increased the flexural strength. This behaviour is attributed to the interfacial interaction between the filler and the matrix. Similar trends were reported by Arbelaiz et al. and Bledzki et al. (Arbelaiz, Fernández et al. 2005, Bledzki, Mamun et al. 2007).

The effect of addition of clay on the flexural strength of the composite was also studied. The composite sample which had no clay showed the highest flexural strength. Addition of clay to the composites reduced the strength. The effect of clay on flexural modulus can be attributed to the poor interaction between the matrix and the filler.

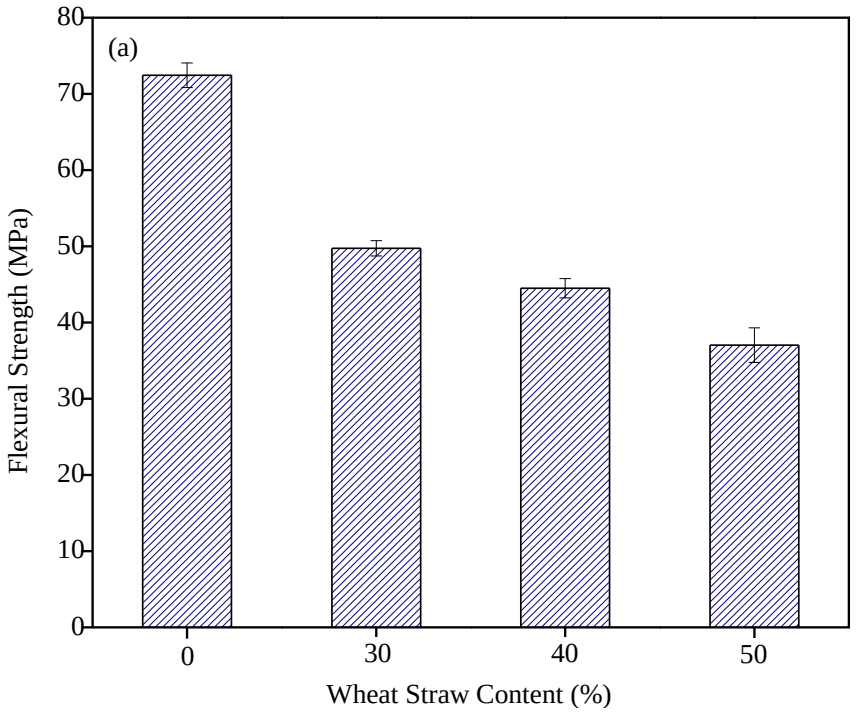
(a)
Flexural Strength (MPa)
80
70
60
50
40
30
20
10
0
0
30
40
50
Wheat Straw Content (%)

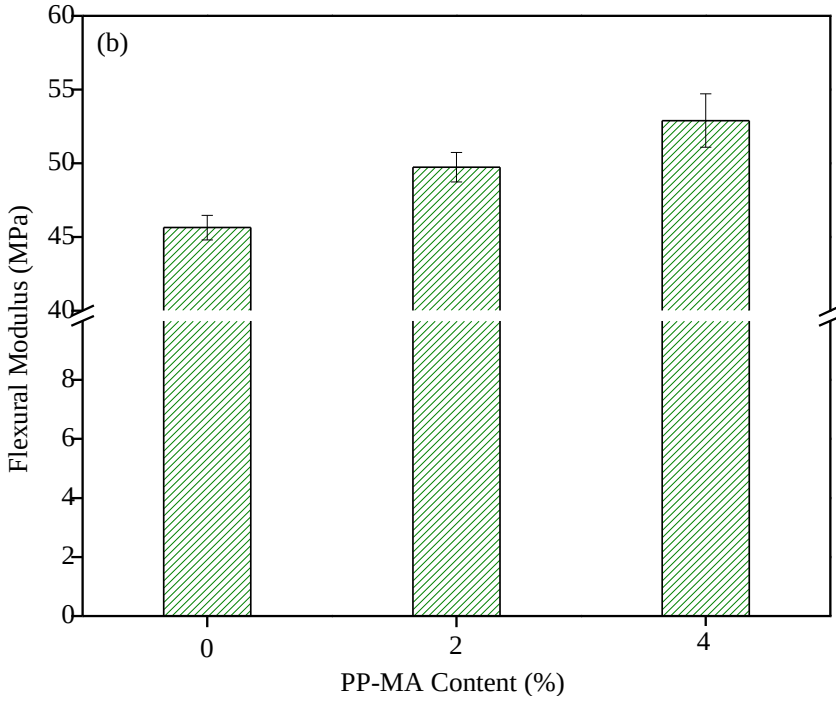
(b)
Flexural Modulus (MPa)
60
55
50
45
40
8
6
4
2
0
0
2
4
PP-MA Content (%)

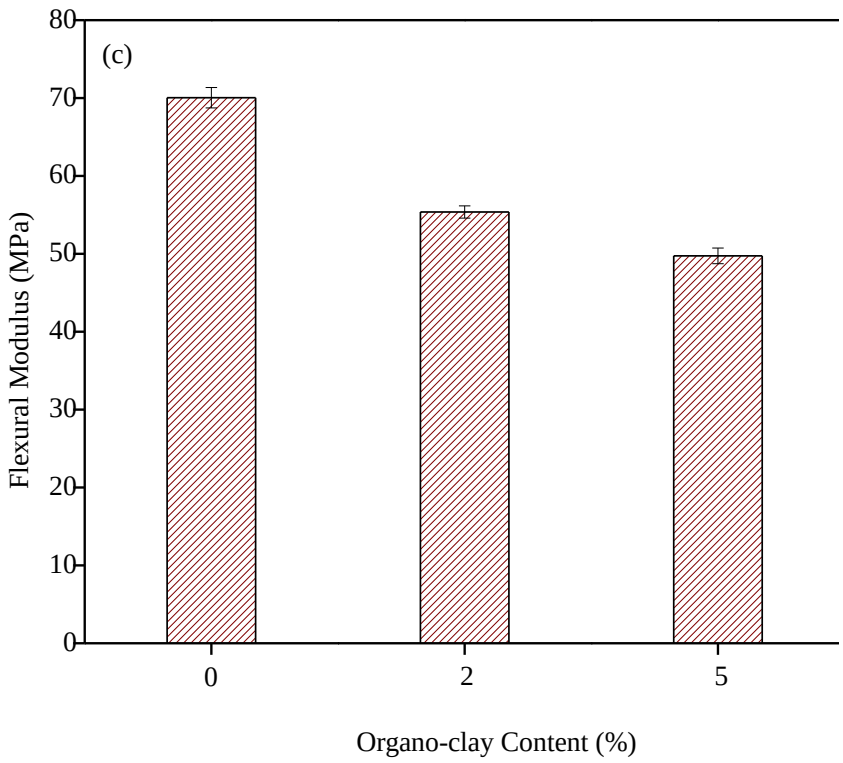

Figure 4-35 Flexural Strength of WSPPC Composites with Respect to (a) WS Content, (b) PP-MA Content, (c) Organo-Clay Content

4.2.9 MECHANICAL BEHAVIOUR MODELING AND OPTIMIZATION

In order to optimize the amount of each component for the optimum improvement in the composite mechanical performance, the flexural modulus and flexural strength were modeled by a constrained mixture design. The interaction parameters between the mixture components were quantified. Factors studied for this analysis were weight percentage of the polypropylene, wheat straw and coupling agent. Due to negligible effect of clay on the mechanical properties of the composites and also to reduce the number of experiments, it was decided to omit the effect of clay from this study.

Since the components of the mixture cannot be worked within the range of 0-100 wt-%, an L-pseudo-component simplex region of constrained mixture design was generated with the constraints set on the polymer from 46 to 70 wt-%, wheat straw from Fine batch from 30 to 50 wt-%, and the coupling agent from 0 to 4 wt-% of the total weight of the composite.

As the minimum number of points is 6 as suggested by Cornell, it is reasonable to take four vertices, one face centroid and one edge centroid as design points [Cornell, 2001]. These points are sufficient enough to accommodate the full second degree scheffe canonical polynomial models to anticipate the existence of nonlinear blending characteristics of the components.

Data obtained from flexural modulus and flexural strength analyses based on the points chosen from mixture design are shown in Table 4-13. As expected the flexural modulus of the composites was enhanced and flexural strength reduced with increasing the amount of gWS while both flexural modulus and strength were enhanced by the amount of PP-MA. Design Expert Software (v. 7.1) was used to analyze the data. The suggested models both for flexural modulus and flexural strength and the Analysis of Variance (ANOVA) of the models are summarized in Table 4-14.

Table 4-13 Flexural Modulus and Flexural Strength of the WSPPCs as a Function of Various Amounts of Mixture Design Components.

Design Points	Polymer (wt-%)	WS (wt-%)	PP-MA (wt-%)	Flex Modulus (MPa)	Flex Strength (MPa)
1	46	50	4	2384	75
2	70	30	0	1680	51
3	66	30	4	1880	73
4	50	50	0	2142	45
5	58	40	2	2308	68
6	56	40	4	2115	74

Table 4-14 Analysis of Variance for Flexural Properties of WSPPCs.

Dependent Variable	Source of variation	SS	DF	MS	F	P-Value
Flexural Modulus	Model	352200	4	88061.33	407.69	0.0371
	Linear Mixture	285300	2	142600.00	660.39	0.0275
	AC	66514.97	1	66514.97	307.94	0.0362
	BC	66949.95	1	66949.95	309.95	0.0361
	Residual	216.00	1	216.00		
	Total	352500	5			
Flexural Strength	Model	790.78	2	395.39	20.97	0.0172
	Linear Mixture	790.78	2	395.39	20.97	0.0172
	Residual	56.55	3	18.85		
	Total	847.33	5			

It was observed that the model is significant based on the F-value (407.69) and that there is only a 3.71 % chance that a model F-value this large could occur due to the noise. It was also found that not only linear mixture component such as the polypropylene, wheat straw and coupling agent are statistically important, but also the interaction between polypropylene and coupling agent (AC) and wheat straw and coupling agent (BC) are significant. Therefore such behaviour introduces nonlinearity to the analysis. Note the insignificant parameters such as interaction between polymer and wheat straw (AB) are not shown in the ANOVA table since they have no effect on the design responses. The following equation was generated for flexural modulus:

$$Flexural\ Modulus = 9.87\ A + 32.97\ B - 6758.38\ C + 70.87\ AC + 71.40\ BC \qquad \text{Equation 4-2}$$

Where A is the weight percentage of polypropylene, B is the weight percentage of wheat straw and C is the weight percentage of coupling agent. A contour plot for the flexural modulus was created and is shown in Figure 4-36.

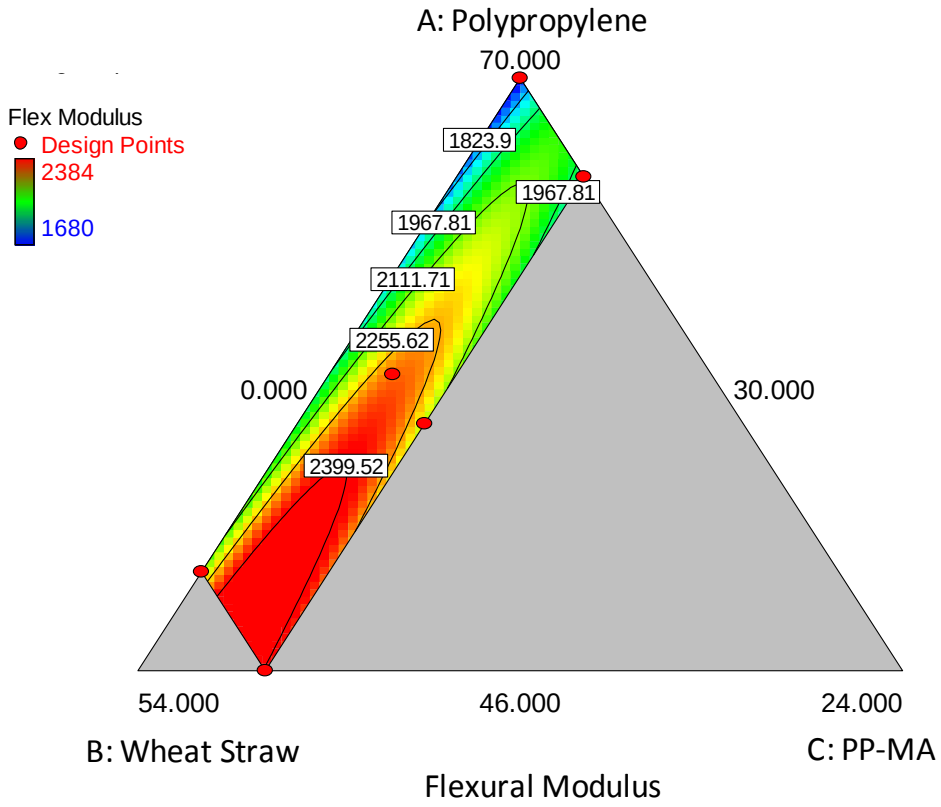

Figure 4-36 Contour Plot of Flexural Modulus Obtained from Design Expert Software

Similarly a model was generated for the flexural strength. It was observed that the model is significant and that there is only a 1.72 % chance that a model F-value this large could occur due to the noise. In this case, only the linear blending characteristics of the components were significant as shown in the ANOVA table and the following equation and contour plot were found for the prediction of the strength of the composites:

$$Flexural\ Strenght = 0.5344\ A + 0.43448\ B + 6.91379\ C \qquad \text{Equation 4-3}$$

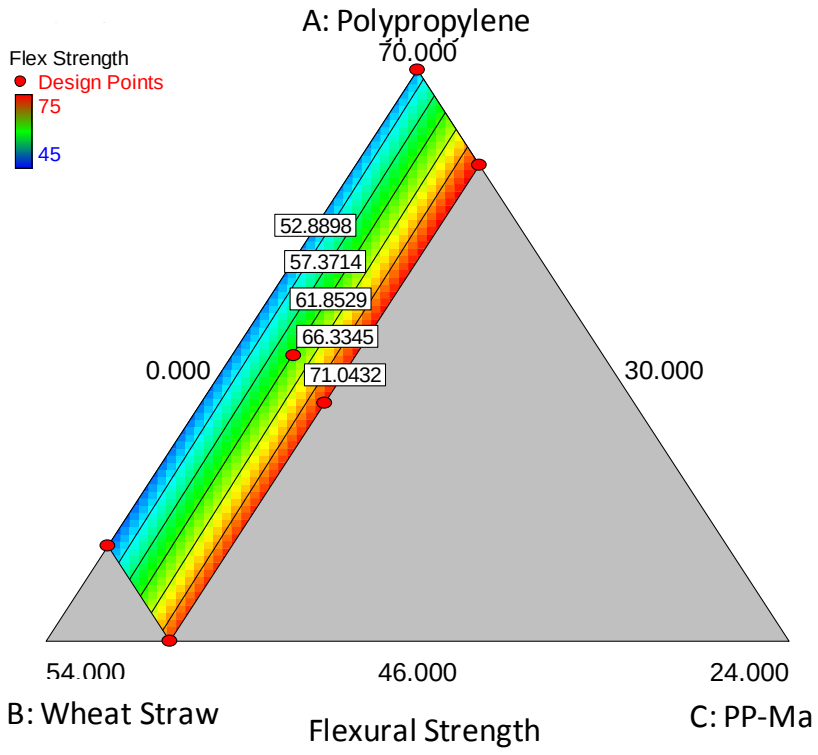

Figure 4-37 Contour Plot of Flexural Strength Obtained from Design Expert Software

A desirability function was introduced to optimize both flexural modulus and strength of composites. This can be done by transforming the estimated response variables y_i (flexural modulus and strength) into desirability variable d_i whose values lie between 0 (least desired) and 1 (most desired). The individual desirability are then combined using the geometric mean according to Equation 4-4:

$$D = (d_1 \times d_2 \times \ldots \times d_k)^{\frac{1}{2}} \qquad \text{Equation 4-4}$$

Where d is the desirability function and k is the number of response variable. The single value of D gives the overall assessment of the desirability of all combined response levels. It should be noted that the value of D falls in the interval [0, 1].

The optimization of desirability function was done by using Design Expert software and the optimization results are presented in Table 4-15 based on three main optimization scenarios. For each scenario few options are presented and different selection could be made based on the final application of the product.

Table 4-15 Optimization Results Based on Desirability Function for Wheat straw Polypropylene Composites

Optimization Scenario #1: Minimizing MA-PP; Maximizing Flex. Modulus and Strength							
Sample	PP	WS	MA-PP	Flex. Mod.	Flex. St.	Desirability	
1	54.314	43.935	1.751	2384.001	60.225	0.658	Selected
2	68.018	30.000	1.982	2065.525	63.089	0.550	

Optimization Scenario #2: Maximizing Wheat Straw; Maximizing Flex. Modulus and Strength							
Sample	PP	WS	MA-PP	Flex. Mod.	Flex. St.	Desirability	
1	46.000	50.000	4.000	2390.000	73.966	0.988	Selected
2	47.776	48.388	3.836	2384.002	73.078	0.951	
3	52.000	44.736	3.264	2383.977	69.798	0.848	
4	55.813	41.771	2.416	2362.505	64.681	0.721	

Optimization Scenario #3: Maximizing Flex. Modulus and Strength							
Sample	PP	WS	MA-PP	Flex. Mod.	Flex. St.	Desirability	
1	46.238	49.762	4.000	2384.002	73.989	0.983	Selected
2	52.000	44.565	3.435	2357.163	70.905	0.911	
3	58.134	38.199	3.667	2160.637	73.019	0.799	
4	61.786	35.000	3.214	2148.495	70.452	0.751	

5 CONCLUSIONS AND RECOMMENDATIONS

The potential use of wheat straw and clay as reinforcements in polypropylene were investigated. The study focused on wheat straw particle size and their thermal stabilities which were correlated with the major chemical components of wheat straw. Ground wheat straw obtained from hammer milling was sieved into three main batches: Large, Mid, and Fine.

To further analyze these batches in more detail, additional sieving was performed and each batch was divided into 6 fractions resulting in a total of 18 fractions. Particle size analysis was done on individual batches along with all the fractions and it was found that most particles were between 100-5,000 µm with aspect ratio mainly in the range 1-10. Higher aspect ratios were found mainly in two fractions 35-100 and 60-100 for the Large and Mid batches. In case of the Fine Batch, aspect ratios were mainly lower than 10 in almost all fractions, except for the fraction 25-35 where 10 wt-% of all particles had aspect ratios higher than 10. It was also found that the main differences in the batches were related to particles in the fraction 35-100. Based on the grinding process, about 44 wt-% of the straw particles were in the Mid batch and the rest of the particles were divided between the Large and the Fine batches.

The amount of lignin and hemicellulose were measured in the 18 fractions of wheat straw particles. It was found that there was a decreasing trend (from 9.5 wt-% to 4.5 wt-%) in the values of lignin as the size of fractions decreased, except for the smallest fraction. The amount of hemicellulose varied in all fractions between 26 wt-% and 29 wt-%.

The thermal stability of the fractions was investigated by TGA analysis. It was found that lignin content did not correlate with the onset of degradation temperature. The particle size correlated well with the thermal stability of the wheat particles. It was found that the

particles which constituted the Large and Mid batches were the most thermally stable particles due to the availability of the larger particles (smaller surface area for thermal degradation). Two main decomposition peaks were obtained for all wheat straw particles by TGA. The first decomposition peak was found to be related to cellulose/hemicellulose decomposition, which happened between 290 ^{o}C and 410 ^{o}C with a decomposition peak at 330 ^{o}C. The second characteristic peak was related mostly to lignin decomposition along with some structural hemicellulose which decomposes at higher temperature.

Hybrid composites of polypropylene matrix with wheat straw and clay were prepared by a co-rotating twin-screw extruder. Maleic anhydride was chosen as the coupling agent to enhance the bonding between the matrix and the natural fiber. The effect of the components in the formulation was correlated to the flexural modulus and strength and to the water absorption. The increase in WS content in a composite increased the flexural modulus and reduced the resistance for water absorption. The increase in PP-MA coupling agent increased the flexural modulus and resistance for water absorption. The increase in clay slightly increased the flexural modulus and reduced the resistance to water absorption.

The morphological study revealed that the wheat straw particles were oriented during the injection molding. The interfacial interaction between the WS particles and PP matrix was significantly higher if coupling agent was added to the composite. This was corroborated by the improved mechanical properties and reduced water absorption. The morphological study revealed the fiber pull-out in cases where coupling agent was not used indicating poor interfacial interaction between the matrix and the filler.

Based on the results obtained in this study, it can be concluded that preparation and utilization of hybrid composites made from wheat straw, clay and polypropylene has a great potential to be used in industries such as transportation and construction. To improve

the thermal and structural properties of the composites the following items should be considered:

1. Modify the grinding system in order to minimize the structural damage caused by hammer milling.
2. Chemical, mechanical, or thermal modification of wheat straw in order to:
    a. Increase the adhesion between the natural fiber and the matrix;
    b. Increase the thermal stability of the wheat straw particles;
    c. Decrease the affinity towards water absorption;
    d. Decrease the natural odour of wheat straw.
3. Modify the compounding processing conditions in order to:
    a. Minimize the filler damage caused by heat and shear forces;
    b. Maximize clay intercalation;
    c. Optimize the homogeneity of the composite.
4. Investigate the properties of the composites at a larger production scale especially in regards to the dispersion of the filler and ease of processing.

REFERENCES

ALEMDAR, A. and SAIN, M., 2008. Isolation and characterization of nanofibers from agricultural residues - Wheat straw and soy hulls. *Bioresource Technology*, **99**(6), pp. 1664-1671.

ARAUJO, J.R., WALDMAN, W.R. and DE PAOLI, M.A., 2008. Thermal properties of high density polyethylene composites with natural fibres: Coupling agent effect. *Polymer Degradation and Stability*, **93**(10), pp. 1770-1775.

ARBELAIZ, A., FERNÁNDEZ, B., RAMOS, J.A., RETEGI, A., LLANO-PONTE, R. and MONDRAGON, I., 2005. Mechanical properties of short flax fibre bundle/polypropylene composites: Influence of matrix/fibre modification, fibre content, water uptake and recycling. *Composites Science and Technology*, **65**(10), pp. 1582-1592.

ASHORI, A. and NOURBAKHSH, A., 2009a. Mechanical behavior of agro-residue-reinforced polypropylene composites. *Journal of Applied Polymer Science.Vol.111*, **111**(5), pp. 2616-2620.

ASHORI, A. and NOURBAKHSH, A., 2009b. Polypropylene Cellulose-Based Composites: The Effect of Bagasse Reinforcement and Polybutadiene Isocyanate Treatment on the Mechanical Properties. *Journal of Applied Polymer Science*, **111**(4), pp. 1684-1689.

ASTM INTERNATIONAL, 2008a. ASTM D 1238 - 04c Standard Test Method for Melt Flow Rates of Thermoplastics by Extrusion Plastometer.

ASTM INTERNATIONAL, 2008b. ASTM D 570 - 98 Standard Test Method for Water Absorption of Plastics.

ASTM INTERNATIONAL, 2008c. ASTM D 7075 - 04 Standard Practice for Evaluating and Reporting Environmental Performance of Biobased Products.

ASTM INTERNATIONAL, 2008d. ASTM D 790 - 03 Standard Test Methods for Flexural Properties of Unreinforced and Reinforced Plastics and Electrical Insulating Materials.

AVELLA, M., BOZZI, C., DELL'ERBA, R., FOCHER, B., MARZETTI, A. and MARTUSCELLI, E., 1995. Steam-exploded wheat straw fibers as reinforcing material for polypropylene-based composites. Characterization and properties. *Angewandte Makromolekulare Chemie*, **233**(1), pp. 149-166.

AVÉROUS, L. and LE DIGABEL, F., 2006. Properties of biocomposites based on lignocellulosic fillers. *Carbohydrate Polymers*, **66**(4), pp. 480-493.

BACHERT, I. and WERNER, F., 2000. Stabilizing plastics in processing and use. *Plastics, Additives and Compounding,* **2**(9), pp. 18-21.

BLEDZKI, A.K., MAMUN, A.A. and FARUK, O., 2007. Abaca fibre reinforced PP composites and comparison with jute and flax fibre PP composites. *Express Polymer Letters,* **1**(11), pp. 755-762.

BLEDZKI, A.K., FARUK, O. and SPERBER, V.E., 2006. Cars from bio-fibres. *Macromolecular Materials and Engineering,* **291**(5), pp. 449-457.

CAO, Y., SHIBATA, S. and FUKUMOTO, I., 2006. Mechanical properties of biodegradable composites reinforced with bagasse fibre before and after alkali treatments. *Composites Part A-Applied Science and Manufacturing,* **37**(3), pp. 423-429.

ESPERT, A., VILAPLANA, F. and KARLSSON, S., 2004. Comparison of water absorption in natural cellulosic fibres from wood and one-year crops in polypropylene composites and its influence on their mechanical properties. *Composites Part A: Applied Science and Manufacturing,* **35**(11), pp. 1267-1276.

FELDMAN, D., 2002. Polymer Weathering: Photo-Oxidation. *Journal of Polymers and the Environment,* **10**(4), pp. 163-173.

FOWLER, P.A., HUGHES, J.M. and ELIAS, R.M., 2006. Biocomposites: technology, environmental credentials and market forces. *Journal of the Science of Food and Agriculture,* **86**(12), pp. 1781-1789.

GALANTI, A.V. and MANTELL, C.L.,1897-JOINT AUTHO, 1965. Polypropylene Fibers and Films. New York: Plenum Press.

GARCIA, M., GARMENDIA, I. and GARCIA, J., 2008. Influence of natural fiber type in eco-composites. *Journal of Applied Polymer Science,* **107**(5), pp. 2994-3004.

GARCIA, O.E.(., INFANTE, R.B.(. and RIVERA, C.J., 1997. Determination of total, soluble and insoluble dietary fibre in two new varieties of Phaseolus vulgaris L. using chemical and enzymatic gravimetric methods. *Food Chemistry,* **59**(1, pp. 171-174), pp. May.

GOLBABAIE, M., 2008. Characterization *of Ontario crop fibers for use in biocomposites (Wheat and Soy bean),* University of Guelph.

GOUANVE, F., MARAIS, S., BESSADOK, A., LANGEVIN, D. and METAYER, M., 2007. Kinetics of water sorption in flax and PET fibers. *European Polymer Journal,* **43**(2), pp. 586-598.

HAMERTON, I., 2006. Book Review: Functional Fillers for Plastics. By Marino Xanthos (Ed.). *Advanced Materials,* **18**(2, pp. 248-248), pp. January.

HOLBERY, J. and HOUSTON, D., 2006. Natural-Fiber-Reinforced Polymer Composites in Automotive Applications. *JOM,* **58**(11), pp. 80-86.

HORNSBY, P.R., HINRICHSEN, E. and TARVERDI, K., 1997a. Preparation and properties of polypropylene composites reinforced with wheat and flax straw fibres. I. Fibre characterization. *Journal of Materials Science,* **32**(2), pp. 443-449.

HORNSBY, P.R., HINRICHSEN, E. and TARVERDI, K., 1997b. Preparation and properties of polypropylene composites reinforced with wheat and flax straw fibres. Part II: analysis of composite microstructure and mechanical properties. *Journal of Materials Science,* **32**, pp. 1009-1015.

JOSEPH, K., VARGHESE, S., KALAPRASAD, G., THOMAS, S., PRASANNAKUMARI, L., KOSHY, P. and PAVITHRAN, C., 1996. Influence of interfacial adhesion on the mechanical properties and fracture behaviour of short sisal fibre reinforced polymer composites. *European Polymer Journal,* **32**(10), pp. 1243-1250.

KÁDÁR, F., SZÁZDI, L., FEKETE, E. and PUKÁNSZKY, B., 2006. Surface characteristics of layered silicates: Influence on the properties of clay/polymer nanocomposites. *Langmuir,* **22**(18), pp. 7848-7854.

KAPUSTAN KRÜGER, P., 2007. *Wheat Straw-Polypropylene Composites*, University of Waterloo.

LE DIGABEL, F., BOQUILLON, N., DOLE, P., MONTIES, B. and AVEROUS, L., 2004. Properties of thermoplastic composites based on wheat straw lignocellulosic fillers. *Journal of Applied Polymer Science,* **93**(1), pp. 428-436.

LEAO, A.L., TEIXEIRA, R.M.F. and FERRAO, P.C., 2008. Production of reinforced composites with natural fibers for industrial applications - Extrusion and injection WPC. *Molecular Crystals and Liquid Crystals,* **484**, pp. 523-532.

LEE, B.J., MCDONALD, A.G. and JAMES, B., 2001. Influence of fiber length on the mechanical properties of wood-fiber/polypropylene prepreg sheets. *Materials Research Innovations,* **4**(2-3), pp. 97-103.

LI, J., TON-THAT, M.- ., LEELAPORNPISIT, W. and UTRACKI, L.A., 2007. Melt compounding of polypropylene-based clay nanocomposites. *Polymer Engineering & Science,* **47**(9), pp. 1447-1458.

LÓPEZ MANCHADO, M.A., ARROYO, M., BIAGIOTTI, J. and KENNY, J.M., 2003. Enhancement of mechanical properties and interfacial adhesion of PP/EPDM/flax fiber

composites using maleic anhydride as a compatibilizer. *Journal of Applied Polymer Science,* **90**(8, pp. 2170-2178), pp. November.

MAIER, C. and CALAFUT, T., 1998. Polypropylene : the definitive user's guide and databook. Norwich, NY: Plastics Design Library.

MANDALIA, T. and BERGAYA, F., 2006. Organo clay mineral-melted polyolefin nanocomposites - Effect of surfactant/CEC ratio. *Journal of Physics and Chemistry of Solids,* **67**(4), pp. 836-845.

MANIAR, K.K., 2004. Polymeric nanocomposites: A review. *Polymer-Plastics Technology and Engineering,* **43**(2), pp. 427-443.

MARCOVICH, N.E., REBOREDO, M.M. and ARANGUREN, M.I., 1998. Dependence of the mechanical properties of woodflour-polymer composites on the moisture content. *Journal of Applied Polymer Science,* **68**(13), pp. 2069-2076.

MENGELOGLU, F. and KARAKUS, K., 2008. Thermal degradation, mechanical properties and morphology of wheat straw flour filled recycled thermoplastic composites. *Sensors,* **8**(1), pp. 500-519.

MIGNEAULT, S., KOUBAA, A., ERCHIQUI, F., CHAALA, A., ENGLUND, K., KRAUSE, C. and WOLCOTT, M., 2008. Effect of fiber length on processing and properties of extruded wood- fiber/HDPE composites. *Journal of Applied Polymer Science,* **110**(2), pp. 1085-1092.

MOHANTY, A.K., MISRA, M. and DRZAL, L.T., eds, 2005. *Natural fibers, biopolymers, and biocomposites.* CRC Press.

MOHANTY, A.K., MISRA, M. and HINRICHSEN, G., 2000. Biofibres, biodegradable polymers and biocomposites: An overview. *Macromolecular Materials and Engineering,* **276**(3-4), pp. 1-24.

MUELLER, D.H. and KROBJILOWSKI, A., 2003. New Discovery in the Properties of Composites Reinforced with Natural Fibers. *Journal of Industrial Textiles,* **33**(2), pp. 111-130.

NG, Z.S., 2008. *Bulk Orientation of Agricultural Filler-Polypropylene Composites,* University of Waterloo.

PANTHAPULAKKAL, S. and SAIN, M., 2006. Injection molded wheat straw and corn stem filled polypropylene composites. Journal *of polymers and the environment* , pp.265-272.

PANTHAPULAKKAL, S., SAIN, M. and LAW, S., 2005. Effect of coupling agents on rice-husk-filled HDPE extruded profiles. *Polymer International,* **54**(1), pp. 137-142.

PANTHAPULAKKAL, S. and SAIN, M., 2007. Studies on the Water Absorption Properties of Short Hemp—Glass Fiber Hybrid Polypropylene Composites. *Journal of Composite Materials,* **41**(15), pp. 1871-1883.

PASCUAL, J., FAGES, E., FENOLLAR, O., GARCÍA, D. and BALART, R., 2009. Influence of the compatibilizer/nanoclay ratio on final properties of polypropylene matrix modified with montmorillonite-based organoclay. *Polymer Bulletin,* **62**(3), pp. 367-380.

PAVLIDOU, S. and PAPASPYRIDES, C.D., 2008. A review on polymer–layered silicate nanocomposites. *Progress in Polymer Science,* **33**(12, pp. 1119-1198), pp. December.

QIAO, X., ZHANG, Y. and ZHANG, Y., 2004. Maleic anhydride grafted polypropylene as a coupling agent for polypropylene composites filled with ink-eliminated waste paper sludge flour. *Journal of Applied Polymer Science,* **91**(4), pp. 2320-2325.

RAMIAH, M.V., 1970. Thermogravimetric and differential thermal analysis of cellulose, hemicellulose, and lignin. *Journal of Applied Polymer Science,* **14**(5), pp. 1323-1337.

RAY, S. and EASTEAL, A.J., 2007. Advances in Polymer-Filler Composites: Macro to Nano. *Materials and Manufacturing Processes.Vol.22,* **22**(6), pp. 741-749.

RAY, S.S. and OKAMOTO, M., 2003. Polymer/layered silicate nanocomposites: a review from preparation to processing. *Progress in Polymer Science,* **28**(11), pp. 1539-1641.

RICHARDS, S. and BOUAZZA, A., 2007. Determination of particle density using water and gas pycnometry. *Geotechnique,* **57**(4), pp. 403-406.

RIZVI, G.M., PARK, C.B. and GUO, G., 2008. Strategies for Processing Wood Plastic Composites with Chemical Blowing Agents. *Journal of Cellular Plastics,* **44**(2), pp. 125-137.

ROWELL, R.M., 2007. Challenges in biomass-thermoplastic composites. *Journal of Polymers and the Environment,* **15**(4), pp. 229-235.

SAHEB, D.N. and JOG, J.P., 1999. Natural fiber polymer composites: A review. *Advances in Polymer Technology,* **18**(4), pp. 351-363.

SAIN, M., WANG, W. and COOPER, P.A., 2006. Study of moisture absorption in natural fiber plastic composites. *Composites Science and Technology,* **66**(3-4), pp. 379-386.

SHARMA, H.S.S., 1996. Compositional analysis of neutral detergent, acid detergent, lignin and humus fractions of mushroom compost. *Thermochimica Acta,* **285**(2), pp. 211-220.

STARK, N.M. and ROWLANDS, R.E., 2003. Effects of wood fiber characteristics on mechanical properties of wood/polypropylene composites. *Wood and Fiber Science,* **35**(2), pp. 167-174.

TAJVIDI, M., NAJAFI, S.K. and MOTEEI, N., 2006. Long-term water uptake behavior of natural fiber/polypropylene composites. *Journal of Applied Polymer Science,* **99**(5), pp. 2199-2203.

THERMO HAAKE, 2002. Instruction Manual MiniLab Rheomex CTW5; Part No. 003-5806; 3-1-067-2.

THOMAS, S., GEORGE, J. and BHAGAWAN, S.S., 1998. Effects of environment on the properties of low-density polyethylene composites reinforced with pineapple-leaf fibre. *Composites Science and Technology (UK).Vol.58,* **58**(9), pp. 1471-1485.

THWE, M.M. and LIAO, K., 2002. Effects of environmental aging on the mechanical properties of bamboo–glass fiber reinforced polymer matrix hybrid composites. *Composites Part A: Applied Science and Manufacturing,* **33**(1), pp. 43-52.

USUKI, A., KOJIMA, Y., KAWASUMI, M., OKADA, A., FUKUSHIMA, Y., KURAUCHI, T. and KAMIGAITO, O., 1993. Synthesis of Nylon 6-Clay Hybrid. *Journal of Materials Research (USA).Vol.8,* **8**(5), pp. 1179-1184.

WAKE, W.C., ED., 19uu. Fillers for plastics. Co-ordinating editor: William C. Wake. London: Iliffe Books [c1971].

WHITE, N.M. and ANSELL, M.P., 1983. Straw-reinforced polyester composites. *Journal of Materials Science,* **18**(5), pp. 1549-1556.

XU, Z., TANG, X., GU, A., FANG, Z. and TONG, L., 2007. Surface- modifiers of clay on mechanical properties of rigid polyurethane foams/organoclay nanocomposites. *Journal of Applied Polymer Science,* **105**(5), pp. 2988-2995.

YAM, K.L., GOGOI, B.K., LAI, C.C. and SELKE, S.E., 1990. Composites from compounding wood fibers with recycled high density polyethylene. *Polymer Engineering and Science,* **30**(11), pp. 693-699.

ZENG, Q.H., YU, A.B., LU, G.Q. and PAUL, D.R., 2005. Clay-based polymer nanocomposites: research and commercial development. *Journal of Nanoscience and Nanotechnology,* **5**(10), pp. 1574-1592.

ZHANG, J.G., JIANG, D.D. and WILKIE, C.A., 2006. Thermal and flame properties of polyethylene and polypropylene nanocomposites based on an oligomerically-modified clay. *Polymer Degradation and Stability,* **91**(2), pp. 298-304.

ZHANG, J.G., JIANG, D.D. and WILKIE, C.A., 2005. Polyethylene and polypropylene nanocomposites based upon an oligomerically modified clay. *Thermochemica Acta*, **430**(1-2), pp. 107-113.

APPENDIX

DIFFERENTIAL SCANNING CALORIMETRY

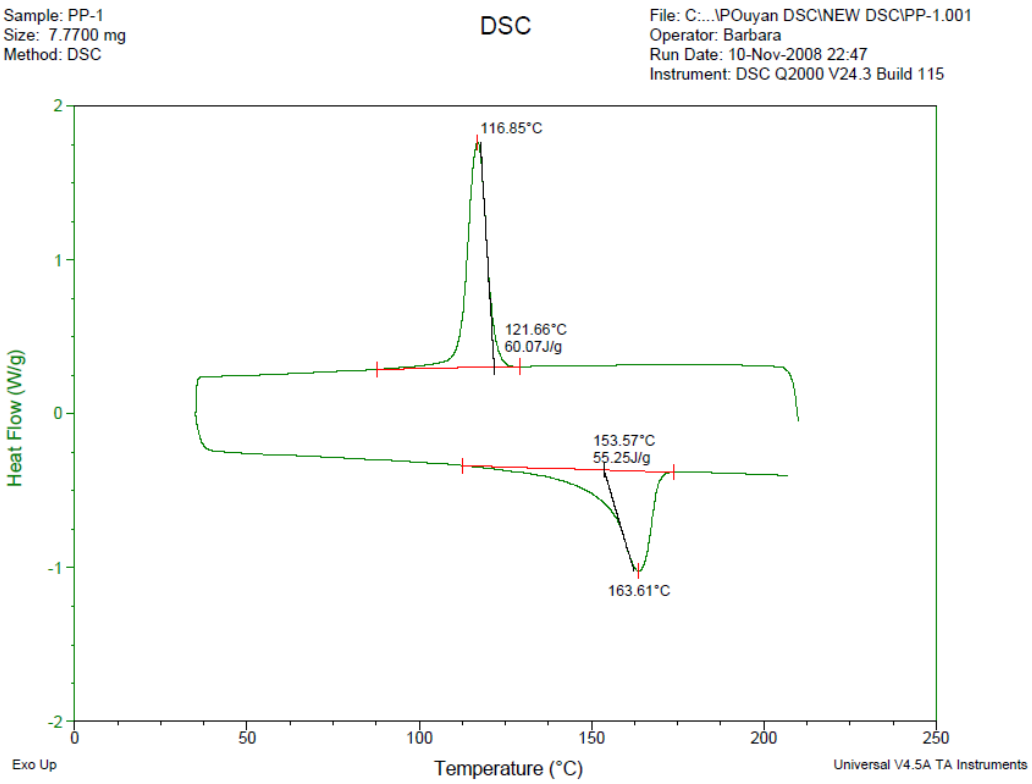

Figure 0-1DSC Curve Run#1

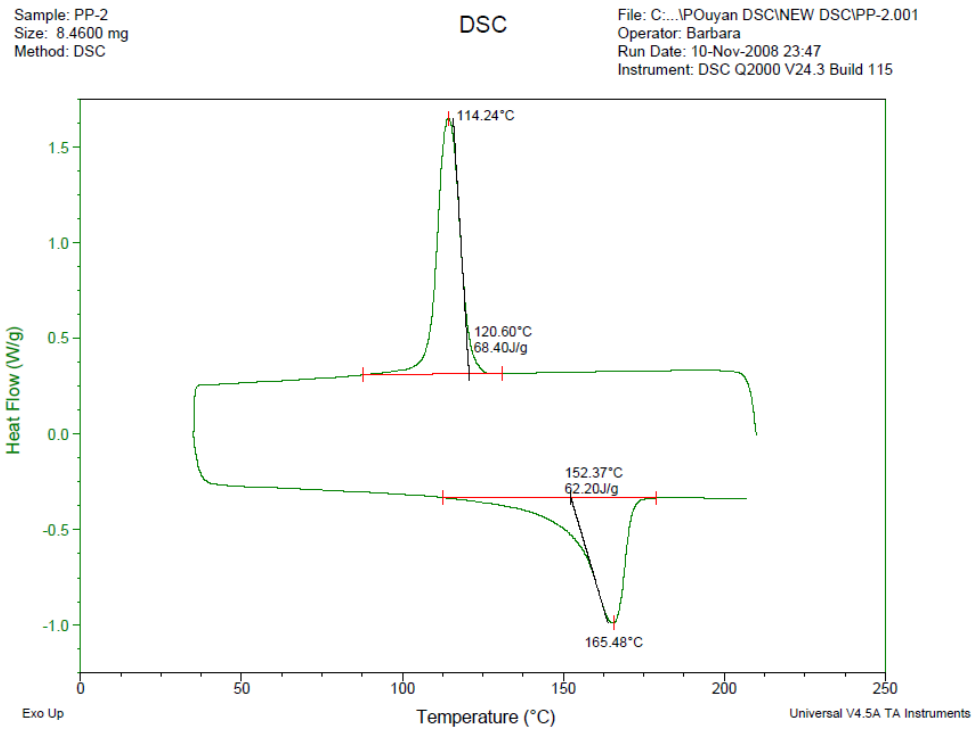

Figure 0-2DSC Curve Run#2

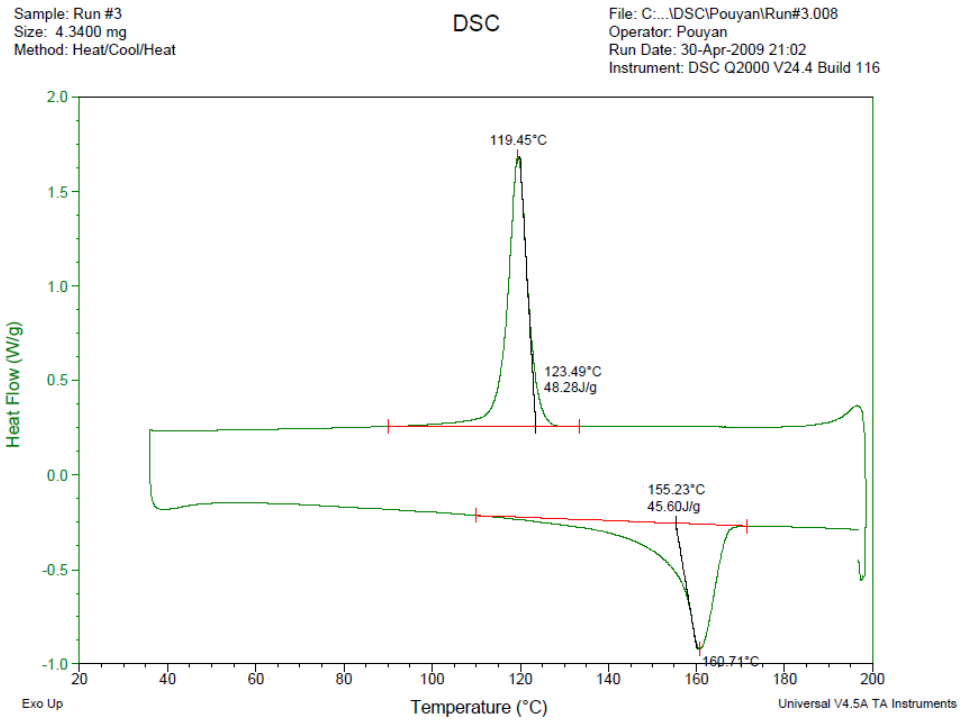

Figure 0-3DSC Curve Run#3

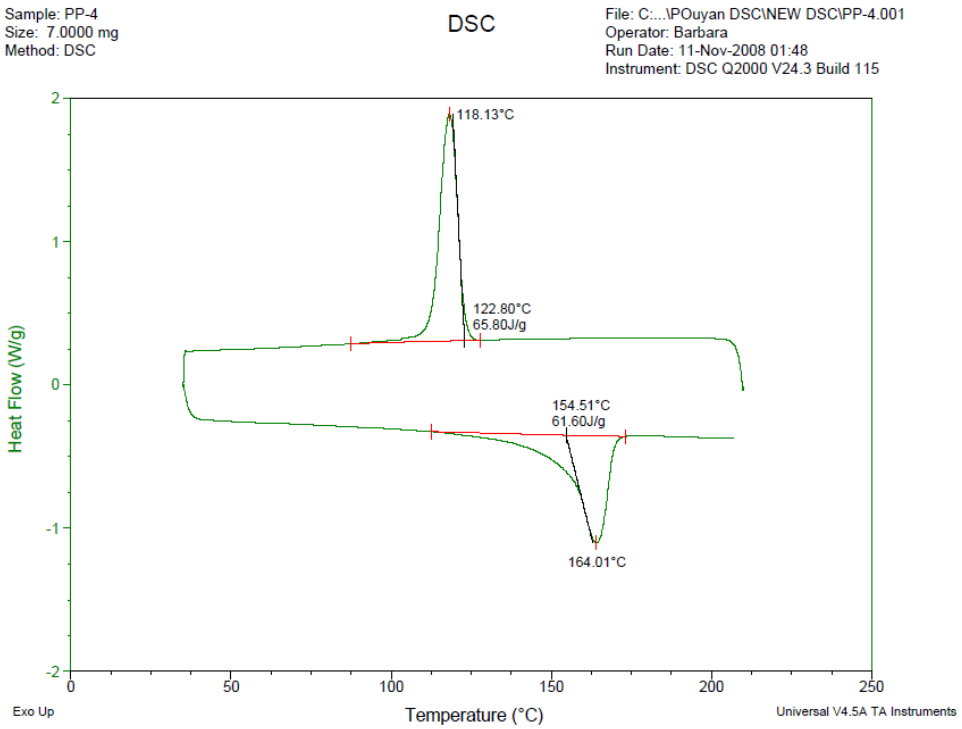

Figure 0-4DSC Curve Run#4

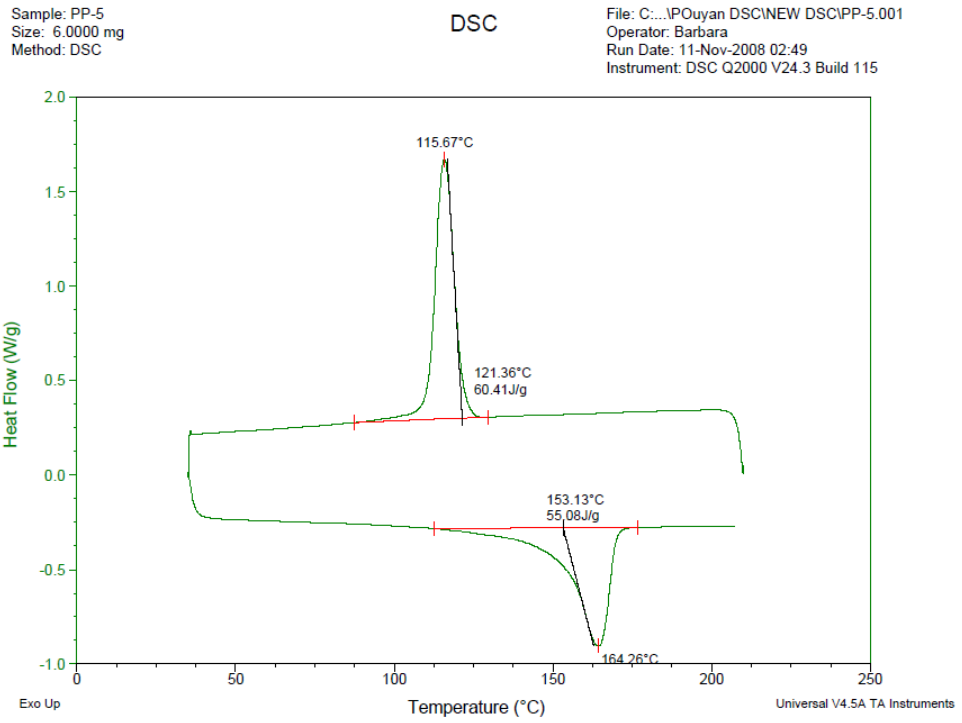

Figure 0-5DSC Curve Run#5

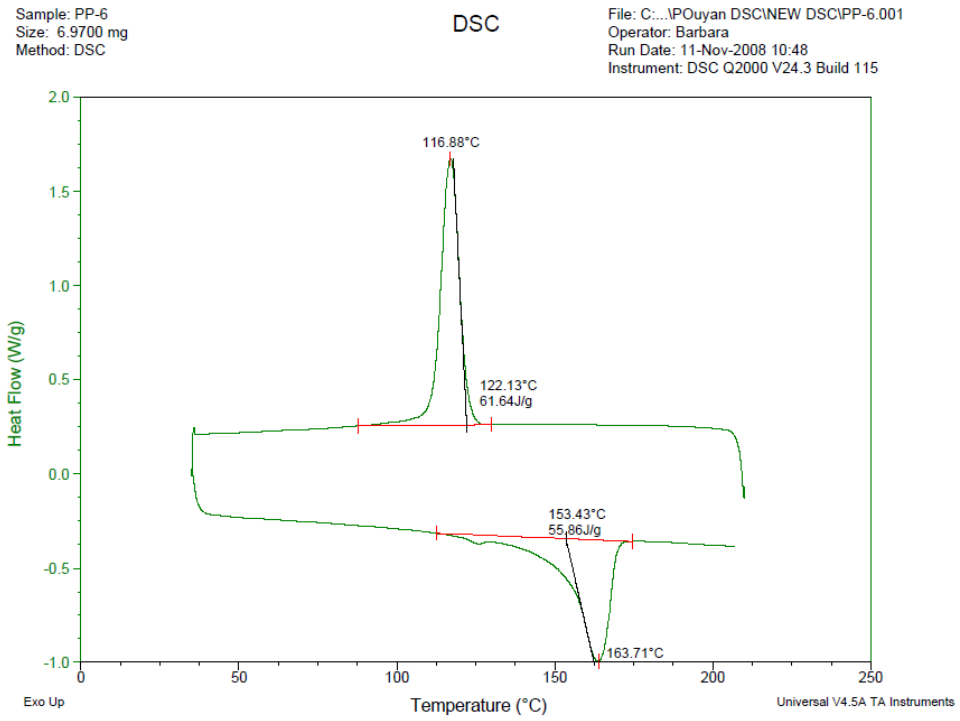

Figure 0-6DSC Curve Run#6

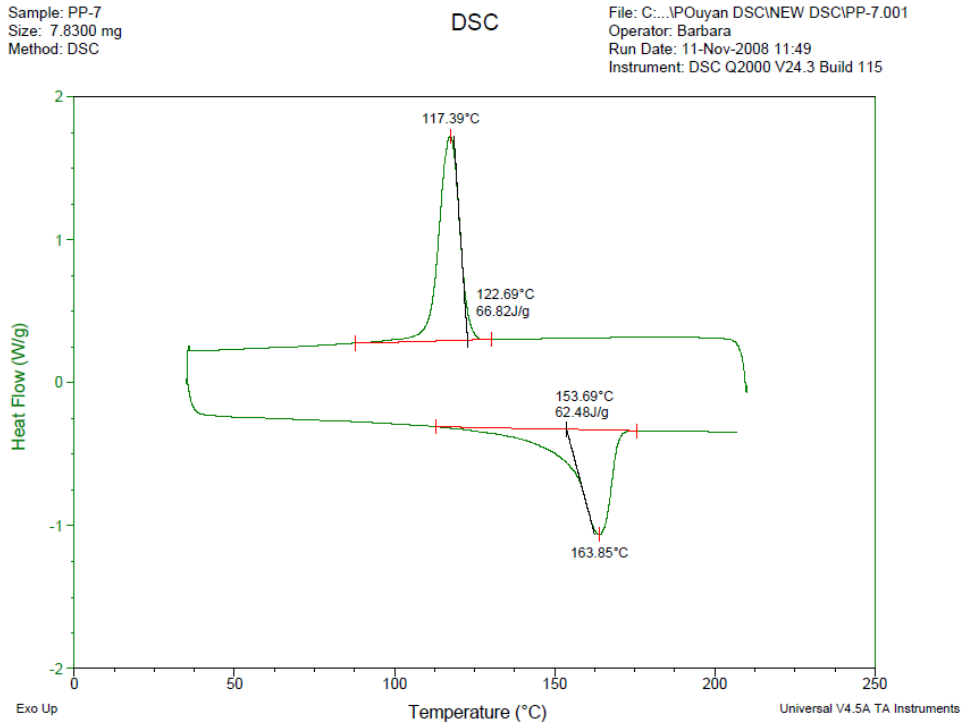

Figure 0-7DSC Curve Run#7

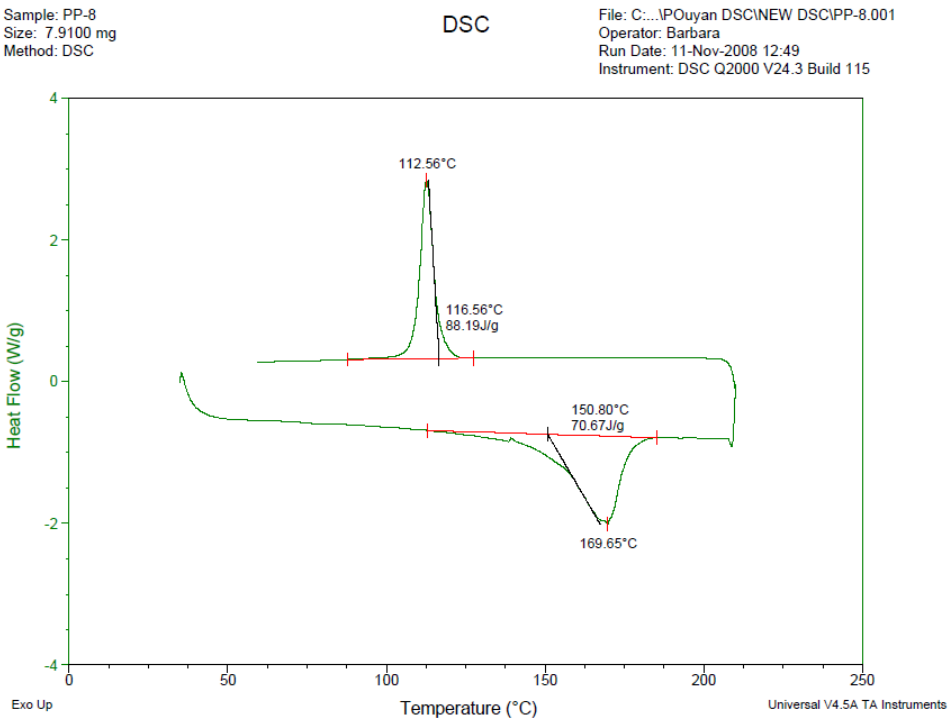

Figure 0-8DSC Curve Run#8

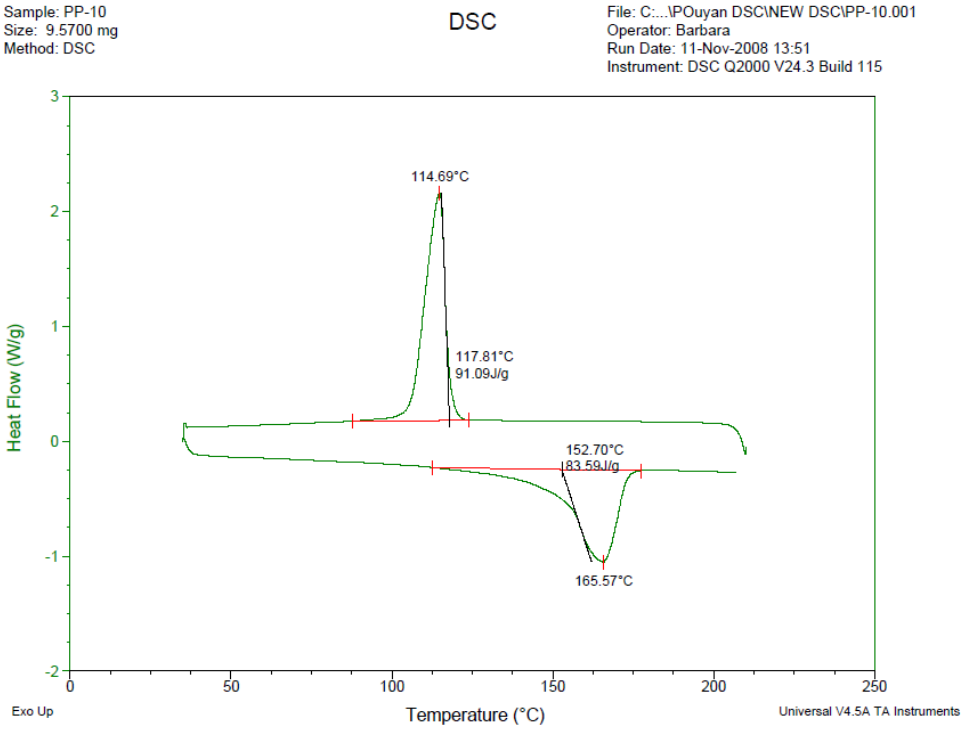

Figure 0-9DSC Curve Run#9

DENSITY MEASUREMENT BY GAS PYCNOMETRY

Table 0-1 Density Measurement From Gas Pycnometry on Large Batch of gWS

Large					
Mass: 0.9609 gm					
Reference Volume : 45.5986019121447 cc					
Sample Chamber Volume: 33.6396886607428 cc					
PF0 (psi)	PI0 (psi)	PI (psi)	PF (psi)	VOLUME (cc)	DENSITY (gm/cc)
00.072	00.071	09.855	05.744	00.542	01.772
00.067	00.068	09.853	05.742	00.573	01.677
00.062	00.062	09.847	05.736	00.557	01.725
00.062	00.061	09.853	05.741	00.579	01.660
00.060	00.058	09.824	05.725	00.593	01.621
00.057	00.056	09.847	05.736	00.588	01.633
00.055	00.054	09.822	05.721	00.582	01.652
00.052	00.052	09.816	05.717	00.595	01.616
00.053	00.053	09.853	05.739	00.599	01.603
00.050	00.050	09.851	05.737	00.604	01.591
				Average Volume : 0.581 cc	
				Average Density: 1.653 +/- 0.054 gm/cc	

Table 0-2 Density Measurement From Gas Pycnometry on Mid Batch of gWS

Mid					
Mass : 1.463 gm					
Reference Volume : 45.5986019121447 cc					
Sample Chamber Volume: 33.6396886607428 cc					
PF0 (psi)	PI0 (psi)	PI (psi)	PF (psi)	VOLUME (cc)	DENSITY (gm/cc)
00.064	00.063	09.853	05.772	00.992	01.475
00.059	00.060	09.847	05.770	01.053	01.389
00.060	00.058	09.851	05.772	01.017	01.438
00.059	00.059	09.853	05.772	01.019	01.436
00.058	00.057	09.849	05.770	01.024	01.429
00.055	00.054	09.853	05.772	01.042	01.404
00.048	00.048	09.841	05.761	01.028	01.424
00.053	00.052	09.843	05.762	00.988	01.481
00.047	00.047	09.837	05.759	01.040	01.407
00.045	00.045	09.839	05.758	01.021	01.432
				Average Volume : 1.022 cc	
				Average Density: 1.431 +/- 0.028 gm/cc	

Table 0-3 Density Measurement From Gas Pycnometry on Fine Batch of gWS

Fine					
Mass : 1.2469 gm					
Reference Volume : 45.5986019121447 cc					
Sample Chamber Volume: 33.6396886607428 cc					
PF0 (psi)	PI0 (psi)	PI (psi)	PF (psi)	VOLUME (cc)	DENSITY (gm/cc)
00.089	00.087	09.839	05.770	00.926	01.347
00.080	00.079	09.827	05.753	00.837	01.490
00.081	00.080	09.837	05.760	00.851	01.466
00.081	00.082	09.827	05.755	00.861	01.448
00.080	00.079	09.822	05.750	00.843	01.479
00.079	00.079	09.855	05.770	00.863	01.444
00.073	00.072	09.853	05.774	00.962	01.296
00.073	00.072	09.849	05.766	00.889	01.402
00.070	00.071	09.845	05.762	00.879	01.418
00.071	00.071	09.845	05.759	00.837	01.490
				Average Volume : 0.875 cc	
				Average Density: 1.425 +/- 0.061 gm/cc	